BULLETIN OF BIOTECHNOLOGY

e-ISSN: 2717-8323

Cilt: 4 Volume: 1 Year: 2023

BULLETIN OF BIOTECHNOLOGY

Cilt: 4 Volume: 1 Year: 2023

Published Biannually

Corresponding Address
Karamanoğlu Mehmetbey University, Faculty of Health, Sciences, Department of Nutrition and Dietetics, Karaman, Turkey
E-mail: mtdogan1@gmail.com
Web: https://www.dergipark.org.tr/biotech

Owner / Publisher
Assist. Prof. Dr. Muhammet DOĞAN
This journal is peer-reviewed and published twice (June, December) a year.

e-ISSN 2717-8323

BULLETIN OF BIOTECHNOLOGY

e-ISSN 2717-8323

Cilt: 4 Volume: 1 Year: 2023

Contents

RESEARCH ARTICLE
Bull Biotechnol (2023) 4(1):1-6
https://doi.org/10.51539/biotech.1215951 Journal homepage: www.dergipark.org.tr/biotech

Bulletin of Biotechnology

5,7,8-trihydroxyflavone Has Anticancer and Apoptotic Effects in Human Androgen-Independet Prostate Cancer PC-3 Cells

Ahmet Karakus[*1], Sevgi Unal Karakus[2], Burak Dagdelen[3]

[*1]*Bartin University, Faculty of Science, Department of Biotechnology, Bartin, Turkiye*
[2]*Bartin University, Faculty of Science, Department of Molecular Biology and Genetics, Bartin, Turkiye*
[3]*Selcuk University, Faculty of Medicine, Department of Medical Biology, Konya Turkiye*

*Corresponding author : akarakus@bartin.edu.tr
Orcid No: https://orcid.org/0000-0003-1458-808X

Received : 07/12/2022
Accepted : 07/01/2023

Abstract: Natural products have been studied to provide alternative treatments against human diseases as they have various medicinal properties. One of these natural products is substances in the class of flavonoids. These bioactive molecules have antioxidant, anti-inflammatory and antitumor activities. The number of studies focusing on these molecules is increasing to discover new therapeutic agents against diseases such as cancer. We aimed to determine the anticancer and apoptotic effects of plant-derived natural 5,7,8-trihydroxyflavone (Nor-wogonin) on androgen-independent human prostate cancer (PC-3) cells *in vitro*. Nor-wogonin concentrations of 10, 20, 40, 80 µM were prepared and applied to human prostate cancer cells for 24 hours. The anticancer effect of flavone was determined by MTT 3-(4,5-dimethylthiazol-2-yl)-diphenyl tetrazolium bromide) method, and its effect on pro-apoptotic and anti-apoptotic genes was determined by Real-Time PCR analysis. According to the obtained data, Nor-wogonin applied to PC-3 cells decreased *in vitro* cell viability due to increasing concentration ($p<0.05$) and the IC_{50} value was calculated as 57.29 µM. In addition, it was determined that Nor-wogonin directed PC-3 cells to apoptosis by acting on various anti-apoptotic and pro-apoptotic gene expressions.

Keywords: Prostate cancer; Nor-wogonin; Anticancer effect; Apoptosis

1 Introduction

Cancer is a serious health problem that accounts for 70% of all deaths worldwide (Cadona et al. 2022). Prostate cancer is the most common aggressive cancer among men (Barsouk et al. 2022). Aggressive and metastatic prostate cancer is among the dangerous, life-threatening tumors and is one of the leading causes of death in men (Apostolatos et al. 2018). Prostate tumors usually occur as a mixture of androgen-dependent and androgen-independent cells (Tang and Porter 1997; Russell et al. 1998). In advanced stage and metastatic prostate cancers, a fatal hormone-resistant disease develops with the growth of tumor cells and the formation of new cells independent of androgen. In this regard, it is important to introduce new treatment strategies and to encourage cells to apoptosis in the treatment of prostate cancers (Huang et al. 2004).

Carcinogenesis is a complex phenomenon involving genetic and epigenetic changes affecting tumor suppressor genes and oncogenes (Shu et al. 2010). In cancer treatment, natural products are becoming important candidates for drug discovery. Especially the phytochemicals in these products have been extensively researched as anticancer therapeutics. These bioactive molecules exert their anticarcinogenic activities by interfering with the formation, development and progression of cancer by regulating cell differentiation, proliferation, angiogenesis, metastasis and apoptosis (Chen et al. 2008). Many successful anticancer drugs currently available contain phytochemicals (Mondal et al. 2011) and some are being investigated in human clinical trials (Sultana 2011).

Flavones constitute one of the subgroups of flavonoids, which are among the most important bioactive compounds among secondary metabolites (Martens and Mithofer 2005). Flavonoids make up the largest group of polyphenols and are abundant in a variety of plant products such as fruits, and vegetables (Pallauf et al. 2017). Besides having biochemical and pharmacological activities, including antioxidant, anticarcinogenic, anti-inflammatory, antiproliferative and antiangiogenic effects, flavones do not have any toxic effects (Havsteen et al. 2002). It has been reported that flavonoids exert their antitumor effects through the induction of apoptosis, some phytochemicals such as tea, zerumbon and

turmeric have been investigated to trigger apoptosis by regulating the down-regulation of Bcl-2 and Bcl-XL in various tumor cells (Aggarwal et al. 2005; Takada et al. 2005; Nishikawa et al. 2006).

Nor-wogonin (5,7,8-trihydroxyflavone) is a polyhydroxy flavone isolated from *Scutellaria baicalensis* with various biological activities such as anticancer, antiviral and antioxidant (Hui et al. 2002; Miyasaki et al. 2013). Nor-wogonin induces apoptosis in HL-60 leukemia cells (Chow et al. 2008) and inhibits cell division by stopping the cell cycle in MDA-MB-231 cell line, leading cells to apoptosis and perform an antiproliferative effect (Abd El-Hafeez et al. 2019). In addition, Nor-wogonin has the potential to inhibit the growth of colorectal cancer cells *in vitro* by triggering apoptosis, autophagy and cell cycle arrest and it is thought to be developed as a possible anticancer agent (Wang et al. 2020).

It is important to define new therapeutics in cancer treatment and to reveal their mechanisms of action in cancerous cells (Eastman et al. 2006). Many studies conducted for this purpose focus on the discovery or development of new therapeutics (Genc et al. 2016, Sahin et al. 2018). In this study, we aimed to determine the anticancer and apoptotic effects of Nor-wogonin on the human prostate (PC-3) cancer cell line.

2 Materials and Method

2.1 Cell line, Cell Culture and Test Compound

Androgen-independent prostate cell PC-3 cells were used in the study. RPMI-1640 medium (Sigma-Aldrich, USA; added into the medium 10% FBS, 100 U/mL penicillin and 0.1 mg/mL streptomycin) was used to feed PC-3 cells. Cells were fed in cell culture flask (TPP; Switzerland) and placed in a humidified incubator (5% CO2, 37°C; N-Biotek, Korean). The cell medium was refreshed on average every 3-4 days and cell passages were performed when the cells reached 90% confluence. The 10, 20, 40, 80 µM concentrations of Nor-wogonin (Cayman Chem, Cas number: 4443-09-8) in RPMI-1640 (for PC-3 cells) medium were prepared.

2.2 Determination of Cell Viability

The cytotoxic effect of Nor-wogonin on PC-3 cell line was determined by MTT (3-(4,5-dimethylthiazol-2-yl)-diphenyl tetrazolium bromide) assay. Cells reaching 90% density were removed from the bottom of the flasks by Trypsin-EDTA solution and counted under an inverted microscope. Cells were seeded into 96-well microplates with $15x10^3$ cells per well. The seeded cells were incubated for 24 h in a CO_2 incubator at 37°C. After incubation, the media in the wells were refreshed, then different concentrations of Nor-wogonin were added to the microplate wells and incubated for 24 hours (Koran et al. 2017).

Then, the cell medium in the microplate was removed and the MTT solution (0.5 mg/mL) was added to each well and incubated for 3 h. After the incubation, MTT solution in the wells was aspirated and 100 µL of dimethyl sulfoxide (DMSO) was added to each well and the incubation was stopped. Optical densities of cells in microplates were determined by spectrophotometer (Thermo, USA) at a wavelength of 570 nm (Mosmann 1983).

The average of the absorbance values obtained from the control wells was calculated and this value was accepted as 100% viable cells. The percentages of viability values in the experimental wells were determined by comparing the absorbance values obtained from Nor-wogonin applied wells to the control absorbance value.

2.3 Determination of the IC_{50} Value

According to the MTT analysis data, it was determined at what dose the high level effect of Nor-wogonin occurred. The effects of the compounds at different applied concentrations were evaluated using the GraphPad Prism 9 program to calculate the inhibitory concentration 50 (IC_{50}) value of the test compound on PC-3 cells. In the studies to be carried out after this step, the determined effective doses were applied to the cells.

2.4 RNA Isolation and Complementary DNA (cDNA) Synthesis

For the total RNA isolation, 1.5 mL of cold PBS was added to each well of 6-well microplates containing 1x106 cells treated with Nor-wogonin IC_{50} values for both PC-3 cells and then cells were scraped from the bottom of the flask. Total RNA isolation from human PC-3 cell line performed in accordance with the manufacturer's protocol (Thermo Fisher Scientific). cDNA synthesis was performed with the following the manufacturer's protocol (Bio-Rad).

2.5 Primer design and gene expression analysis

Polymerase chain reactions (PCR) were performed on a Bio-Rad CFX96 Real-Time PCR cycler and with a master mix (2xqPCRBIO SyGreen Mix Lo-ROX Kit, PCR Biosystems) containing SYBR Green, which was used to obtain gene expression profiles of cDNA samples. The associated genes of primers sequences were designed by Primer3 software program (v. 0.4.0), and they were obtained commercially (Metabion). The specific binding forward and reverse primer sequences of the associated gene and gene symbols are given in Table 1. β-Actin was taken as a housekeeping gene in qPCR studies.

qPCR reaction conditions; after incubation at 95°C for a period of 2 minutes; at 95°C for a period of 5 sec, 40 cycles; at 66°C for a period of 45 sec, 45 cycles; it was set at 74°C for a period of 2 minutes, 45 cycles, and finally at 72°C for a period of 5 minutes, 1 cycle. mRNA expression rates were determined by the comparative threshold cycle (2-ΔΔCt) method (Livak and Schmittgen; 2001). Ct values were normalized with β-actin mRNA expression ratios (Livak and Schmittgen 2001).

Table 1. Forward and reverse primer sequences designed for use in quantitative polymerase chain reaction.

Gene names	Primer Sequences (5'-3')
β-actin	Forward CACCCCAGCCATGTACGTTGC
	Reverse CCAGCCCATGATGGTTCTGAT
bcl-2	Forward GAGGGGCTACGAGTGGGATGC
	Reverse GGAGGAGAAGATGCCCCGGTGC
bax	Forward CCCGAGAGGTCTTTTTCCGAG
	Reverse CCAGCCCATGATGGTTCTGAT
p53	Forward CCTCAGCATCTTATCCGAGTGG
	Reverse GGATGGTGGTACAGTCAGAGC
caspase-3	Forward GCGAATCAATGGACTCTGGAA
	Reverse GTCAACAGGTCCATTTGTTCC

2.6 Statistical analysis

Statistical analyzes were performed with the GraphPad Prism 9 package program. One-way ANOVA was used to detect changes between different groups and Tukey's test was used for multiple comparisons. Quantitative data were analyzed as mean with standard deviation (mean±SD). The degree of significance of the analyzes was given with the symbol (*). p>0.05 (not significant, ns); *p<0.05 (significant); **p<0.01 (very significant); ***p<0.001 (highly significant).

3 Results and Discussion

The cytotoxic effect of Nor-wogonin on the human prostate cancer cell line is shown in Fig. 1. Accordingly, the applied 10 and 20 µM concentrations of flavone did not reveal a significant change in cell viability compared to the control group, while the 40 and 80 µM concentrations significantly decreased the cell viability (*p<0.05). In addition to cell viability assay we detected the IC_{50} values of the Nor-wogonin. The IC_{50} values of Nor-wogonin on PC-3 cells were calculated as 57.29 µM.

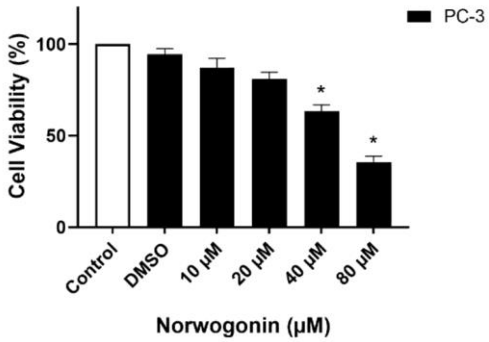

Fig. 1 The % change in viability of PC-3 human prostate cancer cells treated with different concentrations of Nor-wogonin for 24 hours. The data obtained are shown as mean±SD. *p<0.05 vs control group.

The mRNA expression levels of bcl-2, bax, p53 and caspase-3 genes of Nor-wogonin applied to PC-3 and HeLa cells were determined. The mRNA expression levels of the genes were calculated by the $2^{-\Delta\Delta CT}$ method (Livak KJ and Schmittgen 2001). The results were normalized using the mRNA expression level of the β-actin reference gene. mRNA expression rates of bcl-2, bax, p53 and caspase-3 genes were determined. The mRNA expression levels of all genes were evaluated as 1.0 for the control group and the results were given as fold values compared to the control group. The rates of increase and decrease of mRNA expressions of bcl-2, bax, p53 and caspase-3 genes compared to control groups PC-3 cells are given respectively in Fig. 2.

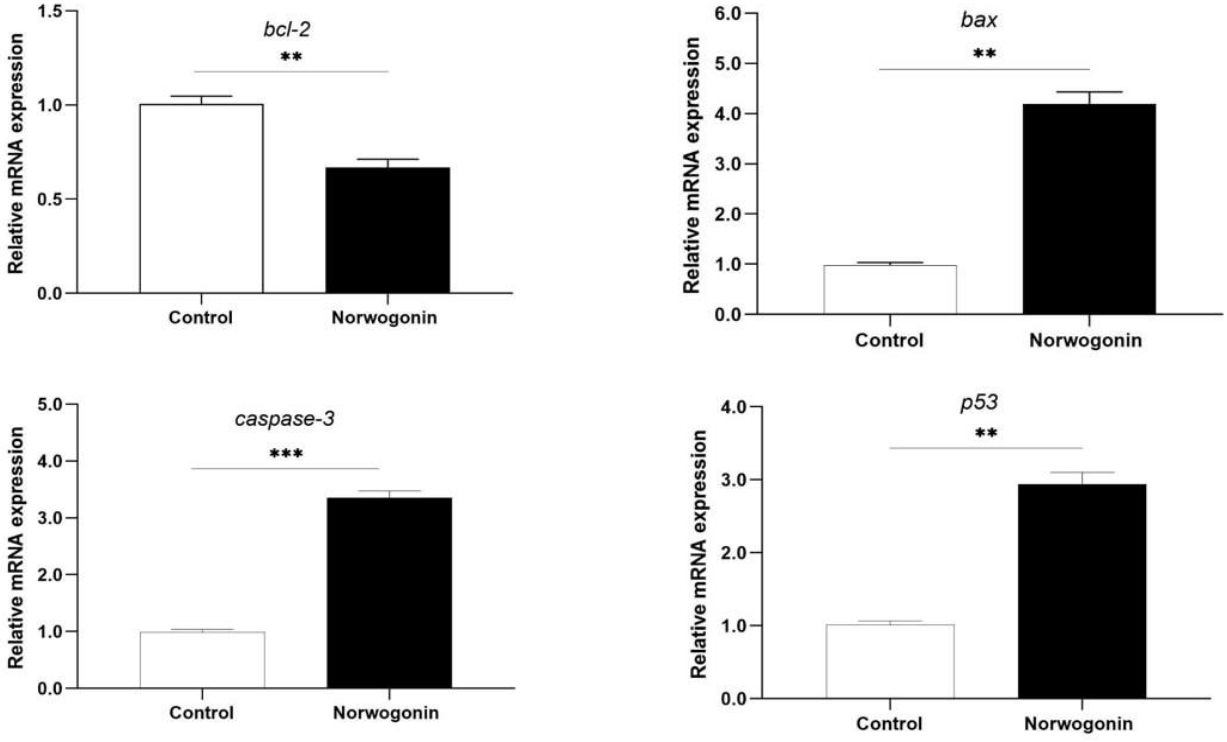

Fig.2 Quantitative changes in the gene expression levels of the control and Nor-wogonin groups in PC-3 cells. Changes in the gene expression levels of bax, bcl-2, p53 and caspase-3 (d) were examined by qPCR. β-Actin was used as a housekeeping gene. mRNA, messenger RNA; qPCR, quantitative polymerase chain reaction.

Prostate cancers are a group of tumors associated with androgen hormone (Panvichian and Pienta 1996, Klocker et al. 1999). Androgen deprivation and estrogen hormone replacement therapies have attracted attention as treatment strategies to reduce the growth of these types of tumors. However, androgen ablation may lead to the development of androgen-independent tumors that are less responsive to conventional chemotherapeutic treatments (Panvichian and Pienta 1996; Klocker et al. 1999).

Studies indicate the availability of herbal-based flavonoid therapies as an alternative method to arrest androgen-independent tumor growth. How flavonoids alter the growth of these types of cells has not been determined, but suggests that they alter the estrogen receptor and expression of hormone-sensitive genes (Denis et al. 1999).

Natural products of plant origin, such as flavonoids, are the leading sources of many medicines and dietary supplements (Hui et al. 2002, Li and Vederas, 2011). The biological effects of Wogonin and Nor-wogonin, which are polyhydroxyflavones and are relatively similar in structure, have been reported (S Patel et al. 2013). The structural difference between Wogonin and Nor-wogonin is due to the presence of a methoxyl (OCH3) group on the C8 of Wog and a hydroxyl (OH) group on the C8 of N-Wog (Huang et al. 2017). Nor-wogonin has been reported to be a more effective apoptotic inducer than Wogonin in human leukemia HL-60 cells (Chow et al. 2008). In another study, it was reported that Nor-wogonin had no toxic effect on rat PC-12 normal adrenal gland cells (Jing et al. 2021). There are not enough studies in the literature with the cytotoxic activity of Nor-wogonin compared to Wogonin. Therefore, in this study, we aim to contribute to the literature by investigating the cytotoxic effect of Nor-wogonin in human androgen-independet prostate cancer cells.

In the studies, the anticancer effect of Nor-wogonin and the IC_{50} values in androgen-independented prostate cancer cells were calculated. In one of these studies, Nor-wogonin was reported to decrease the viability of human triplet breast cancer cells, and the IC_{50} values of Nor-wogonin in MDA-MB-231, HCC70, BT-549, and HCC1806 were 32,24, 39.05, 56.2, and 37.3 μM, respectively (Abd El-Hafeez et al. 2019). In another study, it was emphasized that Nor-wogonin had a cytotoxic effect on HL-60 human leukemia and SW48 human colon cancer cells, and the IC_{50} values of HL-60 and SW48 cells were calculated as 21.7 μM and 15.5 μM, respectively (Chow et al. 2008). In our previous study, we also showed the anticancer effect of Nor-wogonin in human cervical cancer HeLa cell line and determined the IC_{50} value as 32.09 μM (Karakuş and Ünal Karakuş, 2022). According to our findings in this study, Nor-wogonin decreased cell viability in PC-3 cells. While a statistically significant decrease in cell viability was observed at 40 and 80 μM concentrations of Nor-wogonin treated with PC-3 cells, no statistically significant decrease was detected at 10 and 20 μM concentrations. In addition, the IC_{50} value of Nor-wogonin for PC-3 cells was calculated as 57.29 μM.

Natural compounds such as flavonoids are considered important agents for the prevention and treatment of cancer due to their potential therapeutic effects and limited toxicity to healthy cells (Toshiya et al. 2012). In carcinogenesis, flavonoids interfere with intracellular signal transduction pathways, thereby suppressing proliferation, metastasis, angiogenesis and increasing apoptosis (Ravishankar et al. 2013, Srivastava et al. 2016). Controlled by genes in the cell, apoptosis is part of the cell's active death process (Kerr et al. 1972). In our study, we also investigated the expression levels of antiapoptotic bcl-2, proapoptotic bax, caspase-3 and p53 genes, which are involved in apoptotic processes of Nor-wogonin in PC-3 cells. While bcl-2 gene expression decreased in PC-3 cells, the expression of bax, caspase-3 and p53 genes increased.

Activation of the caspase cascade occurs in cells undergoing apoptosis (Estaquier et al. 2012). In this study, Nor-wogonin increased caspase-3 gene expression in both cell lines. Bax and bcl-2 gene expression rate is important in initiating apoptosis (Liu et al. 2005). According to our findings, Nor-wogonin increased the expression rate of bcl-2/bax genes in PC-3 cells.

Tumor suppressor protein p53 is responsible for regulating bax and bcl-2 gene expression, activating cell cycle checkpoints, DNA repair mechanisms and apoptosis response (Farnebo et al. 2010). DNA-damaging agents induce increased p53, which plays a leading role in directly activating the pro-apoptotic bax gene to activate the apoptotic program (Miyashita et al. 1994). In this study, Nor-wogonin increased p53 expression in PC-3 cells.

5 Conclusion

Nor-wogonin showed anticancer effect in PC-3 human prostate cancer cells and induced apoptosis by showing increased bax, caspase-3 and p53 gene expression and decreased bcl-2 gene expression. However, further studies are needed to better understand how Nor-wogonin affects the molecular mechanisms in cell death and to determine its biocompatibility levels.

Acknowledgements

This research was supported by Bartin University Scientific Research Projects Coordination Commission with project number 2021-FEN-B-001.

Conflict of interest disclosure:

The authors of this study declare that they have no conflict of interest.

References

Abd El-Hafeez AA, Khalifa HO, Mahdy EAM, Sharma V, Hosoi T, Ghosh P, Ozawa K, Montano MM, Fujimura T, Ibrahim ARN, Abdelhamid MAA, Pack SP, Shouman SA, Kawamoto S (2019) Anticancer effect of nor-wogonin (5, 7, 8-trihydroxyflavone) on human triple-negative breast cancer cells via downregulation of TAK1, NF-κB, and STAT3. Pharmacol Rep 71(2):289-298

Aggarwal BB, Shishodia S, Takada Y, Banerjee S, Newman RA, Bueso-Ramos CE, Price JE (2005) Curcumin suppresses the paclitaxel-induced nuclear factor-kappaB pathway in breast cancer cells and inhibits lung metastasis of human breast cancer in nude mice. Clin Cancer Res 11:7490-7498

Barsouk A, Padala SA, Vakiti A, Mohammed A, Saginala K, Thandra KC, Rawla P, Barsouk A (2020) Epidemiology, Staging and Management of Prostate Cancer. Medical Sciences 8(3):28

Cadona FC, Dantas RF, de Mello GH, Silva-Jr FP (2022). Natural products targeting into cancer hallmarks: An update on caffeine, theobromine, and (+)-catechin. Critical Reviews in Food Science and Nutrition 62(26):7222-7241

Chen D, Dou QP (2008) Tea polyphenols and their roles in cancer prevention and chemotherapy. Int J Mol Sci 9 (7):1196- 1206

Chow JM, Huang GC, Shen SC, Wu CY, Lin CW, Chen YC (2008) Differential apoptotic effect of wogonin and nor-wogonin via stimulation of ROS production in human leukemia cells. J Cell Biochem 103:1394–1404

Denis L, Morton MS, Griffiths K (1999) Diet and its preventive role in prostatic disease. Eur Urol 35, 377–387

Eastman A, Perez RP (2006) New targets and challenges in the molecular therapeutics of cancer. Br J Clin Pharmacol 62(1):5-14

Estaquier J, Vallette F, Vayssiere JL, Mignotte B (2012) The mitochondrial pathways of apoptosis. Adv Exp Med Biol 942:157-83

Farnebo M, Bykov VJ, Wiman KG (2010) The p53 tumor suppressor: a master regulator of diverse cellular processes and therapeutic target in cancer. Biochem Biophys Res Commun 396:85-89

Genc M, Karagoz Genc Z, Tekin S, Sandal S, Sirajuddin M, Hadda Taibi B, Sekerci M (2016) Design, Synthesis, *in vitro* Antiproliferative Activity, Binding Modeling of 1,2,4,-Triazoles as New Anti-Breast Cancer Agents. Acta Chim Slov 63(4):726-737

Havsteen BH (2002) The biochemistry and medical significance of the flavonoids. Pharmacology & therapeutics 96(2-3):67-202

Huang GC, Chow JM, Shen SC, Yang LY, Lin CW, Chen, YC (2007) Wogonin but not Nor-wogonin inhibits lipopolysaccharide and lipoteichoic acid-induced iNOS gene expression and NO production in macrophages. Int Immunopharmacol 7(8):1054-1063

Huang YT, Chueh SC, Teng CM, Guh JH (2004) Investigation of ouabain-induced anticancer effect in human androgen-independent prostate cancer PC-3 cells. Biochem Pharmacol 15;67(4):727-33

Hui KM, Huen MS, Wang HY, Zheng H, Sigel E, Baur R, Xue H (2002) Anxiolytic effect of wogonin, a benzodiazepine receptor ligand isolated from Scutellaria baicalensis Georgi. Biochemical pharmacology 64(9):1415-1424

Jing L, Gao R, Zhang J, Zhang D, Shao J, Jia Z, Ma H (2021) Norwogonin attenuates hypoxia-induced oxidative stress and apoptosis in PC12 cells. BMC Complementary Medicine and Therapies 21(1):1-12

Karakuş A, Karakuş SÜ (2022) Nor-wogonin'in İnsan Rahim Ağzı Kanseri Hücrelerinde Antikanser ve Apoptotik Etkileri. Avrupa Bilim ve Teknoloji Dergisi (34):617-622

Kerr JF, Wyllie AH, Currie AR (1972) Apoptosis: a basic biological phenomenon with wide-ranging implications in tissue kinetics. Br J Cancer 26(4):239-257

Klocker H, Culig Z, Eder IE, Nessler-Menardi C, Hobisch A, et al (1999) Mechanism of androgen receptor activation and possible implications for chemoprevention trials. Eur Urol 35,413-419

Koran K, Tekin Ç, Çalışkan E, Tekin S, Sandal S, Görgülü AO (2017) Synthesis, structural and thermal characterizations and *in vitro* cytotoxic activities of new cyclotriphosphazene derivatives. Phosphorus Sulfur Silicon Relat Elem 192(9):1002-1011

Li JW, Vederas JC (2011) Drug discovery and natural products: end of era or an endless frontier? Biomed Khim 57(2):148-160

Liu J, Huang R, Lin D, Peng J, Wu X, Lin Q (2005) Expression of survivin and bax/bcl-2 in peroxisome proliferator activated receptor-γ ligands induces apoptosis on human myeloid leukemia cells *in vitro*. Ann Oncol 16:455-459

Livak KJ, Schmittgen TD (2001) Analysis of relative gene expression data using real-time quantitative PCR and the $2^{-\Delta\Delta CT}$ method. Methods 25(4):402-408

Miyasaki Y, Rabenstein JD, Rhea J, Crouch ML, Mocek UM, Kittell PE, Liu GY (2013) Isolation and characterization of antimicrobial compounds in plant extracts against multidrug-resistant Acinetobacter baumannii. PloS one 8(4):e61594

Miyashita T, Krajewski S, Krajewska M, Wang HG, Lin H, Liebermann DA (1994) Tumor suppressor p53 is a regulator of bcl-2 and bax gene expression *in vitro* and *in vivo*. Oncogene 9:1799-1805

Mondal S, Bandyopadhyay S, Ghosh M, Mukhopadhyay S, Roy S, Mandal C (2011) Natural Products: Promising Resources For Cancer Drug Discovery. Anticancer Agents Med Chem 12(1):49-75

Mosmann T (1983) Rapid colorimetric assay for cellular growth and survival: Application to proliferation and cytotoxicity assays. J Immunol Methods 65 (1):55-63

Nishikawa T, Nakajima T, Moriguchi M, Jo M, Sekoguchi S, Ishii M, Takashima H, Katagishi T, Kimura H, Minami M, Itoh Y, Kagawa K, Okanoue T (2006) A green tea polyphenol, epigalocatechin-3-gallate, induces apoptosis of human hepatocellular carcinoma, possibly through inhibition of Bcl-2 family proteins. J Hepatol 44:1074–1082

Pallauf K, Duckstein N, Rimbach GA (2017) Literature review of flavonoids and lifespan in model organisms. Proc Nutr Soc 76:145–162

Panvichian R and Pienta KJ (1996) Hormonal and chemotherapeutic systemic therapy for metastatic prostate cancer. Cancer Control 3:493–500

Ravishankar D, Rajora AK, Greco F, Osborn HMI (2013) Flavonoids as prospective compounds for anti-cancer therapy. Int. J Biochem Cell Biol 45:2821–2831

Russell PJ, Bennett S, Stricker P (1998) Growth factor involvement in progression of prostate cancer. Clin Chem 44:705-23

S Patel P, Joshee N, M Rimando A, Parajuli P (2013) Anti-cancer scopes and associated mechanisms of Scutellaria extract and flavonoid wogonin. Curr Cancer Ther Rev 9(1):34-42

Sahin O, Ozdemir UO, Seferoglu N, Genc ZK, Kaya K, Aydiner B, Tekin S, Seferoglu Z (2018) New platinum (II) and palladium (II) complexes of coumarin-thiazole Schiff base with a fluorescent chemosensor properties: Synthesis, spectroscopic characterization, X-ray structure determination, in vitro anticancer activity on various human carcinoma cell lines and computational studies. J Photochem. Photobiol B 178:428-439

Shu L, Cheung KL, Khor TO, Chen C, Kong AN (2010) Phytochemicals: cancer chemoprevention and suppression of tumor onset and metastasis. Cancer Metastasis Rev 29 (3):483-502

Srivastava S, Somasagara RR, Hegde M, Nishana M, Tadi SK, Srivastava M, Choudhary B, Raghavan SC (2016) Quercetin, a Natural Flavonoid Interacts with DNA, Arrests Cell Cycle and

Causes Tumor Regression by Activating Mitochondrial Pathway of Apoptosis Sci Rep (12)6:24049

Sultana N (2011) Clinically useful anticancer, antitumor, and antiwrinkle agent, ursolic acid and related derivatives as medicinally important natural product. J Enzyme Inhib Med Chem 0:1-27

Takada Y, Murakami A, Aggarwal BB (2005) Zerumbone abolishes NF-kappaB and IkappaBalpha kinase activation leading to suppression of antiapoptotic and metastatic gene expression, upregulation of apoptosis, and downregulation of invasion. Oncogene 24:6957–6969

Tang DG and Porter AT (1997) Target to apoptosis: a hopeful weapon for prostate cancer. Prostate 32:284-93

Toshiya K, Testuya T, Akira H, Takuji T (2012) Cancer chemoprevention through the induction of apoptosis by natural compounds. Biophys Chem 3(2):156-173

Wang Z, Zhang Q, Zhou L, Liu G, Wu Q, Chen C (2020) Norwogonin flavone suppresses the growth of human colon cancer cells via mitochondrial mediated apoptosis, autophagy induction and triggering G2/M phase cell cycle arrest. J Buon 25(3):1449-1454

RESEARCH ARTICLE
Bull Biotechnol (2023) 4(1):7-12
https://doi.org/10.51539/biotech.1213740 Journal homepage: www.dergipark.org.tr/biotech

Bulletin of Biotechnology

Evaluation of insecticidal and enzyme activity potentials of essential oils and extracts of *Chenopodium botrys* L. against storage products pests

Ali Rıza Tüfekçi[1]*, Hüseyin Akşit[2], Samed Şimşek[3], Ömer Cem Karakoç[4], Şevki Adem[5], Zeyad Adil Hameed[6], Mehmet Nuri Atalar[7], Ahmet Rıdvan Topkara[8]

[*1] *Department of Chemistry, Faculty of Science, Çankırı Karatekin University, Çankırı, Turkey.*
[2] *Department of Analytical Chemistry, Faculty of Pharmacy, Erzincan Binali Yıldırım University, Erzincan, Turkey.*
[3] *Department of Medical Services and Techniques, Çayırlı Vocational School, Erzincan Binali Yıldırım University, Erzincan, Turkey.*
[4] *Food and Agriculture Vocational School, Çankırı Karatekin University, Çankırı, Turkey.*
[5] *Department of Chemistry, Faculty of Science, Çankırı Karatekin University, Çankırı, Turkey.*
[6] *Department of Chemistry, Faculty of Science, Çankırı Karatekin University, Çankırı, Turkey.*
[7] *Department of Biochemistry, Faculty of Science and Arts, Igdır University Igdır, Turkey.*
[8] *Çankırı Karatekin University, Çankırı, Turkey.*

*Corresponding author : areb@karatekin.edu.tr
Orcid No: https://orcid.org/0000-0002-2951-3657

Received : 04/12/2022
Accepted : 09/06/2023

Abstract: Investigating the insecticidal properties of *Chenopodium botrys* L. plant extracts is valuable for pest control and agricultural practices. *C. botrys* L. plant extracts may exhibit various enzymatic activities, such as protease, amylase, lipase, and antioxidant activities. Investigating these enzymatic properties provides insights into the plant's biochemical composition and potential applications. This study was aimed to reveal the insecticidal activity and enzyme activity of the essential oil and extracts obtained by different solvent and extraction methods by using the aerial part of the plant. Plant material was collected from Erzincan. The essential oil of *C. botrys* L. plant was obtained by steam distillation using Neo-Clavenger device. The remaining aqueous part was extracted with the solvent ethylacetate and n-butanol, respectively. In the end, five extracts were obtained: essential oil (CB-EO), untreated aqueous extract (CB-F), ethylacetate (CB-EA), n-butanol (CB-nBu) and processed aqueous extract (CB-L). The effects of five extracts on both insecticidal (against *Sitophilus granarius* and *Tribolium castaneum*) and enzyme activities (acetylcholinesterase, xanthine oxidase (XO) and tyrosinase) were studied. It has been determined that CB-F and CB-nBu extracts have an activation effect against tyrosinase enzyme with IC_{50} values of 250 and 423 µg/mL, respectively. At the end of 48 hours, CB-EA extract was determined to cause 20% death against the adult insects of *Sitophilus granarius* as a result of contact toxicity test. As a result of GC-MS analysis of essential oil, α-Eudesmol compound was analyzed as the main component. In conclusion, studying the enzyme and insecticidal activities of *C. botrys* plant extracts is significant due to its potential applications in pest control, biotechnology, natural product discovery, and sustainable agriculture.

Keywords: Biological activity; Phenolic compounds; Spinachaceae family; Essential oils

1 Introduction

Chenopodium plant species are from the Spinachaceae family and their leaves resemble crow's feet. These plant species are grown in different parts of the world as a leafy plant and as a secondary cereal crop. This plant species can also be in the form of an annual or perennial shrub in herbaceous form. The species included in the family are generally distributed in most of Europe, Asia and North America. They spread in a wide variety of areas such as arid regions, soils rich in nitrogen potassium, coasts, roads, fields and riversides (Akman et al. 2007; Yıldırımlı 2003; Tozoğlu 2011). Recently, interest in the crowbar plant has been growing in many countries, especially in Europe, and research has been increasing. The *Chenopodium botrys* L. plant has traditionally been used for medicinal purposes. This information is based on folklore, not proven information on the threshold of scientific data. *C. botrys*, the scent of incense gives it characteristic meanings. As a result of scientific studies, it has been determined that the essential oil of the plant shows antibacterial and antifungal activity because it contains sesquiterpene compounds containing oxygen (Mahboubi et al. 2011; Andov et al. 2014; Morteza-Semnani 2017).

Plants are the main source of many bioactive compounds. Therefore, it has been reported in many studies that they

significantly affect enzyme activities both as extracts and as pure compounds. Many phycochemicals have been reported that specifically affect the enzyme activities of acetylcholinesterase (AChE), Xanthine oxidase (XO), and Tyrosinase (Kebbi et al. 2021; Yırtıcı et al. 2022). Therefore, the potential effects of the obtained extracts on these three enzymes were investigated in this study.

The world population is increasing day by day and as an effect of global warming, food supply to the population will cause great problems in the coming years. The overall pandemic conditions have made this situation even more obvious for humanity. Therefore, the supply of food, its safe transportation and limited resources are a big problem for humanity, which depends on agricultural systems. The current global agricultural production needs to be protected from many factors, from harvest to table. The biggest problem comes from warehouse pests, which also constitute a large insect team. These insects, which are harmful to cereals, can easily adapt themselves to environmental conditions and can live even in difficult conditions.

Storage pests are classified as primary pests and secondary pests, depending on their diet and amount. *Sitophilus granarius* and *Tribolium castaneum* are considered one of the primary pests. Due to the harmful effects of this pest, serious losses are experienced in stored products (Singh et al. 2009). The widely used approach to control warehouse pests in the world is pesticides and especially fumigants (Mutungi et al. 2014).

However, in recent years, serious concerns caused by pesticides in agricultural products, increasing demand for storage products due to diseases and increasing demand have led to the development of environmentally friendly approaches for the protection and cultivation of these products (Alkan et al. 2019). For this reason, natural origin plants and natural organic compounds obtained from them, which are naturally safe for people to consume, have started to be used for these purposes. Natural compounds, which have an insect repellent or killing effect on insects, destroy insects with many mechanisms. compounds that mostly target enzyme systems immediately stop the pest from living. If such natural compounds or enzyme inhibitors or activating compounds are found, this problem can be directly reduced to a minimum.

The mechanism of action of insecticides on insects is becoming more elucidated by the day. The importance of the enzyme system in insects has emerged. Inhibition or activation of AChE by natural insecticides can affect the movement and balance of the organism or organisms exposed to it. AChE is typically synthesized in nerve, muscle, and some blood-related cells. The enzyme is localized extracellularly in excitable tissues, both nerve and muscle. The enzyme acetylcholinesterase hydrolyzes acetylcholine to choline and acetic acid. The formed choline is transported back to the nerve centers to form new ACh molecules (Purves et al. 2008). Acetylcholine is a neurotransmitter found at the intersections of nerves and muscles, in lymph nodes in the visceral motor systems, and in various parts of the central nervous system. Studies show that acetylcholine affects the speed of individual neurons. AChE inhibitors are used in the treatment of Alzheimer's disease, glaucoma, smooth muscle weakness and various autonomic nervous system disorders (Taylor et al. 2009).

Xanthine oxidase (XO) acts as an important source of oxygen-derived free radicals that cause oxidative damage before and after biological events in living tissues. XO enzyme is among the most important factors of joint inflammation in relation to hyperuricemia in the joints, as it causes uric acid to accumulate in the joint area. Natural products provide a broad pool of XO inhibitors that can turn into critical products. Today, the potential to develop successful natural products to prevent or control XO-related diseases is still largely unexplored.

The enzyme tyrosinase, also known as phenol oxidase, is known to be a copper enzyme commonly found in plants, insects, animals and microorganisms (Yang et al. 2005, Liu et al. 2006). For vertebrates and plants it is crucial for the formation of pigmentation and for biological processes such as the browning of fruits and vegetables. It is the key enzyme involved in the formation of melanin in melanocytes. Tyrosinase catalyzes both the hydroxylation of monophenols and the oxidation of o-diphenols to o-quinones. In insects, tyrosinase is a widespread enzyme that plays an important role in normal developmental processes such as cuticular stratification, scleritization, wound healing, opsonin production, and encapsulation and nodulation to defend against foreign pathogens (Wang et al. 2005; Ma and Kanost 2000). Diphenolase is the essential insect enzyme in the oxidation of catecholamine to its corresponding kinins, which are then metabolized to melanin or crosslinking proteins in sclerotin.

In this study, *C. botrys*, known as "yapışkan kazayağı" among the people, was collected in the central district of Erzincan in our country. In this study, it was aimed to reveal the insecticidal activity and enzyme activity potential of the essential oil and extracts obtained by different solvent and extraction methods by using the aerial part of the plant. The purpose of this study can be expressed in several steps. Firstly; is to eliminate the damage of this insect species, which is a storage pest, to grains with completely natural plant-derived products. In addition, it was aimed to determine the effects on acetylcholine esterase, tyrosinase and xo enzymes and to determine the content of essential oil components by GC-MS technique.

2 Materials and Method

2.1 Plant Material and Extraction

C. botrys plant was collected from the Central region of Erzincan province during the flowering period of June-July. Prof. Dr. Ali Kandemir validated the taxonomic identity of the plant material, and a voucher specimen (EBYU 11627) has been deposited at the Herbarium of the Faculty of Pharmacy, Erzincan Binali Yıldırım University. The aerial parts of 1000 g *C. botrys* plant were cut with scissors and boiled in water for approximately 3 hours at 110 °C in the Neo clavenger apparatus. The essential oil collected in the collection chamber of the Clavenger apparatus was taken into

glass vials and a small amount of sodium sulfate was added into it to remove the water (CB-EO). Total of 650 µl of essential oil was obtained. On the other hand, the remaining aqueous part was separated from the pulp with the help of filter paper. Slightly separated from the supernatant portion and this was recorded as the untreated aqueous portion (CB-F). The aqueous fraction was first extracted with ethylacetate and the solvent of the extract was evaporated (CB-EA, yield % 2.7, 2.7 gr). The remaining aqueous was then extracted with n-butanol and its solvent was evaporated (CB-nBu, yield % 4.6, 4.6 gr). At the end of these processes, the remaining aqueous portion was placed in a separate container (CB-L). Especially CB-F and CB-L extracts were dehydrated in the lyophilizer. Extracts were stored in the dark and at +4 °C until study time.

2.2 Production of insect cultures

Adult individuals belonging to *S. granarius* and *T. castaneum* insect species were used for insecticide activity studies. The cultivation of both insect species was carried out by modifying the methods of Karakoç et al (2006). In order to obtain the same stage adults from *S. granarius* to be studied, 1/3 of wheat was placed in 1 L glass jars and 500 adults were released on average and they were expected to lay eggs for 7 days. Adult individuals released after this period were collected. For obtaining *T. castaneum* eggs, nutrient medium consisting of sifted 70% flour and 30% dry yeast was prepared. Approximately 500 adults were placed in a 1-liter spawning jar containing a mixture of sifted flour and yeast. The eggs obtained as a result of the sieving process made from the laying jar with an interval of 3 days were transferred to the nutrient medium containing cracked wheat and yeast. The culture was incubated at 27±2 °C, 50±10% humidity and dark conditions, and adults 2-4 weeks old were used in the experiments.

Application of insecticidal activity tests; The extracts were prepared with acetone as a 10% plant extract/acetone (weight volume) mixture. This mixture was applied to the insect with a micro applicator at a dose of 1 µl/insect for each insect. In the control group, 1 µl of pure acetone was applied to each insect. In all treatments, 10 adult beetles were used in all replicates. The treated adult insects were transferred to 60 mm plastic petri dishes and incubated at 27±2 °C. After 24 hours, the data obtained were recorded. Analysis of variance was performed with the results obtained. Differences between treatments were determined by Tukey multiple comparison test.

2.3 GC/MS analysis

The analysis of the essential oil components was determined by Thermo Scientific brand Trace 1310 model GC-MS (gas chromatography-mass spectrometry) device. A DB-5MS capillary column (30 m x 0.25 mm inner diameter and 0.25 µm) was used on the device. 100 µl of EO sample was prepared by dissolving in 1.5 ml of chloroform. The carrier gas was helium at a flow rate of 1 ml/min and injections were in split mode (50:1). The mass-spectrometer interface temperature was set at 280 ºC. The temperature of the ion source was 250 ºC, electron energy 70 eV. Initial temperature for column oven temperature started at 60°C and held there for 2 minutes, increased to 200°C at a rate of 8°C/min and held for 3 minutes and increased to 250°C at a rate of 8°C/min. and hold for 3 minutes. The total run time was 32 minutes. The percentages of the essential oil components were calculated using peak areas without any correction factors. Identification and accuracy of compounds were confirmed using current Wiley, NIST and MS libraries.

2.4 Enzyme activity tests

Acetylcholine esterase (AChE) enzyme activity measurements of the extracts were made in vitro under laboratory conditions by making some changes in the Ellman method (Ellman et al. 1961). Accordingly, the reaction mixture consists of 0.1 M Tris-HCl (pH 8.0), 0.5 mM acetylcholine iodate, 0.5 mM EDTA, 0.025 mM DTNB and 0.05% sodium citrate solution. AChE enzyme activity was evaluated by measuring the absorbance of the yellow 5-thio-2-nitrobenzoate anion at 412 nm with the enzyme solution added to the medium.

The tyrosinase inhibitory activity properties of the extracts and essential oil were determined by the dopachrome method used by Sarıkurkcu et al. (Sarıkurkcu et al. 2018). Accordingly, 25 mL of each extractant was taken from the stock extract solutions prepared in DMSO at a ratio of 1:1 and 40 mL of tyrosinase solution and 100 mL of sodium phosphate buffer (pH 6.8) were added and mixed. The mixture was incubated at 25°C for 15 minutes. After adding 40 mL of L-DOPA, the mixture was incubated again at 25°C for 10 minutes. Absorbance was measured at 492 nm. The inhibitory effect of the scutellarin compound, which was used as a positive control, on the tyrosinase enzyme was determined. For this, 1 mg of the scutellarin compound was weighed and dissolved in 1mL of DMSO, then diluted ten times with distilled water. Enzyme activity was tested at five different scutellarin concentrations.

The inhibition activity measurements of the extract and essential oil against the Xanthine oxidase (XO) enzyme were determined by performing minor modifications to the methods mentioned in the literature (Bustanji et al. 2010; Mohammed et al. 2010; Sweeney et al. 2001; Chiang et al. 1994). For each experiment, the solution and substrate containing the enzyme were freshly prepared just before the experimental studies. The solution mixture contains 80 mM sodium pyrophosphate buffer (pH = 8.5), 0.120 mM xanthine and 0.1 unit of XO enzyme and the reaction takes place in this mixture. Absorbance was measured for the formation of uric acid at 295 nm at 25°C. Thus, the initial rate of the reaction was calculated. Each extract was first dissolved in buffer solution and added to the reaction mixture to determine the inhibitory effect at a concentration of 200 µg/ml.

3 Results

Five essential oils (CB-EO), untreated aqueous extract (CB-F), ethylacetate (CB-EA), n-butanol (CB-nBu), and processed aqueous extract (CB-L) from the aerial parts of *C. botrys* plant extract was obtained. Insecticidal activities of these extracts were determined by contact toxicity tests against *Sitophilus granarius* and *Tribolium castaneum* storage pests. It was determined that only CB-EA extract caused 19.31% death to

adult insects of *Sitophilus granarius* (F= 37.23; df = 5,12; P<0.05). The other extracts, especially the essential oil, did not show any effect for the two insects. At the same time, acetylcholinesterase, xanthine oxidase (XO) and tyrosinase enzymes of the same extracts were examined in the concentration range of 0-1 mg/mL. As a result of the enzyme activity test, it was determined that only the CB-F coded extract had an activation effect on the tyrosinase enzyme. Content analysis of essential oil was done with GC-MS device. GC-MS chromatogram of CB-EO extract is given in Figure 1 and analysis result is given in Table 1. A total of 58 component analyzes were determined according to the GC-MS analysis result. α-Eudesmol compound was analyzed as the main component. The results were evaluated by comparing with the results of the Wiley and NIST library.

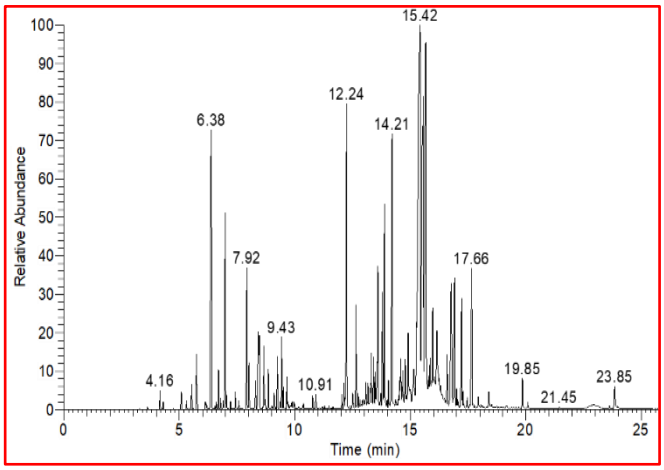

Fig. 1 GC-MS chromotogram of CB-EO

Table 1 Chemical compositions of *C. botrys* essential oils (CB-EO).

RT	Compounds Name	% Area
4.16	4-Hydroxy-4-methyl-2-pentanone	0.22
5.08	Bornylene	0.28
5.53	α-pinene	0.43
5.74	α-Fenchene	1.10
6.13	Sabinene	0.22
6.37	α-Myrcene	7.52
6.69	3-Carene	0.47
6.98	Limonene	2.92
7.42	γ-Terpinene	0.23
7.92	Fenchone	2.41
8.01	Linalool	0.77
8.30	Fenchyl alcohol	0.44
8.45	Trans-2-pinanol	2.61
8.66	Cis-sabinene hydrate	1.02
8.85	9-hydroxy-linalool	0.49
9.09	Borneol	0.20
9.24	4-Terpineol	0.74
9.50	cis-Piperitol	0.24
9.66	trans-Piperitol	0.48
10.77	α-Fenchyl acetate	0.18
10.91	p-Menth-1-en-9-ol	0.22
12.12	(-)-α-Elemene	0.33
12.23	β-Eudesmol acetate	5.78
12.50	α-Gurjunene	0.28
12.64	Caryophyllene	1.36
13.07	α-Humulene	0.29
13.17	δ-Cadinene	0.29
13.31	Eremophilene	0.90
13.40	Germacrene-D	0.56
13.48	α-Selinene	0.37
13.59	α-Muurolene	2.58
13.79	α-Amorphene	1.76
13.88	Germacrene B	3.17
14.05	Spathulenol	0.31
14.20	Elemen	5.70
14.58	Alloaromadendrene oxide	1.13
14.67	Caryophyllene oxide	0.51
14.77	Veridiflorol	0.65
14.90	Globulol	1.30
14.99	Cubenol	0.28
15.14	Spathulenol	0.81
15.26	α-Guaiene	0.27
15.40	α-Eudesmol	13.2
15.55	Veridiflorol	8.43
15.66	Elemol	8.91
15.85	Isoaromadendrene epoxide	0.33
15.97	Juniper camphor	1.01
16.15	γ-himachalene	1.49
16.59	Aromadendrene oxide	0.72
16.76	(Z)-valerenyl acetate	3.38
16.91	γ-Gurjunene	2.75
17.00	Farnesene	0.23
17.22	Isospathulenol	2.06
17.65	trans-Longipinocarveol	3.03
17.94	α-copaene-11-ol	0.23
18.40	Hexadecanoic acid	0.30
19.85	Phytol	0.39
23.85	Hexadecanoic acid, methyl ester	0.54

The effects of the extracts on the enzyme activities are shown in Table 2. While CB-L and CB-nBu extracts showed an inhibitory effect on AChE enzyme activity, the same extracts activated the activity of XO and tyrosinase enzymes.

Table 2 Effects of extracts on Acetylcholine esterase (AChE), Xanthine oxidase (XO), and Tyrosinase enzymes activities.

Extracts	AChE (IC_{50})	XO (AC_{50})	Tyrosinase (AC_{50})
CB-L	460 µg/mL	604 µg/mL	250 µg/mL
CB-nBu	376 µg/mL	493 µg/mL	423 µg/mL
CB-F	-	641 µg/mL	-
CB-EA	-	-	-
CB-EO	-	-	-

The contact toxicity effects of essential oil and extracts obtained from *C. botry* plant on *S. granarius* and *T. castneum* insects after 24 hours are given in Table 3. It was determined that CB-EA extract had a mortality rate of approximately 20% against *S. granarius*, while it had a mortality rate of approximately 4.5% against *T. castneum*. However, the other extracts and essential oil showed no effect.

Table 3 Contact effect of different extracts of *C. botrys* against S. granarius and T. castneum after 24 hours.

Extracts	% Mortality±StDev	
	S. granarius	***T. castaneum***
Control	0.00±0.00b[1]	0.00±0.00b
CB-EO	0.00±0.00b	0.00±0.00b
CB-F	0.00±0.00b	0.00±0.00b
CB-EA	19.31±1.66a	4.53±3.41a
CB-nBu	0.00±0.00b	0.00±0.00b
CB-L	0.00±0.00b	0.00±0.00b

[1]Different letters in the same column indicate that the means are statistically significantly different. (Anova P<0,05, Tukey test).

4 Discussion

In studies on the essential oil analysis of the *C. botry* plant, the essential oil differs in terms of amount and composition. Bicyclic sesquiterpenoids were found in *C. botrys* (Kokanova-Nedialkova et al. 2009). The smell that gives the plant its unique smell is due to monoterpenes and sesquiterpenes (Kletter et al. 2001). As a result of *C. botrys* of GC-MS analysis; monoterpenes (camphor, δ-3-caren, fenchone, linalool, menthone, nerol, β-pinene, pulegone, terpineol-4, and thujone) and sesquiterpenes (β-elemene, elemol, and β-eudesmol) compounds, as well as mucus anserine of anserine compound. It has been found to be responsible for its aromatic, herbaceous, earthy, dull, heavy and pine-like odor (Buchbauer et al. 1995). The first essential oil analysis of the *C. botry* plant mentions the ascaridiol compound and is a bicyclic monoterpene species with a very unusual bridging peroxide functional group. It was determined that this plant species, also known as crow's feet in our country, contains the compound 2-(4a.8-dimethyl-1.2.3.4.4a.5.6.7-octahydro-naphthalen-2-yl)-prop-2-en-1-ol (Karabörklü et al. 2011). In their study conducted in Özer et al (2017) determined the essential oil content of the *C. botry* plant they collected from the provinces of Isparta, Konya and Afyon. unlike us, they determined ledol, elemol, germacrene D-4-ol and eudesm-7(11)-en-4-ol compounds as the main components. In addition, this group examined the effects of essential oils on acetylcholinesterase (AChE), butyrylcholinesterase (BChE), and tyrosinase enzymes and found a little activity against tyrosinase enzyme (Özer et al. 2017). These results are important in that they show similarities with our study results. In another study, the effect of essential oil obtained from the same plant species on three different storage pests of *T. castaneum* beetle was investigated by a fumigant effect experiment. They found a high inhibitory effect there (Kumar and Pandey 2021).

Tyrosinase, xanthine oxidase, and acetylcholinesterase are enzymes that play an important role in normal insect development. For this reason, it may be possible to control the damages that will be caused by inhibiting or activating enzymes, as disrupting the working potential will directly affect the life of the insect. Although CB-L and CB-nBu extracts are very strong, they appear to have moderate enzyme activities. With further studies, compounds that cause changes in enzyme activities can be determined. The low activity values may be due to the low amount of effective compounds.

5 Conclusion

This study is about the insecticide and enzyme activity properties of *C. botrys*, which is used for its pleasant aromatic odor and medicinal properties. Scientific studies support the medical potential of *C. botrys* in developing new drugs. Different isomers of ascaridole of different origins have been identified in *C. botrys* oil. The absence of ascaridol compound in this plant species proves that it has negative effects on both insecticide and enzyme activity. In conclusion, research into the enzyme and insecticidal properties of *C. botrys* plant extracts is important because of its potential uses in biotechnology, sustainable agriculture, pest management, and the creation of new natural products.

Acknowledgements

The authors thanks to Ali Kandemir (Erzincan Binali Yıldırım University) for his kind assistance in identifying the plant and assigning the herbarium number.

Authors' contributions:

All authors contributed equally to this work.

Conflict of interest disclosure:

No conflict of interest was declared by the authors.Citation in text

References

Ahmad NS, Farman M, Najmi MH, Mian KB, Hasan A (2008) Pharmacological basis for use of *Pistacia integerrima* leaves in hyperuricemia and gout. J Ethnopharmacol 117:478-482

Akman Y, Güney K, Ketenoğlu O, Hamzaoğlu E, Kurt L, Tuğ N (2007) Angiospermae. Palme Yayıncılık, Ankara

Alkan M, Ertürk S (2019) Insecticidal efficacy and repellency of trans-anethole against four stored-product insect pests. J Agr Sci 26(1): 64-70

Andov AL, Karapandzova M, Cvetkovikj I, Stefkov G, Kulevanova S (2014) Chemical composition of *Chenopodium botrys* L. (Chenopodiaceae) essential oil. Maced Pharm Bull 60(1): 45-51

Buchbauer G, Jirovetz L, Wasicky M, Walter J, Nikiforov A (1995) Headspace volatiles of *Chenopodium botrys* (Chenopodiaceae). J Essent Oil Res 7:305-308

Bustanji Y, Hudaib M, Tawaha K, Mohammad M, Almasri I, Hamed S (2010) In vitro xanthine oxidase inhibition by selected Jordanian medicinal plants. Jordan J Pharm Sci 4(1):49-56

Ellman GL, Courtney KD, Andres V, Feather-Stone RM (1961) A new and rapid colorimetric determination of acetylcholinesterase activity. Biochem Pharmacol 7(2): 88-95

Fagugli RM, Gentile G, Ferrara G, Brugnano R (2008) Acute renal and hepatic failure associated with allopurinol treatment. Clin Nephrol 70:523-526

Gullo VP, McAlpine J, Lam KS, Baker D, Petersen F 2006. Drug discovery from natural products. Ind Microbiol Biotechnol 33:523-31

Huang CY, Yeh TF, Hsu FL, Lin CY, Chang ST, Chang HT (2018) Xanthine oxidase inhibitory activity and thermostability of cinnamaldehyde-chemotype leaf oil of *Cinnamomum osmophloeum* microencapsulated with β-cyclodextrin. Molecules 23(5):1107

Karakoç ÖC, Gökçe A, Telci İ (2006) Fumigant activity of some plant essential oils against *Sitophilus oryzae* L., *Sitophilus granarius* L. (Col.: Curculionidae) and Acanthoscelides obtectus Say. (Col.: Bruchidae). Türk Entomol Derg 30(2):123-135

Karabörklü S, Ayvaz A, Yilmaz S, Akbulut M (2011) Chemical composition and fumigant toxicity of some essential oils against *Ephestia kuehniella*. J Econ Entomol 104:1212-1219

Kebbi S, Noman L, Demirtas I, Bensouici C, Adem S, Benayache S, Benayache F, Seghiri R, Gok M (2021). In vitro Antioxidant and Anticholinesterase Activities of Senecio massaicus Essential Oil and Its Molecular Docking Studies as a Potential Inhibitor of Covid-19 and Alzheimer's Diseases. J of Bio Act Pro from Nat, 11(4), 380-394.

Kletter C, Krichbaum M (2001) Tibetan medicinal plants. Medpharm Scientific Publishers 241-246

Kokanova-Nedialkova Z, Nedialkov PT, Nikolov SD (2009) The genus *Chenopodium*: Phytochemistry, ethnopharmacology and pharmacology. Phcog Rev 3:280-306

Kumar R, Pandey PS (2021) Insecticidal activity of essential oils against three stored product beetles in stored wheat. J Entomol Zool Stud 9(1):387-389

Liu G, Yang L, Fan T, Cong R, Tang Z, Sun W, Zhu L (2006) Purification and characterization of phenoloxidase from crab *Charybdis japonica*. Fish Shellfish Immunol 20(1):47-57

Ma C, Kanost MR (2000) A β1, 3-glucan recognition protein from an insect, *Manduca sexta*, agglutinates microorganisms and activates the phenoloxidase cascade. J Biol Chem 275(11):7505-7514

Mahboubi M, Ghazian BF, Farzin N (2011) Chemical composition and antimicrobial activity of *Chenopodium botrys* L. essential oil. J Essent Oil-Bear Plants 14(4):498-503

Mohammad MK, Almasri IM, Tawaha K, Al-Nadaf A, Hudaib M, Al-Khatib HS (2010) Antioxidant, antihyperuricemic and xanthine oxidase inhibitory activities of *Hyoscyamus reticulatus*. Pharm Biol 48:1376-1383

Morteza-Semnani K (2015) A Review on *Chenopodium botrys* L.: Traditional uses, chemical composition and biological activities. Pharm Biomed Res 1(2):1-9

Mutungi CM, Affognon H, Njoroge AW, Baributsa D, Murdock LL 2014. Storage of mung bean (*Vigna radiata* [L.] Wilczek) and pigeonpea grains (*Cajanus cajan* [L.] Millsp) in hermetic triple-layer bags stops losses caused by *Callosobruchus maculatus* (F.)(Coleoptera: Bruchidae). J Stored Prod Res 58:39-47

Ozer MS, Sarikurkcu C, Ceylan O, Akdeniz I, Tepe B (2017). A comprehensive study on chemical composition, antioxidant and enzyme inhibition activities of the essential oils of *Chenopodium botrys* collected from three different parts of Turkey. Ind Crops Prod 107:326-331

Purves D, Augustine GJ, Fitzpatrick D, Hall WC, LaMantia AS, McNamara JO, White LE (2008) Neuroscience, The 4th Edition. Sinauer Associates, Sunderland, MA, USA

Sarikurkc C, Kirkan B, Ozer MS, Ceylan O, Atilgan N, Cengiz M, Tepe B (2018) Chemical characterization and biological activity of *Onosma gigantea* extracts. Ind Crops Prod 115:323-329

Singh CB, Jayas DS, Paliwal JNDG, White NDG (2009) Detection of insect-damaged wheat kernels using near-infrared hyperspectral imaging. J Stored Prod Res 45(3):151-158

Taylor P, Camp S, Radić Z (2009) Encyclopedia of neuroscience (Squire, L.R., Editor-in-Chief). Academic Press, Elsevier Inc. pp 5–7

Tozoğlu F (2011) Erzincan kirazı (cerasus erzincanica; Ş.Yıldırımlı) sap ve tohum kısımlarının antioksidan aktivitelerinin belirlenmesi. Erzincan Üniversitesi, F Bil Ens, Erzincan, 51s. (Yüksek Lisans Tezi)

Yang Y, Wang Z, Xu SY (2005) Enzymology property of polyphenol oxidase from Lily. Sci Technol in Indust, 26:99-102

Yıldırımlı Ş (2003) The chorology of the Turkish species of Chenopodiaceae, Cistaceae, Convolvulaceae, Cornaceae and Corylaceae families. Ot Sist Bot Dergisi 10(1):203-215

Yırtıcı Ü, Ergene A, Atalar MN. Adem, Ş. (2022). Phytochemical composition, antioxidant, enzyme inhibition, antimicrobial effects, and molecular docking studies of Centaurea sivasica. S Afr J of Bot, 144, 58-71.

Wang SD, Luo WC, Xu SJ, Ding Q (2005) Inhibitory effects of 4-dodecylresorcinol on the phenoloxidase of the diamondback moth *Plutella xylostella* (L.)(Lepidoptera Plutellidae). Pestic Biochem Physiol 82(1):52-58

RESEARCH ARTICLE
Bull Biotechnol (2023) 4(1):13-16
https://doi.org/10.51539/biotech.1215927 Journal homepage: www.dergipark.org.tr/biotech

Bulletin of Biotechnology

Determination of sun protection potential of *Hibiscus rosa-sinensis* as natural additive for cosmetic industry

Ali Saglam[1], Meltem Asan-Ozusaglam[1*], Irem Celik[1]

[1]*University of Aksaray, Faculty of Science and Letters, Department of Molecular Biology and Genetic, Aksaray, Turkey

*Corresponding author : meltemozusaglam@gmail.com
Orcid No: https://orcid.org/0000-0002-3638-1306

Received : 07/12/2022
Accepted : 09/06/2023

Abstract: Harmful rays coming from the sun cause negative effects on the human body. Sunscreens and UV protective products are used to reduce and prevent these negative effects. Plants have been used in medicine and cosmetics for centuries, and have the potential to treat skin diseases. Consumers tend to use sunscreens that contain natural ingredients instead of synthetic sunscreens. In this study, the in vitro solar protection factor (SPF) values of water extracts from flowers and leaves of *Hibiscus rosa-sinensis* were investigated. The SPF values of the water extracts and commercially available cream mixtures were also examined. The SPF values of the extracts were measured at the wavelengths of 290-320 nm of UV-B ultraviolet rays reaching the earth from the sun. SPF values of *H. rosa-sinensis* flower and leaf extracts were determined as 11.77 and 22.10. The leaf extract has the highest SPF value (21.70) in 10 mL concentration among the prepared extract and cream mixtures. Therefore, *H. rosa-sinensis* extracts with high SPF values may have the potential to be used as natural additives in the cosmetic industries.

Keywords: Camellia; sun protection factor (SPF); extracts; cream.

1 Introduction

Nowadays, there is a significant increase in skin cancer caused by the harmful effects of the sun and environmental factors (Dorj et al. 2018). With the thinning of the ozone layer, harmful sun rays come directly to the earth and cause harm to people. Therefore, an increase in the incidence of skin cancer is observed (McMichael 1993; McKenzie et al. 2003). It is necessary to use sunscreens to prevent abnormalities that occur on the skin surface in varying forms and structures. Sunscreens are substances that can be applied to the skin in different ways, interfering with the sun's rays and reducing their harmful effects (Osterwalder and Lim 2007).

All rays of different wavelengths emitted from the sun are called the "electromagnetic spectrum of the sun" (Petrazzuoli 2000). UV radiation forms a specific part of the electromagnetic spectrum that has a shorter wavelength and higher energy than visible light. There are 3 types of UV of sunlight falling on the earth's surface; UVC (200-290 nm), UVB (290-320 nm), and UVA (320-400 nm). UV rays constitute 5% of the rays reaching the earth. UVA wavelength is in the range of 320-400 nm and it constitutes about 90% of UV rays. UVA rays can damage human cells by penetrating up to 100 µm deep to the skin surface. It causes sagging and wrinkles by causing loss of elasticity in human skin. Thus, it causes premature aging of the skin. UVA rays cause enzyme inactivation, protein denaturation, cell organelles and cell membrane damage (Azevedo et al. 1999). UVB is one of the ultraviolet rays reaching the surface of earth, although the majority of it is filtered by the atmosphere, with a wavelength of 290-320 nm. UVB rays are the type of rays that have the most effect on the formation of melanin pigment in the skin and sunburns (Azevedo et al. 1999). UVC is UV rays with the highest energy and lowest wavelength (200-290 nm) (Dutra et al. 2004).

Plants have historically been an important source of a wide variety of secondary metabolites used as pharmaceuticals, food additives, colours, agrochemicals, etc.(Al-Snafi 2015). *Hibiscus rosa-sinensis*, known as the Camellia, is a hairless shrub commonly grown in the tropics (Nadkarni 1996). Camellia has been used in traditional medicine to regulate menstruation and stimulate blood circulation. The flower has been used in diabetes, leprosy, regulating the menstrual cycle, liver ailments, stomachaches, cough suppressant, eye problems, miscarriage problems, and as an aphrodisiac. The leaves are used in the treatment of headache, dysentery, diarrhea, arthritis, boils and cough (Chopra and Rashid 1969; Jadhav et al. 2009; Pekamwar et al. 2013; Nath and Yaday 2015). Phytochemical analysis showed that *H. rosa-sinensis* leaf extract is rich in protein, free amino acids, carbohydrates, steroids and essential oils as well as phenolic compounds (Divya et al. 2013). The main cause of antioxidant effects in herbal products is phenolic compounds, which filter UV rays (Del Valle et al. 2020).

In the field of cosmetics, products with natural ingredients developed using plants are at the forefront. In our study, the sun protection factor (SPF) of water extracts from *H. rosa-sinensis* and commercial cream and the extract mixtures were investigated in vitro and their potential to be used as natural sunscreen additives in the cosmetic industry was determined.

2 Materials and Method

2.1 Plant Material

H. rosa-sinensis flower and leaf samples were collected from Alata Horticultural Research Institute (Mersin-Turkey) (Figure 1A.).

2.2 Preparation of Extracts

H. rosa-sinensis flower and leaf samples were dried in an airy environment and ground with a Waring-blender. For extraction, 10 g of powdered fruit sample was extracted in a hot water bath with 30 mL of water for 6 hours each day for 2 days (Figure 1B). After extraction, the solvents were evaporated. The extracts were then stored at 4°C in dry conditions until use (Figure 1C).

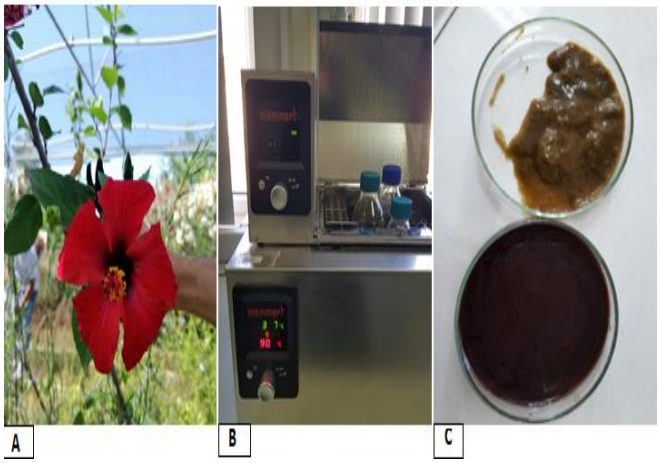

Fig. 1 *H. rosa-sinensis* (A) and Preparation of the Extracts (B-C)

2.3 Determination of SPF

H. rosa-sinensis flower and leaf water extracts (2 µg/µL) were weighed and mixed in ethanol (96%) with a vortex device until homogeneous. Then, the mixture was read in a spectrophotometer (Beckman Coulter) in the wavelength range of 290-320 nm with 3 repetitions at 5 nm intervals. The obtained values were calculated using the Mansur equation (1) (Mansur et al. 1986).

Equation 1

$$\textbf{SPF} = \text{CF x } \sum_{290}^{320} EE(\lambda)\text{x } I(\lambda)\text{x } Abs\ (\lambda)$$

2.4 Determination of SPF of Extract and Cream Mixtures

In addition to determining the SPF values of the extracts, the SPF values of the extract and cream mixture were also examined. For this purpose, the modified method was used according to Asan-Ozusaglam and Celik (2023). Commercial cream and *H. rosa-sinensis* flower or leaf extracts were mixed and the mixture was made up to final volume (10 mL) with distilled water. The prepared mixtures were diluted with ethanol (40%) to the final volume of 2.5 mL, 5 mL and 10 mL concentrations and measured in 3 replications at 5 nm intervals using a spectrophotometer (Beckman Coulter) in the wavelength range of 290 nm-320 nm. SPF values of cream and extract mixtures were calculated using the Mansur equation (1) as mentioned above.

2.3 Statistical Analysis

The SPF data of *H. rosa-sinensis* flower and leaf extracts and cream mixtures were analyzed using GNU SPSS version software. Statistical significance was confirmed by one-way analysis of variance (ANOVA) with Tukey's post-hoc test. The difference between the data was considered statistically significant at the $p<0.05$ level.

3 Results and Discussion

SPF values of *H. rosa-sinensis* flower and leaf extracts were determined in vitro spectrophotometrically. The SPF value of the leaf water extract (22.10) was found to be higher than the SPF value of the flower extract (11.77) (Table 1 and 2).

Table 1 SPF Values of Camellia Flower Water Extract

	SPF Values		
λ (nm)	**CFx EE(λ)xI(λ)x Ab (λ)1**	**CFx EE(λ)xI(λ)x Ab (λ)2**	**CFx EE(λ)xI(λ)x Ab (λ)3**
290	0.28	0.23	0.24
295	1.18	1.08	1.23
300	3.71	3.51	3.70
305	3.74	3.53	3.82
310	2.01	1.90	2.02
315	0.88	0.83	0.88
320	0.18	0.17	0.19
Total SPF	**11.98**	**11.25**	**12.08**
Mean±SD	**11.77±0.46**		

Table 2 SPF Values of Camellia Leaf Water Extract

	SPF Values		
λ (nm)	**CFx EE(λ)xI(λ)x Ab (λ)1**	**CFx EE(λ)xI(λ)x Ab (λ)2**	**CFx EE(λ)xI(λ)x Ab (λ)3**
290	0.34	0.36	0.35
295	1.83	1.85	1.83
300	6.36	6.43	6.46
305	7.11	7.17	7.21
310	4.05	4.09	4.11
315	1.85	1.86	1.86
320	0.40	0.40	0.40
Total SPF	**21.94**	**22.16**	**22.22**
Mean±SD	**22.10±0.15**		

After determining the SPF values of the extracts alone, they were mixed with commercial cream and then the SPF values of the cream-mixture were evaluated. The results are given in Figure 2. The SPF value of the commercial cream as a control was also determined. Cream mixtures with *H. rosa-sinensis* flower and leaf water extracts showed higher SPF values at 10 mL concentration (20.67 and 21.70) compared to the control group (1.26).

Lokapure et al. (2014) determined the SPF value of the extracts from *H. rosa-sinensis* flower with 90% ethanol and the SPF value of the extract gel mixtures. They determined the SPF value of *H. rosa-sinensis* flower extract as 3.88±0.01 and the SPF value of flower extract-gel mixtures as 12.54±0.05. In another study using the extract of *H. rosa-sinensis* flower obtained with 90% ethanol, the UV absorption value of the extract was determined in the range of 200 nm – 400 nm. The results indicated that it has very high absorption (1.26) at 200 nm, high absorption at 280 nm (0.3), and moderate absorption (0.2-0.1) ability above 300 nm (Sidram et al. 2011). Dwivedi (2022) determined the SPF value of 40 µg/mL – 50 µg/mL – 60 µg/mL concentrations of *H. rosa-sinensis* flower extract obtained with 80% ethanol. The SPF values were found as 0.565, 0.691, 0.974, respectively. The differences between the results obtained in the current study and those of the literature may be due to many factors such as the solvent used in the extraction, the extraction method or the growing conditions of plant (Osorio-Tobón 2020).

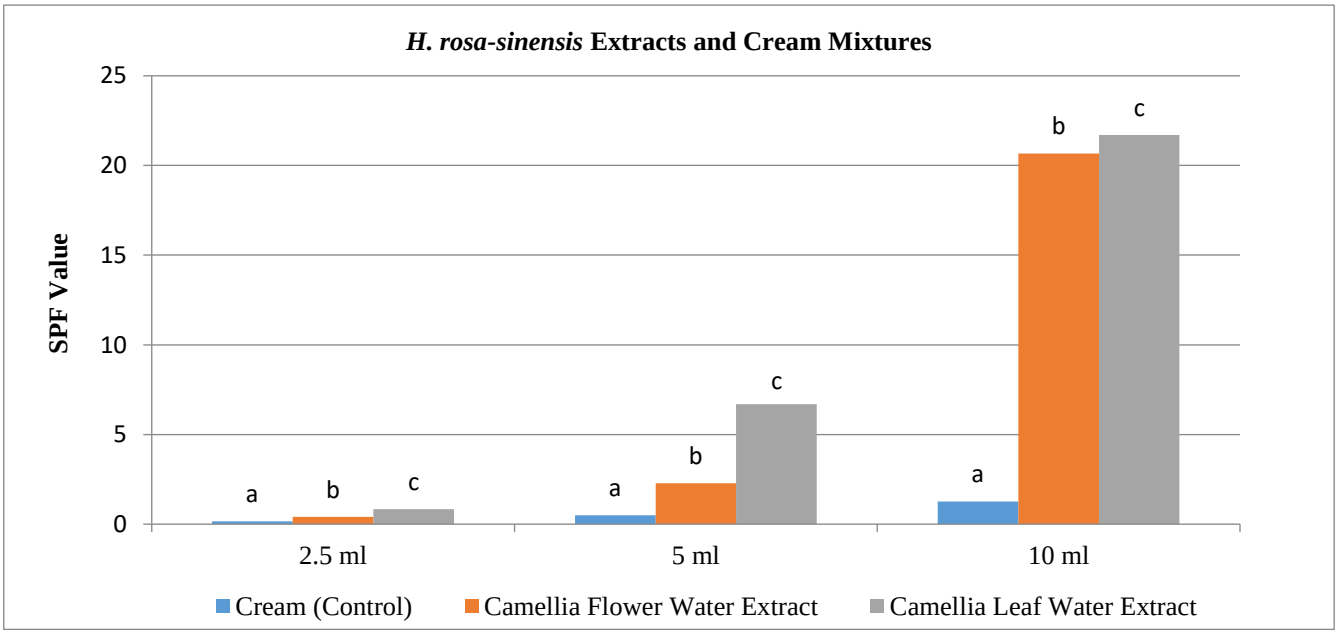

Fig. 2 SPF Values of *H. rosa-sinensis* Flower and Leaf Extracts and Cream Mixture
Different letters indicate significant difference at $p<0.05$ between samples.

5 Conclusion

Recent studies have shown that most synthetic sunscreens have adverse effects on the skin. Using the sun protection properties of plant extracts, cost-effective and readily available natural preservatives can be obtained. In the current study, UV absorption capacities and sun protection properties of water extracts obtained from *H. rosa-sinensis* flowers and leaves were determined. *H. rosa-sinensis* water extracts with high SPF values may have the potential to be used as natural sunscreen additives in the cosmetic industry. Therefore, the Camellia water extracts may be safer and cheaper alternative sources for the cosmetic industry after further in vivo studies.

Authors' contributions: The authors were equally contributed in writing the manuscript and are equally responsible for plagiarism.

References

Al-Snafi AE (2015) Therapeutic properties of medicinal plants: a review of their detoxification capacity and protective effects (part 1). Asian J Pharmaceut Sci Techol 5(4): 257-270

Asan-Ozusaglam M, Celik I (2023) White pitahaya as a natural additive: potential usage in cosmetic industry. Foods Raw Mater 11(1): 57-63

Azevedo JS, Viana Jr NS, Vianna Soares CD (1999) UVA/UVB sunscreen determination by second-order derivative ultraviolet spectrophotometry. Il Farmaco 54(9): 573-578

Chopra RN, Rashid A (1969) The archegonia of Splachnobryum. Bryologist 72(4): 525-527

Del Valle JC, Buide ML, Whittall JB, Valladares F, Narbona E (2020) UV radiation increases phenolic compound protection but decreases reproduction in *Silene littorea*. *PloS one*, 15(6): e0231611

Divya MJ, Sowmia C, Dhanya KP, & Joona K (2013) Screening of antioxidant, anticancer activity and phytochemicals in methanolic extract of *Hibiscus rosa-sinensis* leaf extract. Res J Pharm Biol Chem Sci 4(2): 1308-1316

Dorj UO, Lee KK, Choi JY, Lee M (2018) The skin cancer classification using deep convolutional neural network. Multimed Tools Appl 77(8): 9909-9924

Dutra EA, Kedor-Hackmann ERM, Santoro MIRM (2004) Determination of sun protection factor (SPF) of sunscreens by ultraviolet spectrophotometry. Rev Bras Ciênc Farm 40(3): 381-385

Dwivedi AK, (2022) Spectrophotometric Determination of Sun Screen Potential of Selected Medicinal Plants. Int J Pharm Sci Rev Res 74(2): 104-107

Jadhav VM, Thorat RM, Kadam VJ, Sathe NS (2009) Traditional medicinal uses of *Hibiscus rosa-sinensis*. J Pharm Res 2(8): 1220-1222

Lokapure SG, Patil SS, Phutane KR, Mohite SK, Magdum CS (2014) In vitro Evaluation of Sun Protection factor and Diffusion study of *Hibiscus rosa-sinensis* L flower Extract Gel. Res J Pharm Technol 7(6): 643-647

Mansur JS, Breder MNR, Mansur MCA, Azulay RD (1986) Determinação do fator de proteção solarpor espectrofotometria. An Bras Dermatol 61: 121-124

McKenzie RL, Björn LO, Bais A, Ilyasd M (2003) Changes in biologically active ultraviolet radiation reaching the Earth's surface. Photochem Photobiol Sci 2(1): 5-15

McMichael AJ (1993) Planetary overload: global environmental change and the health of the human species. Cambridge University Press. pp 186-191

Nadkarni KM (1996) [Indian materia medica]; Dr. KM Nadkarni's Indian materia medica: with Ayurvedic, Unani-Tibbi, Siddha, allopathic, homeopathic, naturopathic & home remedies, appendices & indexes. 1 (Vol. 1). Popular Prakashan

Nath P, Yadav AK (2015) Acute and sub-acute oral toxicity assessment of the methanolic extract from leaves of *Hibiscus rosa-sinensis* L. in mice. J Intercult Ethnopharmacol 4(1): 70-73

Osorio-Tobón JF (2020). Recent advances and comparisons of conventional and alternative extraction techniques of phenolic compounds. J Food Sci Technol 57(12): 4299–4315

Osterwalder U, Lim HW (2007) Novel developments in photoprotection: Part I. In Photodermatology CRC Press. pp 279-296

Pekamwar SS, Kalyankar TM, Jadhav AC (2013) *Hibiscus rosa-sinensis*: a review on ornamental plant. World J Pharm Pharm Sci (WJPPS) 2(6): 4719-4727

Petrazzuoli M (2000) Advances in sunscreens. Curr Probl Dermatol 12(6): 287-290

Sidram AN, Lokapure SG, Kalyane NV (2011) Study on anti-solar activity of ethanolic extract of flower of *Hibiscus Rosa-sinensis* Linn. Research J Pharm and Tech 4(3): 472-473

RESEARCH ARTICLE
Bull Biotechnol (2023) 4(1):17-29
https://doi.org/10.51539/biotech.1262979 Journal homepage: www.dergipark.org.tr/biotech

Bulletin of Biotechnology

Functional and structural identification of iron-binding proteins on tomato (*Solanum lycopersicum* L.) proteome via *in silico* approaches

Yiğit Küçükçobanoğlu[1*], Lale Yıldız Aktaş[1]

[*1]*Department of Biology, Faculty of Science, Ege University, İzmir, Turkey*

*Corresponding author : y.kucukcobanoglu@gmail.com
Orcid No: https://orcid.org/0000-0002-9856-5506

Received : 10/03/2023
Accepted : 09/06/2023

Abstract: Iron-plant interactions have crucial roles in crop production growth and development. In this study, we have analyzed the whole proteome of tomato (*Solanum lycopersicum* L.) plants for iron-binding proteins. A total of 213 iron-binding protein candidates were identified in the study. Out of these 213 proteins, 45 were selected for modeling and validated with a high confidence level by using different computational analyses. Results showed that Glu, Cys, Asp, and His amino acid residues were indicators of iron-binding proteins. Besides, mechanistic insights of iron-binding proteins were analyzed by molecular dynamics simulations. Simulation results proved the conformational stabilization of proteins. Validated proteins were further analyzed for subcellular localization, clustered for molecular functions and biological processes. According to the results, iron-binding proteins were mostly located in the chloroplast. Also, these proteins are involved in different molecular and biological roles ranging from oxidation-reduction processes and electron transport chain to protein repair mechanisms. This report provides structural and functional properties of iron-binding proteins for tomato proteome. The study may assist in future research on plant physiology, protein engineering, or bioengineering.

Keywords: iron-binding proteins; tomato; structural bioinformatics; functional analysis; three-dimensional modeling

1 Introduction

Metal ions have a vital role in biological reactions, including photosynthesis, respiration, and water oxidation in living organisms (Lu et al. 2013). The importance of metal ions in these processes comes forward due to their ability to bind proteins. (Garcia et al. 2006). Among metals, iron (Fe) (an essential micronutrient for plants) has roles in several processes like photosynthesis, respiration, or DNA synthesis on plant growth and development (Briat et al. 1995). Different oxidation states of Fe exist in nature, like reduced ferrous (Fe^{+2}) or oxidized ferric (Fe^{+3}) (Pehkonen, 1995). Iron-binding proteins are essential cofactors for the plant cells (Andreini et al. 2017). Iron-binding proteins are a component of chloroplast proteins like Rieske proteins, which have a crucial role in photosynthesis (Allen, 2004; Briat et al. 2007). Furthermore, iron-binding proteins take charge of DNA metabolism or protein translation metabolic pathways (Braymer and Lill 2017).

Metalloproteins (proteins that contain metal ions) are important protein classes with their catalytic, regulatory, or structural roles via metal atoms (Shi and Chance, 2008). In the last decades, several analysis techniques have been used to investigate metalloproteins based on mass spectrometry like inductively coupled plasma-mass spectrometry (ICP-MS) (Pröfrock and Prange 2012), nuclear analytical techniques like high-resolution spatial speciation analysis by synchrotron radiation X-ray fluorescence (SR-XRF) (Pushie et al. 2014), or affinity techniques like immobilized metal affinity chromatography (IMAC) (Chang et al. 2017). However, these analytical techniques have limitations due to time-consuming processes for sample preparation and data acquisition. Additionally, these techniques are expensive for instrumentation and chemical supply. Given all these disadvantages, using new approaches such as computational biology has become inevitable to focus on these significant proteins.

Nowadays, developments based on bioinformatics make it feasible to analyze big data of the whole genome or proteome. Iron-binding proteins can be identified, modeled, or functionally analyzed using bioinformatics tools for plant proteomes. Iron-binding sites of proteins can be analyzed by using protein sequences or structures with online tools like MetalPredator (Valasatava et al. 2016), MetSite (Sodhi et al. 2004), MetalloPred (Naik et al. 2011), or IonCom (Hu et al. 2016). Besides, there are various bioinformatic tools available like MetalS^2 (Andreini et al. 2013), MetalS^3 (Valasatava et al.

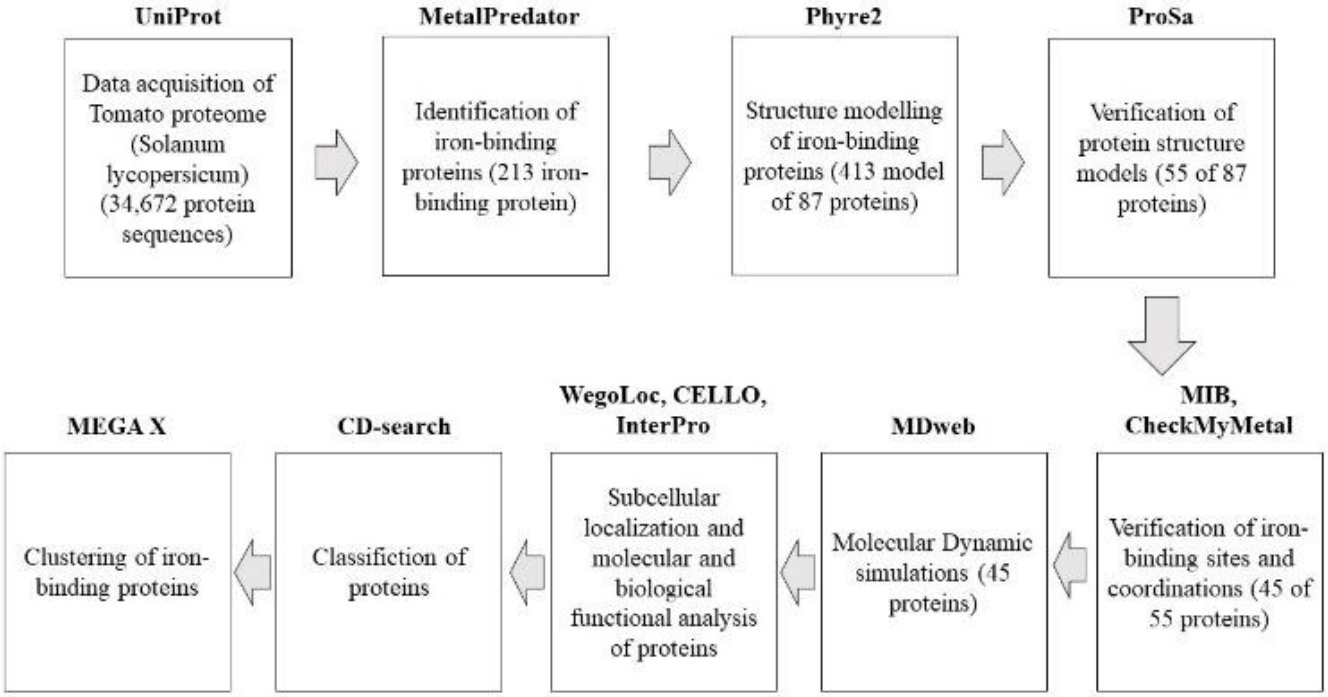

Fig. 1 Schematic demonstration of the analysis workflow for identifying and classifying iron-binding proteins from the tomato proteome

2014), MIonSite (Qiao and Xie 2019), MetalDetector V2.0 (Passerini et al. 2011), CheckMyMetal (CMM) (Zheng et al. 2017). The interaction of binding sites of metalloproteins with transition metals like iron, zinc, copper, manganese, and cadmium makes them possible to identify by using sequence or structural information of proteins via bioinformatic tools. In addition, the MetalPredator tool is a specified tool for finding iron-binding proteins using Hidden Markov Model profiles (HMM) and structural motif bindings of iron (Valasatava et al. 2016). *Xanthomonas translucens* pv. *Undulosa* proteome was analyzed for iron-binding proteins, and ~9.8% of the proteome had iron-binding protein motifs using *in silico* approaches. These proteins had different functions like transport or carbohydrate metabolism (Sharma et al. 2017). In another research, iron-binding proteins of wheat proteome were analyzed, and results showed that iron-binding proteins were involved in 21% of biological processes and 39% of molecular functions (Verma et al. 2017).

Tomato (*Solanum lycopersicum* L.) is included in the Solanaceae family, which contains most of the economic crops like potato or pepper. With over 10000 cultivars, tomato is cultivated in a 5 million ha area, and its production was estimated at 180 million tons worldwide in 2019 (FAO, 2020). Due to the importance of tomato crop production, understanding the interactions between iron metal ions and tomato proteome can benefit crop growth and development.

The literature review showed no research on iron-binding proteins on the whole tomato (*S. lycopersicum*) proteome. This study aimed at identifying, classifying, and 3D modeling the iron-binding proteins on tomato proteome using *in silico* analyses. A summarized scheme of the workflow is illustrated in Fig. 1. The results highlight the understanding of the functions of iron-binding proteins in tomato, which could be beneficial for new challenges for tomato crop growth and development. Also, these results can offer different approaches to iron-related nutrient management for crop production.

2 Materials and Method

2.1 Dataset acquisition of tomato (*S. lycopersicum*) proteome

Tomato (*S. lycopersicum*) proteome has 34672 proteins based on UniProt database as reference proteome (Proteome ID: UP000004994). The protein sequence dataset of the whole tomato proteome was downloaded in FASTA format from the UniProt database (https://www.uniprot.org/proteomes/UP000004994).

2.2 Identification of iron-binding proteins

The whole proteome sequence dataset of tomato was analyzed using an online MetalPredator program to identify iron-binding proteins (Valasatava et al. 2016). MetalPredator identifies proteins using Pfam domains and iron-binding motifs called Minimal Functional sites (MFSs) with e-value lower than 10^{-3}.

2.3 Modeling structures of iron-binding proteins

Three-dimensional (3D) structures of identified iron-binding proteins were modeled using online Protein Homology/Analogy Recognition Engine V2.0 (Phyre2) software. Phyre2 is a sequence-based modeling program for protein 3D structures that uses advanced remote homology (Kelley et al. 2015). Modeled 3D structures were selected according to the criteria: confidence ≥ 90%, query ≥ 50%, and identification ≥ 30%. Filtered structures quality was verified by the ProSA-web program using structure templates (Wiederstein and Sippl, 2007). ProSA-web program verifies models by z-scores depending on C^{α} potentials of protein structure coordinates.

2.4 Determination of iron-binding sites on verified protein models

Verified 3D models of iron-binding proteins were analyzed using Metal Ion-Binding site prediction and docking server (MIB) to identify Fe^{2+} and Fe^{3+} binding structure models (Lin et al. 2016). MIB analyses were based on the fragment transformation method using structure models, and the tool aligns the structure to metal ion binding residues. The results were analyzed depending on the alignment scores of iron-binding motifs.

CheckMyMetal (CMM) program was used for both validation and coordination geometries of iron-binding sites on protein structures (Zheng et al. 2017). The CMM program can evaluate structures for geometrical and other irregularities in iron-binding sites with different parameters such as bond valences or metal-binding sites. Three-dimensional protein structures were visualized using Mol* 3D viewer (Sehnal et al. 2021).

2.5 Molecular dynamics simulations of iron-binding proteins

Iron-binding structure models of iron-binding proteins were analyzed via MDweb server for molecular dynamics (MD) simulations (Hospital et al. 2012). MDweb server can perform MD simulations using different algorithms like AMBER, GROMACS, or NAMD. In our study, AMBER Full MD setup -ff99SB* (Hornak & Simmerling, including Best &Hummer psi modification)- toolkit was used for setup, solvation, and equilibration. In this toolkit, sodium ions have been used for neutralization, and octahedron box of TIP3P water molecules with a spacing distance of 15 Å was used for solvation. The energy minimization of the structure was completed in 500 steps of the conjugate gradient with a force constant of 50Kcal/mol. The equilibration step was started with heating solvent to 300k, then continued with reducing the force constant respectively 5.0 Kcal/mol, 2.5 Kcal/mol, 1 Kcal/mol, and finally completed by simulation without restrains. Simple box solvent molecular dynamics simulations were performed via a constant Number of particles, Pressure, and Temperature (NPT) with 2.0 fs time steps, 2.5 ps total time, 300k temperature, and 50 output frequency steps. For the results, the root mean square deviation (RMSD) was determined for protein backbone residues and ligands.

2.6 Subcellular localization, molecular functions, and biological process analysis of iron-binding proteins

Cellular and subcellular localization of iron-binding proteins were analyzed by using weighted gene ontology term-based subcellular localization prediction (WegoLog) (Chi and Nam, 2012) and subcellular localization predictor (CELLO V2.5) web tools (Yu et al. 2006). Both web tools are used for analyzing sequence similarity and gene ontology information to predict the subcellular localization of proteins based on a support vector machine (SVM) classifier. But tools have been using different datasets to analyze localization, such as BaCello dataset for WegoLoc and Park and Kneisha dataset for Cello.

Functional analysis of identified and verified iron-binding proteins was performed using online InterPro software, which classifies proteins into families and predicts domains and important sites (Blum et al. 2021). The program uses predictive models known as signatures and classifies proteins for subcellular localization, biological processes, and molecular functions.

2.7 Classification and clustering of iron-binding proteins

The identified 55 iron-binding proteins were classified for functional domains using the Conserved Domain Database (CDD) tool on the National Centre for Biological Institute database (Marchler-Bauer et al. 2010). CDD search tool classification analysis was performed for the criteria: CDD–58235 position-specific scoring matrix (PSSM) database with an expectation value (e-value) of 0.01.

Iron-binding protein sequences were clustered using the maximum parsimony method with 2000 bootstrap replications of the Subtree-Pruning-Regrafting (SPR) algorithm in the MEGA X program (Kumar et al. 2018). The phylogenetic tree was visualized using the EvolView v3 web tool (Subramanian et al. 2019).

3 Results

3.1 Identification and structure modeling of iron-binding proteins on tomato proteome

The tomato proteome dataset, which includes 34672 protein sequences, was retrieved from the UniProt database. The proteome dataset was analyzed to determine iron-binding proteins via MFSs using the MetalPredator program. Approximately 0.6% of whole tomato proteome, corresponding to 213 proteins, were identified as iron-binding proteins depending on Pfam patterns on minimal functional sites of proteins. Potential 213 iron-binding proteins have been 3D modeled using protein sequences on Phyre2 software. The 3D protein structure modeling results showed 413 candidate models for 87 protein sequences. The candidate protein models were filtered according to the criteria: confidence ≥ 90%, query ≥ 50%, and identification ≥ 30%. Filtered models were selected for structure quality analysis. Finally, filtered structure model quality was verified by the ProSA-web program depending on the z-scores of structure models (Supplementary Table S1). Results have shown that the ProSA-web program verified 55 protein structures.

3.2 Determination of iron-binding sites on verified protein models

The selected 55 iron-binding protein models were analyzed using the MIB program to identify both Fe^{2+} and Fe^{3+} binding motifs on 3D protein structures. Iron had two convertible oxidation states, Fe^{2+} and Fe^{3+}, involved in different biochemical pathways. MIB program analyses were based on protein structures and used to predict iron-binding residues. The results showed that 50 of 55 identified proteins were modeled and could bind both Fe^{2+} and Fe^{3+} (Supplementary Table S2). Glutamic acid (Glu), Cysteine (Cys), Aspartic acid (Asp), and Histidine (His) amino acids residues were involved in the iron bindings of proteins, and the distribution of iron-binding amino acid residues was shown in Fig. 2. According to the results, Fe^{2+} binding residues were determined as 37 Cys, 21 Glu, 19 Asp, 19 His, 5 Asn, and 4 Ala, while Fe^{3+} binding residues were 33 Cys, 32 Glu, 16 Asp, 11 His, 4 Gln, and 2 Ala amino acids. The binding residues of each iron-binding protein were addressed in Supplementary Table S2

Validation and coordination geometry analyses of iron-binding protein structures were performed by using CheckMyMetal (CMM) web tool. Results showed that 45 of 50 iron-binding proteins were verified at a high confidence level, 42 Fe^{2+} binding sites and 41 Fe^{3+} binding sites were determined with various geometries on iron-binding proteins. Coordination geometries of many iron-binding protein structures were classified as freely bound. These structures did not show any coordination geometry with iron ions because the poor coordination caused deviation from the ideal geometry. Besides, different coordination geometries like square planar, trigonal planar, trigonal bipyramidal, or tetrahedral by CMM analysis were observed. Fe^{2+} binding protein geometries indicated 20 poorly coordinated, 12 free coordination, 8 square planar coordination, and 2 tetrahedral coordination. Also, Fe^{3+} binding protein geometries revealed 17 free coordination, 16 poorly coordinated, 3 square planar coordination, 2 tetrahedral and trigonal bipyramidal coordination, and 1 trigonal planar coordination (Supplementary Table S3). Selected 3D structure images of iron-binding proteins were illustrated in Fig. 3.

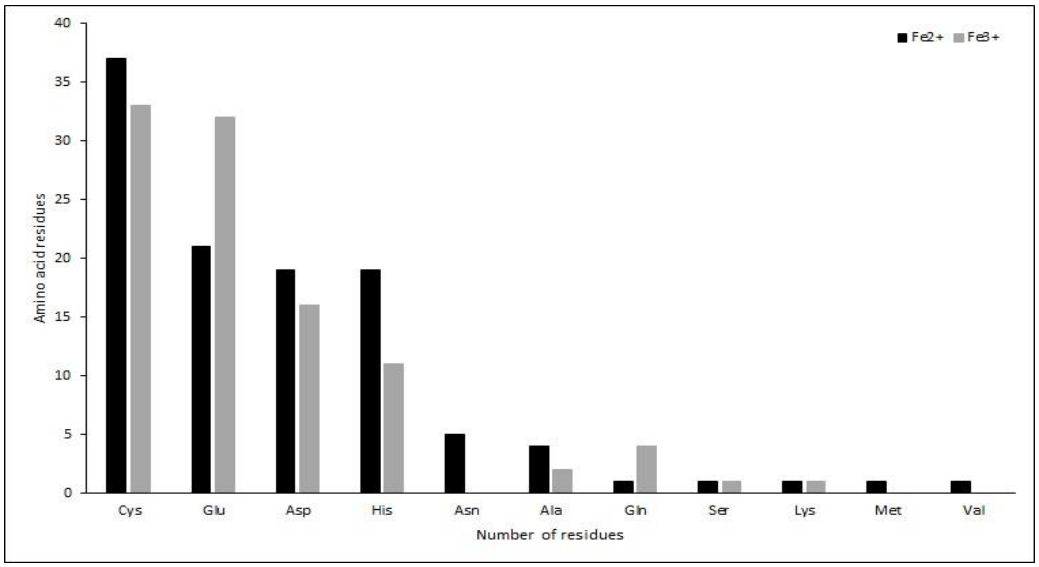

Fig. 2 Distribution of iron-binding amino acid residues

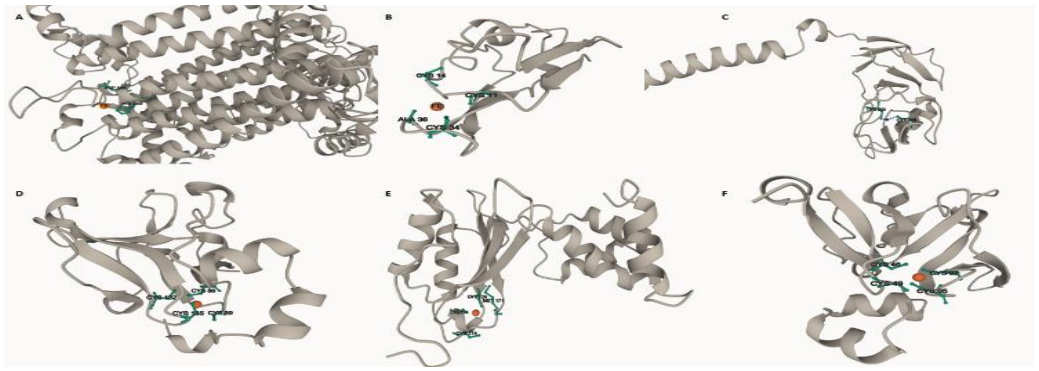

Fig. 3 Visualization of iron-binding proteins in three dimensional structures and coordination geometries; A)sp|Q2MIA0|PSAA_SOLLC protein Fe^{2+} square planar coordination geometry, B)sp|Q2MI49|PSAC_SOLLC protein Fe^{3+} square planar coordination geometry, C)tr|A0A3Q7JLM2|A0A3Q7JLM2_SOLLC protein Fe^{3+} trigonal planar coordination geometry, D)tr|A0A3Q7ERR3|A0A3Q7ERR3_SOLLC protein Fe^{3+} trigonal bipyramidal coordination geometry, E)tr|A0A3Q7I5P3|A0A3Q7I5P3_SOLLC protein Fe^{2+} tetrahedral coordination geometry, F)tr|A0A3Q7EI02|A0A3Q7EI02_SOLLC protein Fe^{3+} tetrahedral coordination geometry

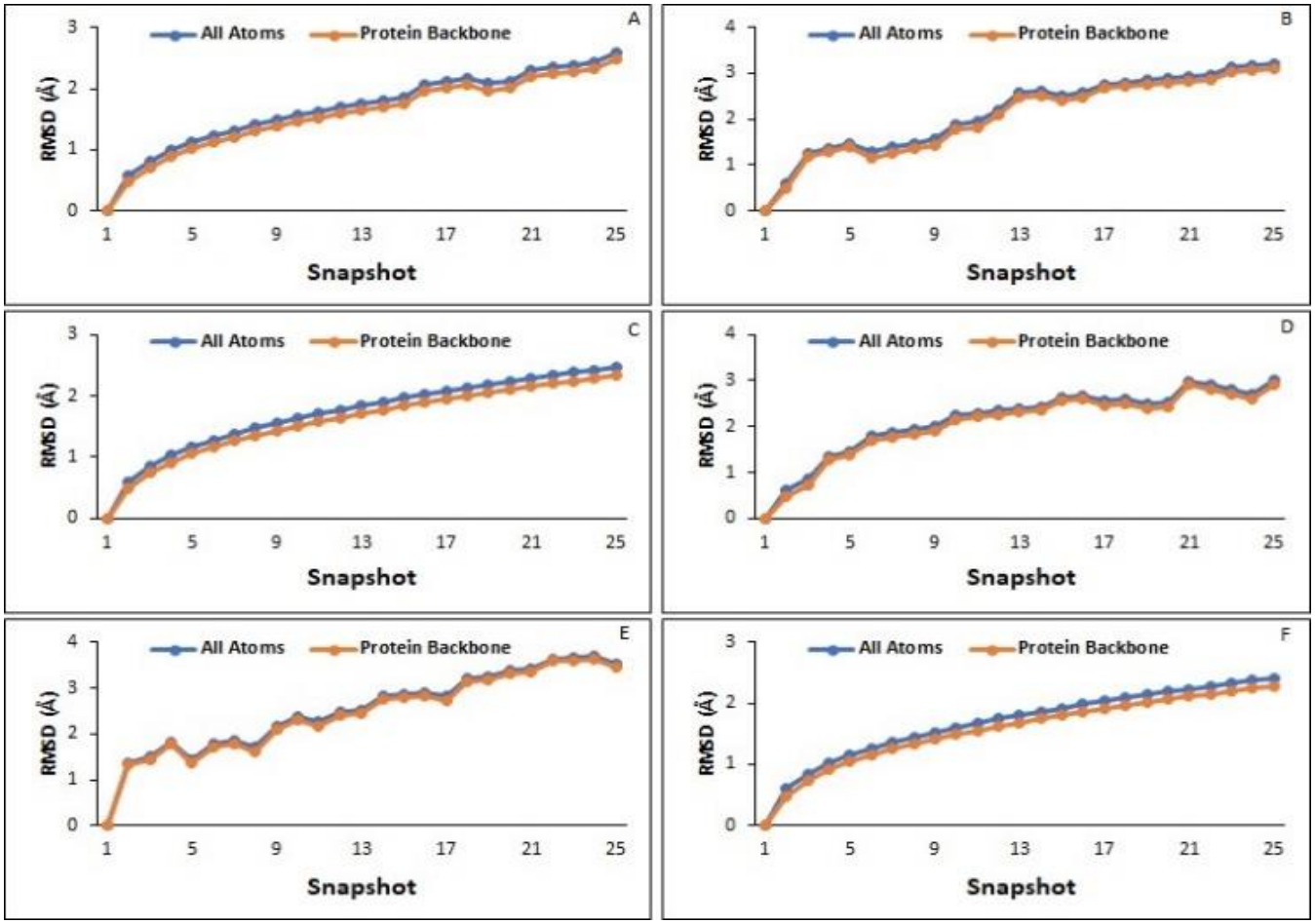

Fig. 4 RMSD results of iron-binding proteins A)sp|Q2MIA0|PSAA_SOLLC Fe^{2+}, B)sp|Q2MI49|PSAC_SOLLC Fe^{3+}, C)tr|A0A3Q7JLM2|A0A3Q7JLM2_SOLLC Fe^{3+}, D)tr|A0A3Q7ERR3|A0A3Q7ERR3_SOLLC Fe^{3+}, E)tr|A0A3Q7I5P3|A0A3Q7I5P3_SOLLC Fe^{2+}, F)tr|A0A3Q7EI02|A0A3Q7EI02_SOLLC Fe^{3+}

3.3 Molecular dynamics simulations of iron-binding proteins

After the iron-binding site verification at 45 iron-binding proteins, docked structures for both Fe^{2+} and Fe^{3+} via MIB have been selected for MD simulations. MD simulations were performed to investigate the mechanistic insight of iron-binding proteins. Structural changes of proteins were determined using RMSD analysis for 25 snapshots. Results showed that the time evolution of average RMSD values on all proteins varied between 1,626 Å - 2,994 Å for Fe^{2+} and 1,626 Å - 2,140 Å for Fe^{3+} (Supplementary Table S4). The time-course changes of RMSD distribution plots for selected proteins compared to protein backbones were shown in Fig. 4. According to the MD simulation results, iron-protein binding structures achieved stable conformations in the simulations.

3.4 Subcellular localization, molecular functions, and biological process analysis of iron-binding proteins

The remaining 45 proteins with high confidence levels were analyzed to determine subcellular localization, molecular function, and biological process. Subcellular localization analyses were completed using WegoLoc and CELLO v2.5 web tools. Cellular components, molecular functions, and biological processes were analyzed using the InterPro web tool. Subcellular localization of iron-binding proteins analyzed via WegoLoc showed that proteins were localized in the chloroplast (33%), cytoplasm (31%), mitochondrion (29%), and nucleus (7%) (Fig. 5a). CELLO v2.5 analysis results showed that subcellular localizations of the iron-binding proteins were chloroplastic (33%), nuclear (24%), mitochondrial (20%), cytoplasmic (9%) extracellular (7%), and plasma membranal (7%) (Fig. 5b). Total 16 protein was found as consistent localizations for both WegoLoc and CELLO v2.5 programs (Supplementary Table S5).

Molecular and functional analyses of iron-binding proteins were performed using InterPro web tool. Results showed that analyzed iron-binding proteins were involved in 51 biological processes, 128 molecular functions, and 15 cellular components. iron-binding proteins were checked for their implication in biological processes showing that a large part was related to oxidation-reduction processes and electron transport chain (14%), and tricarboxylic acid cycle (8%). Other functions (6%) were determined as protein repair, oxidative stress, rRNA processing, rRNA methylation, tRNA methylation, and photosynthesis. Also, a small part of the proteins belonged to another 11 processes with different rates like DNA repair (4%) or tRNA modification (2%) (Fig. 6).

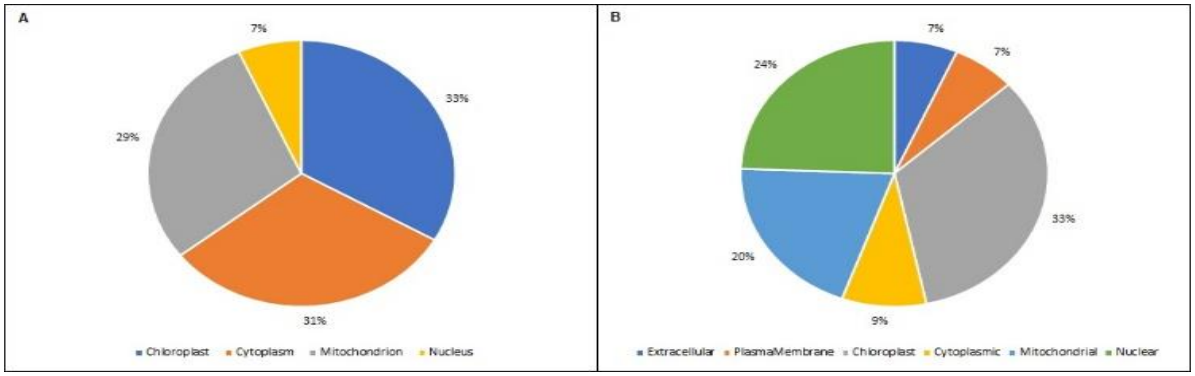

Fig. 5 Subcellular localization of iron-binding proteins; A) WegoLoc analysis, B) CELLO v2.5 analysis

Molecular functions of iron-binding proteins were mostly classified as 20% iron-sulfur cluster binding, 13% electron transfer activity, and 11% for 2 iron-2 sulfur (2Fe-2S) cluster binding. The other molecular functions were 9% catalytic activity, 7% oxidoreductase activity, and 6% iron 4 sulfur cluster binding (Fig. 7).

In addition, the analyzed iron-binding proteins were joined into cellular components. Most of the proteins were part of membranes (20%). Other proteins were determined as components at photosystems I, thylakoid, integral components of membranes, and nucleus (13%). A small part of the proteins were components of the thylakoid membrane, chloroplast, mitochondrion, and molybdopterin synthase complex (7%) (Fig. 8).

3.5 Classification and clustering of iron-binding proteins

Selected high confidence level 45 iron-binding proteins were classified for functional domains using the CDD search tool. These functionally classified proteins were clustered using the maximum parsimony method with 2000 bootstrap on the MEGA X program. iron-binding proteins were classified into 28 superfamily categories, which were assembled into 15 categories depending on their biological or molecular functions. These categories were oxidation-reduction, protein repair, posttranslational modifications, gene regulation, metal-ion binding, DNA binding, rRNA processing, ATP metabolism, translation, tRNA modification, DNA repair, electron transfer, photosynthesis mechanisms, and reductase and transferase activities (Fig. 9).

The roles of iron-binding proteins were demonstrated through ferredoxin in electron transfer, succinate dehydrogenase in oxidation-reduction processes, Rieske in photosynthesis, and thioredoxin in gene regulation (Supplementary Table 1). All the identified iron-binding proteins were associated with important roles in different metabolic pathways of tomato plants.

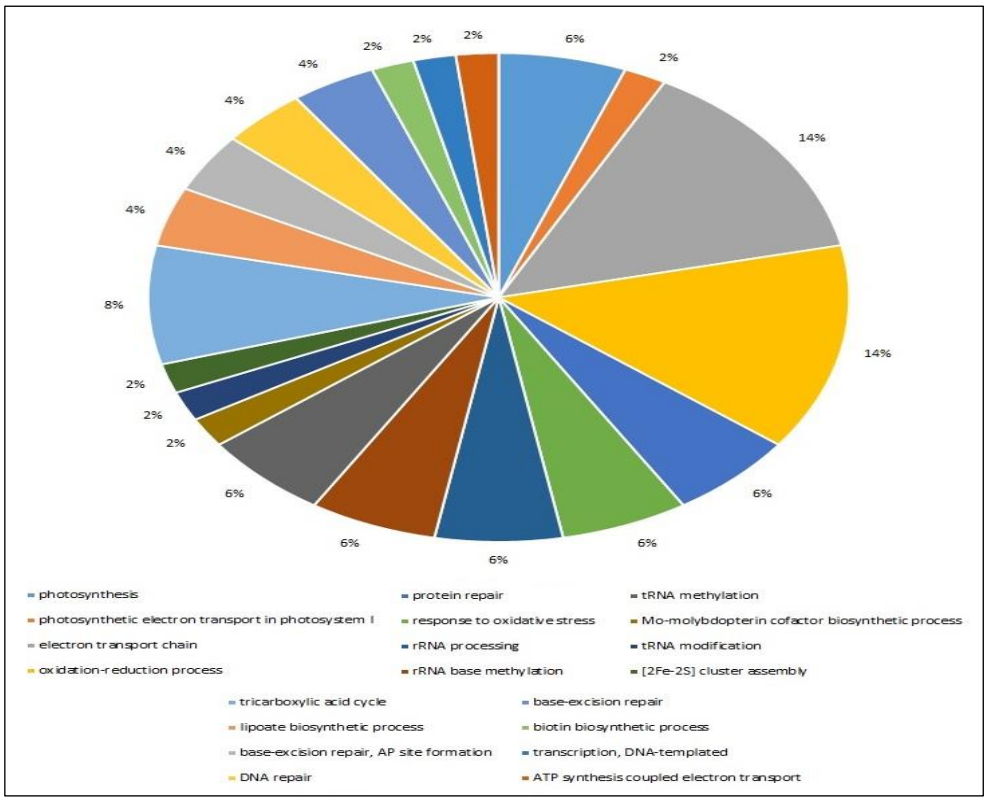

Fig. 6 Biological processes involving iron-binding proteins

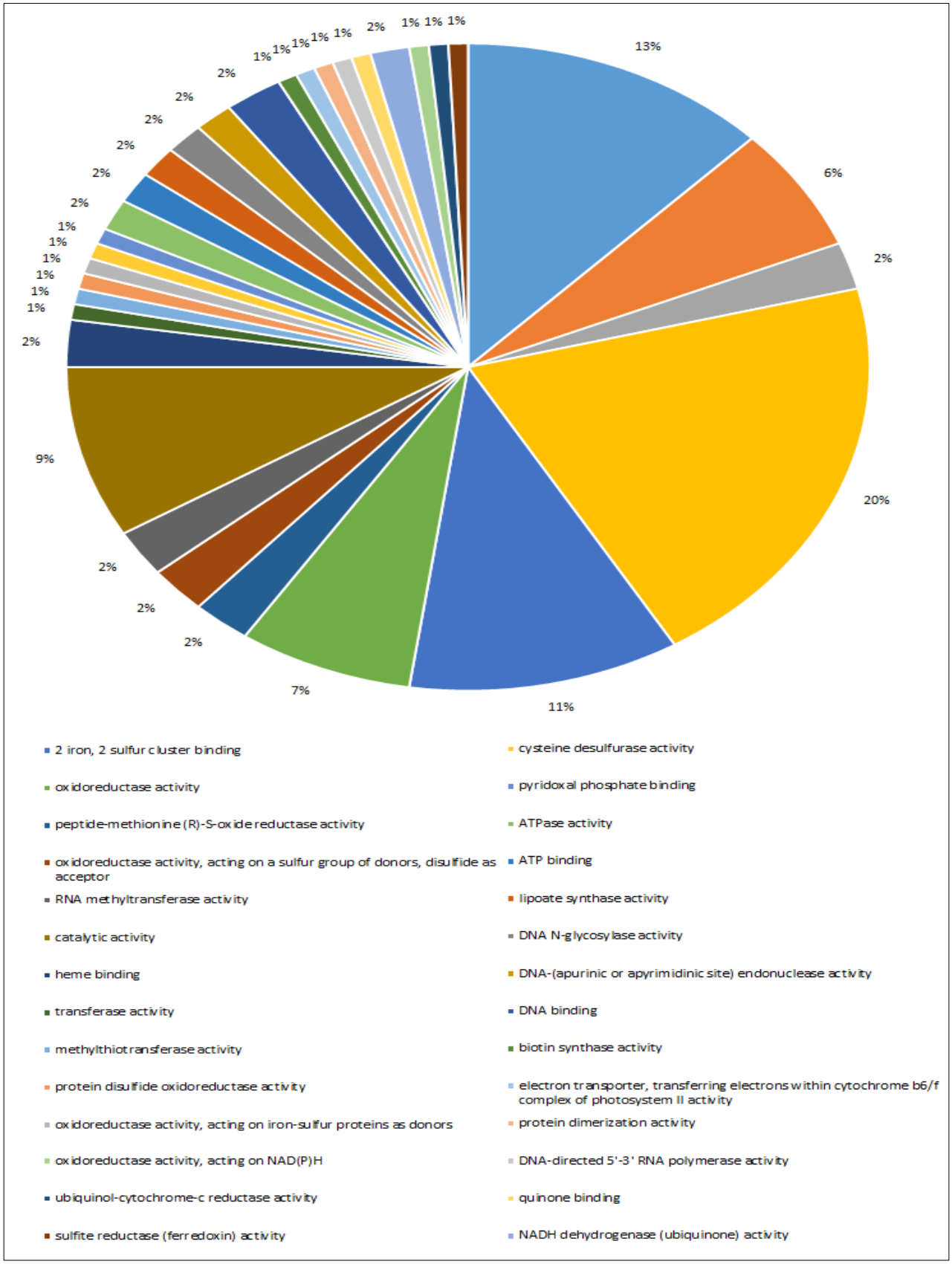

Fig. 7 Molecular functions involving iron-binding proteins

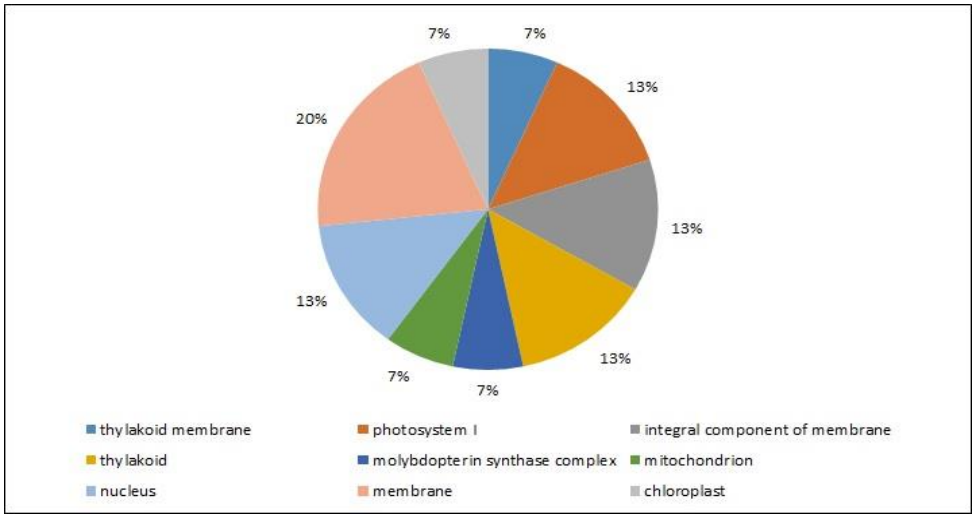

Fig. 8 Cellular components involving iron-binding proteins

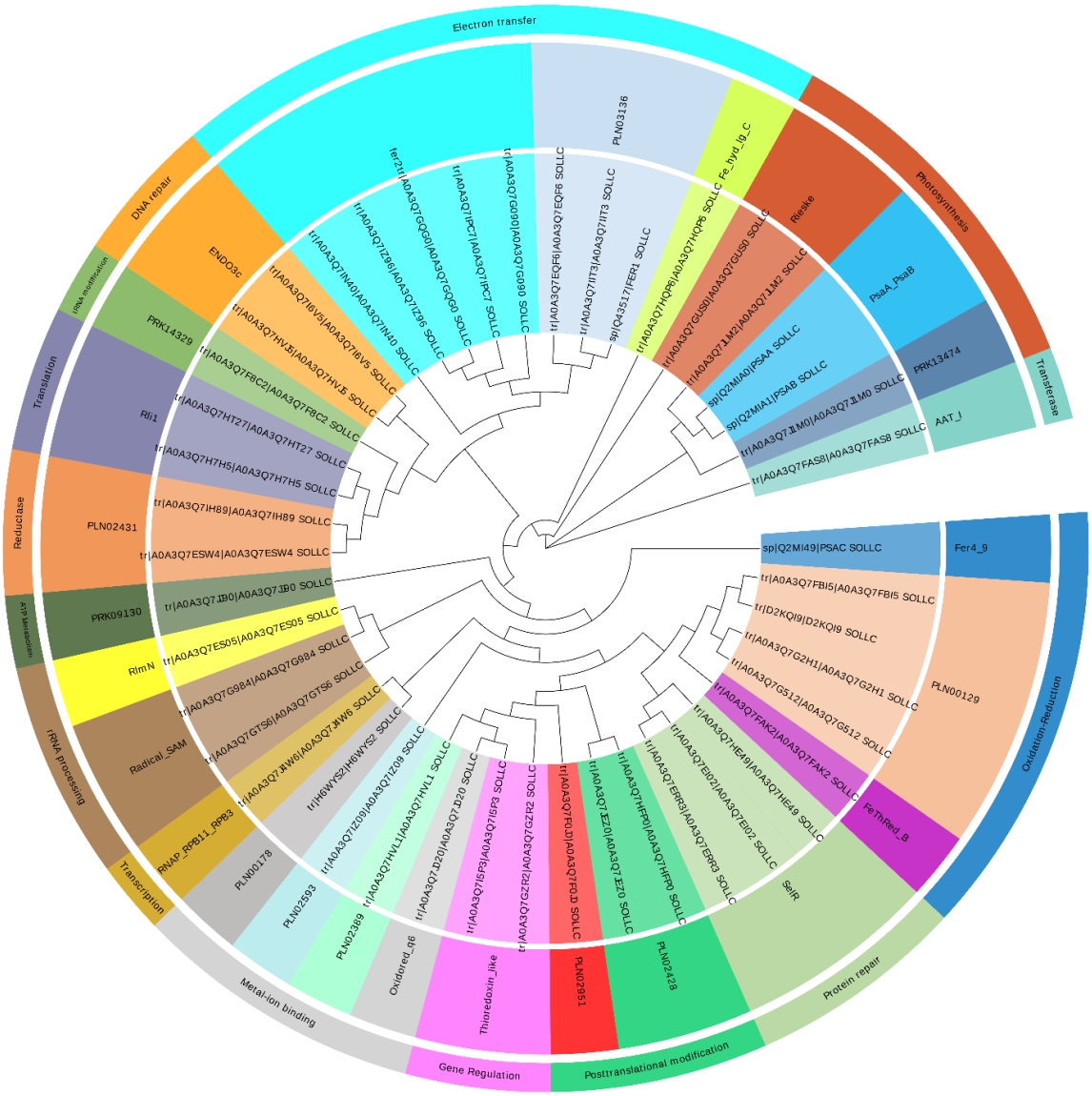

Fig. 9 Functional classification of clustered iron-binding proteins

4 Discussion

Tomato is an economic crop with many cultivars worldwide. Iron is one of the essential micronutrients, and it has a crucial role in plant growth and development. In this study, iron-binding proteins of tomato proteome have been identified, classified, and analyzed for biological functions. In the first step of the study, the MetalPredator program was used to find iron-binding proteins on tomato proteome sequences. MetalPredator is a customized program for iron-binding proteins and uses the HMM model profiles for Pfam domains and structural motifs defined as MFSs via MetalPDB (Andreini et al. 2012; Valasatava et al. 2016; Putignano et al. 2018). MetalPredator has been used for various bacterial proteomes like *Paenibacillus polymyxa* for iron-binding biosynthesis (Li et al. 2021) or *Spironucleus salmonicida* for stress response genes (Stairs et al. 2019). Also, wheat proteome has been analyzed for iron-binding proteins using the MetalloPred tool, and approximately 1.1% of wheat proteome has been determined as iron-binding proteins (Verma et al. 2017). Our results showed that 0.6% of tomato proteome contained iron-binding proteins. There is no report in the literature addressing iron-binding proteins in tomato plants, especially the determination of iron-binding proteins using MetalPredator. This study demonstrates, for the first time, a complete analysis of all iron-binding proteins of the tomato proteome.

Metal ions bind to proteins as ligands by donating an electron pair. The side chains of cysteine (Johnson et al. 2005), histidine (Ciofi-Baffoni et al. 2018), glutamic acid (Chaud et al. 2002), and aspartic acid (Caetano-Silva et al. 2015) residues interact with both Fe^{2+} and Fe^{3+} ions. Iron-binding residues interaction sites are analyzed by setting an iron-ion binding template of at least 3.5 Å between the metal ion and two residues (Lin et al. 2016). In this study, MIB analysis showed Fe^{2+} and Fe^{3+} ion interactions on 50 iron-binding proteins. Both Fe^{2+} and Fe^{3+} ion binding were related to the canonical metal-binding sites. These sites are located at the interface of two domains connected by a single long α-helix (Vigouroux et al. 2020). Analyzed proteins had an interaction with mostly cysteine (Cys), aspartic acid (Asp), histidine (His), and glutamic acid (Glu) residues. Besides, a fewer number of the analyzed proteins interacted with glutamine (Gln), tyrosine (Try), asparagine (Asn), alanine (Ala), methionine (Met), valine (Val), and lysine (Lys) residues. Respectively, free γ- and δ- carboxyl groups of aspartic and glutamic acid residues could bind iron ions (Storcksdieck et al. 2007). Iron ions could bind with histidine residues due to the imidazole side chain (Nemirovskiy and Gross, 1996). Cysteine residues could bind iron ions due to sulfur groups (Giles et al. 2003). Additionally, 89% of coordinating atoms bind to side chains of Asp, His, Glu, and Cys residues (called canonical amino acids) on iron-ion binding sites (Sánchez-Aparicio et al. 2021). Another study reported that the major iron-ion binding protein residues of sea cucumber as His, Glu, Cys, and Asp amino acids (Sun et al. 2017). According to the literature, our results are coherent with previous reports for metal-ion binding sites on proteins.

Iron has two interconvertible oxidation states: Fe^{2+} and Fe^{3+}. Consequently, Fe ions can be implicated in vital oxidation-reduction reactions in biological systems. Those reactions are a part of significant processes like respiration, photosynthesis, or DNA synthesis. Depending on the oxidation states of iron, it can be in different coordination environments (Sánchez et al. 2017). In our study, most iron-binding proteins showed free or poor coordination. Iron ions were primarily coordinated by O or N atoms in the first coordination sphere, but if lone pair of electrons occupies more space than a bonding pair, deviation from ideal geometry may occur (Gillespie, 1992). Reports showing that various protein complexes without the ideal designated geometries are consistent with our results (McLaughlin et al. 2012). Our coordination geometries analysis for Fe^{2+} binding proteins displayed 18% as square planar and 4% as tetrahedral geometries. On the other hand, Fe^{3+} binding proteins showed 6% square planar and 4% for trigonal bipyramidal and tetrahedral coordination geometries. In both cases, square planar geometry was supported by negatively charged amino acids like Glu or His to prevent higher coordination numbers (Pascualini et al. 2015). The square planar geometry can also arise from the arrangement of four binding pyridine units on the bis-porphyrin heme protein model (Chen et al. 1999). Square planar geometry corresponds to a high-field and low-spin electronic arrangement like in pheophytin, an electron carrier of chlorophyll (Bechaieb et al. 2018). Tetrahedral coordination geometry on iron-binding complexes has been proceeded by inorganic sulfides or protein-based ligands like cysteine residues (Pandelia et al. 2015). Also, tetrahedral coordination in iron-binding proteins is regulated by coordinating four cysteine sulfur atoms like in Rubredoxin (Todorovic and Teixeira, 2018). Trigonal bipyramidal coordination geometry can be promoted by coordinating N and three O atoms like on YtgA protein (Luo et al. 2019). Various coordination geometries resulted from differences in electronegativity between iron and amino acid residues.

MD simulations were performed to understand the mechanistic insight of iron-binding proteins via structural conformations. Iron ions were docked into targeted residues iron-binding proteins using the MIB tool. MD simulations showed that protein structures have stable conformations according to the average RMSD values (between 1,626 Å - 2,994 Å for Fe^{2+} and 1,626 Å - 2,140 Å for Fe^{3+}). Evaluating the accuracy of the dynamic binding process is complicated due to multiple iron coordinating geometries (Hu and Shelver, 2003). In this study, Q2MI49|PSAC_SOLLC protein showed square planar geometry for Fe^{3+} via Cys11, Cys14, Cys34, and Ala36. The RMSD values for these residues were respectively changing (0.06 Å, 0.04 Å, 0.03 Å, 0.07 Å) when compared with the protein backbone. Furthermore, A0A3Q7EI02_SOLLC protein showed tetrahedral coordination geometry via Cys46, Cys49, Cys92, and Cys95, with RMSD values of 0,01 Å, 0,22 Å, 0,03 Å, 0,01 Å when compared with the protein backbone (Data not shown). Although lower RMSD values have proved conformational stabilization of analyzed iron-binding proteins, differently charged areas generated by the side chains of amino acid residues could be the reason for the issue (Bernacchioni et al. 2016).

Both subcellular localization analysis results in WegoLoc and Cello v2.5 showed that iron-binding proteins were mostly localized in the chloroplast. Total 16 protein were detected in

similar localization. These are 9 proteins for chloroplast, 4 proteins for mitochondrion, 2 proteins for nucleus and 1 protein for cytoplasm (Supplementary Table S5). However, there were differences between these analyses in other localizations because WegoLoc and Cello use different datasets. WegoLoc tool is based on the BaCello dataset for plants with 491 proteins (Pierleoni et al. 2006). Meanwhile, the Cello v2.5 tool is based on Park and Kneisha dataset with 7589 eukaryotic proteins (Yu et al. 2006). Regarding datasets, results from the Cello v2.5 tool could be considered more accurate than WegoLoc for plants.

This study classified 45 high confidence level iron-binding proteins from different protein families according to subcellular localization, molecular functions, and biological processes. These proteins have essential roles in electron transfer, catalytic activity, metal ion binding, protein repair, and oxidation reduction processes. Iron-binding proteins plays important roles as both carrier proteins and metalloproteins in plant metabolism including from photosynthesis to protein repair. Carrier iron-binding proteins take charge for moving ions and molecules across the membranes. Also, metalloproteins are contains metal ions as cofactors. In this study, determined iron-binding proteins commonly act as carrier proteins for electron transfer and oxidation reduction processes. On the other hand, other iron-binding proteins act as metalloproteins for metal-ion binding or Fe-S clusters. The biological and molecular functions of these high confidence level iron-binding proteins were presented (Fig. 9, Supplementary Table 1), and the descriptions were derived from InterPro (Blum et al. 2021) and NCBI-CDD (Marchler-Bauer et al. 2010) databases.

Functional domains of the identified proteins were analyzed by detecting homologs using the CDD search tool and protein super families clustered via the sequences using the maximum parsimony method. This method is a character-based phylogenetic tree construction method (Kannan and Wheeler, 2012) and offers better performance than the maximum likelihood method due to the high heterogeneity of sequence datasets (Kolaczkowski and Thornton, 2004).

5 Conclusion

In this study, using computational methods, iron-binding proteins of tomato proteome were identified via structural formations at high confidence level. A total of 42 iron-binding proteins were identified via 3D structures, metal ion binding geometries, and structural conformations (MD analysis) on tomato proteome. Different tools were used to analyze the identified iron-binding proteins subcellular localization, molecular function, and biological process roles. Two different subcellular localization tools proved that iron-binding proteins are primarily localized in the chloroplast. These proteins are commonly involved in oxidation-reduction biological processes. Molecular functions of iron-binding come forward on iron-sulfur cluster binding and electron transfer activity. Finally, iron-binding proteins were classified as superfamilies and clustered for homologous proteins. Clustered proteins revealed the importance of iron-binding proteins on electron transfer and oxidation-reduction processes. Results showed that iron-binding proteins play important roles in the growth and development of tomato plants through biochemical and physiological functions. These results provide a base for iron-binding proteome analyses using computational plant sciences methods. Considering these proteomic analyses will be more critical in the future for research areas like protein engineering or bioengineering.

Acknowledgements

This study is funded by Ege University Scientific Research Projects (FDK-2019-21028), Council of Higher Education Scholarship 100/2000, and TUBITAK 2211c scholarship.

Authors' contributions:

Yiğit Küçükçobanoğlu and Lale Yıldız Aktaş contributed to the study conception, design, data collection, writing - orginal draft preparation, writing-, review and editing.

Conflict of interest disclosure:

The authors declare that they have no conflict of interest.

References

Allen JF (2004) Cytochrome b6f: structure for signalling and vectorial metabolism. Trends Plant Sci 9:130–137.

Andreini C, Cavallaro G, Lorenzini S, Rosato A (2012) MetalPDB: a database of metal sites in biological macromolecular structures. Nucleic Acids Res 41:D312–D319.

Andreini C, Cavallaro G, Rosato A, Valasatava Y (2013) MetalS2: a tool for the structural alignment of minimal functional sites in metal-binding proteins and nucleic acids. J Chem Inf Model 53:3064–3075.

Andreini C, Rosato A, Banci L (2017) The relationship between environmental dioxygen and iron-sulfur proteins explored at the genome level. PLoS One 12:e0171279.

Bechaieb R, Lakhdar ZB, Gérard H (2018) DFT and TD-DFT studies of Mg-substitution in chlorophyll by Cr (II), Fe (II) and Ni (II). Chemistry Africa 1:79–86.

Bernacchioni C, Pozzi C, di Pisa F, Mangani S, Turano P (2016) Ferroxidase Activity in Eukaryotic Ferritin is Controlled by Accessory-Iron-Binding Sites in the Catalytic Cavity. Chemistry–A European Journal 22:16213–16219.

Bertsova Y v, Kostyrko VA, Baykov AA, Bogachev A v (2014) Localization-controlled specificity of FAD: threonine flavin transferases in Klebsiella pneumoniae and its implications for the mechanism of Na+-translocating NADH: quinone oxidoreductase. Biochimica et Biophysica Acta (BBA)-Bioenergetics 1837:1122–1129.

Blum M, Chang H-Y, Chuguransky S, Grego T, Kandasaamy S, Mitchell A, Nuka G, Paysan-Lafosse T, Qureshi M, Raj S (2021) The InterPro protein families and domains database: 20 years on. Nucleic Acids Res 49:D344–D354.

Borukhov S, Nudler E (2008) RNA polymerase: the vehicle of transcription. Trends Microbiol 16:126–134.

Braymer JJ, Lill R (2017) Iron–sulfur cluster biogenesis and trafficking in mitochondria. Journal of Biological Chemistry 292:12754–12763.

Briat J-F, Curie C, Gaymard F (2007) Iron utilization and metabolism in plants. Curr Opin Plant Biol 10:276–282.

Briat J-F, Fobis-Loisy I, Grignon N, Lobréaux S, Pascal N, Savino G, Thoiron S, von Wirén N, van Wuytswinkel O (1995) Cellular and molecular aspects of iron metabolism in plants. Biol Cell 84:69–81.

Caetano-Silva ME, Bertoldo-Pacheco MT, Paes-Leme AF, Netto FM (2015) Iron-binding peptides from whey protein hydrolysates: Evaluation, isolation and sequencing by LC–MS/MS. Food Research International 71:132–139.

Chang Y-Y, Li H, Sun H (2017) Immobilized metal affinity chromatography (IMAC) for metalloproteomics and phosphoproteomics In: Inorganic and Organometallic Transition Metal Complexes with Biological Molecules and Living Cells , pp 329–353. Elsevier.

Chaud M v, Izumi C, Nahaal Z, Shuhama T, Bianchi M de LP, Freitas O de (2002) Iron derivatives from casein hydrolysates as a potential source in the treatment of iron deficiency. J Agric Food Chem 50:871–877.

Chen LX, Lee PL, Gosztola D, Svec WA, Montano PA, Wasielewski MR (1999) Time-resolved X-ray absorption determination of structural changes following photoinduced electron transfer within Bis-porphyrin Heme protein models. J Phys Chem B 103:3270–3274.

Chi S-M, Nam D (2012) WegoLoc: accurate prediction of protein subcellular localization using weighted Gene Ontology terms. Bioinformatics 28:1028–1030.

Ciofi-Baffoni S, Nasta V, Banci L (2018) Protein networks in the maturation of human iron–sulfur proteins. Metallomics 10:49–72.

DeFraia CT, Wang Y, Yao J, Mou Z (2013) Elongator subunit 3 positively regulates plant immunity through its histone acetyltransferase and radical S-adenosylmethionine domains. BMC Plant Biol 13:1–13.

Dong J, Lai R, Nielsen K, Fekete CA, Qiu H, Hinnebusch AG (2004) The Essential ATP-binding Cassette Protein RLI1 Functions in Translation by Promoting Preinitiation Complex Assembly*♦. Journal of Biological Chemistry 279:42157–42168.

Dutta S, Teresinski HJ, Smith MD (2014) A split-ubiquitin yeast two-hybrid screen to examine the substrate specificity of atToc159 and atToc132, two Arabidopsis chloroplast preprotein import receptors. PLoS One 9:e95026.

FAO F (2020) FAOSTAT statistical database. Rome: Food and Agriculture Organisation of the United Nations.

Freedman RB, Hirst TR, Tuite MF (1994) Protein disulphide isomerase: building bridges in protein folding. Trends Biochem Sci 19:331–336.

Garcia JS, de Magalhães CS, Arruda MAZ (2006) Trends in metal-binding and metalloprotein analysis. Talanta 69:1–15.

Giles NM, Watts AB, Giles GI, Fry FH, Littlechild JA, Jacob C (2003) Metal and redox modulation of cysteine protein function. Chem Biol 10:677–693.

Gillespie RJ (1992) The VSEPR model revisited. Chem Soc Rev 21:59–69.

Gueguen V, Macherel D, Jaquinod M, Douce R, Bourguignon J (2000) Fatty acid and lipoic acid biosynthesis in higher plant mitochondria. Journal of Biological Chemistry 275:5016–5025.

Hase T, Schürmann P, Knaff DB (2006) The interaction of ferredoxin with ferredoxin-dependent enzymes In: Photosystem I , pp 477–498. Springer.

Hospital A, Andrio P, Fenollosa C, Cicin-Sain D, Orozco M, Gelpí JL (2012) MDWeb and MDMoby: an integrated web-based platform for molecular dynamics simulations. Bioinformatics 28:1278–1279.

Houston NL, Fan C, Xiang Q-Y, Schulze J-M, Jung R, Boston RS (2005) Phylogenetic analyses identify 10 classes of the protein disulfide isomerase family in plants, including single-domain protein disulfide isomerase-related proteins. Plant Physiol 137:762–778.

Hu X, Dong Q, Yang J, Zhang Y (2016) Recognizing metal and acid radical ion-binding sites by integrating ab initio modeling with template-based transferals. Bioinformatics 32:3260–3269.

Hu X, Shelver WH (2003) Docking studies of matrix metalloproteinase inhibitors: zinc parameter optimization to improve the binding free energy prediction. J Mol Graph Model 22:115–126.

Jahns P, Graf M, Munekage Y, Shikanai T (2002) Single point mutation in the Rieske iron–sulfur subunit of cytochrome b6/f leads to an altered pH dependence of plastoquinol oxidation in Arabidopsis. FEBS Lett 519:99–102.

Jin S, Hu Y, Fu H, Jiang S, Xiong Y, Qiao H, Zhang W, Gong Y, Wu Y (2021) Identification and characterization of the succinate dehydrogenase complex iron sulfur subunit B gene in the Oriental River Prawn, Macrobrachium nipponense. Front Genet 12.

Johnson DC, Dean DR, Smith AD, Johnson MK (2005) Structure, function, and formation of biological iron-sulfur clusters. Annu Rev Biochem 74:247.

Kannan L, Wheeler WC (2012) Maximum parsimony on phylogenetic networks. Algorithms for Molecular Biology 7:1–10.

Kelley LA, Mezulis S, Yates CM, Wass MN, Sternberg MJE (2015) The Phyre2 web portal for protein modeling, prediction and analysis. Nat Protoc 10:845–858.

Kolaczkowski B, Thornton JW (2004) Performance of maximum parsimony and likelihood phylogenetics when evolution is heterogeneous. Nature 431:980–984.

Kumar S, Stecher G, Li M, Knyaz C, Tamura K (2018) MEGA X: molecular evolutionary genetics analysis across computing platforms. Mol Biol Evol 35:1547.

Kurisu G, Kusunoki M, Katoh E, Yamazaki T, Teshima K, Onda Y, Kimata-Ariga Y, Hase T (2001) Structure of the electron transfer complex between ferredoxin and ferredoxin-NADP+ reductase. Nat Struct Biol 8:117–121.

Li Q, Li Y, Li X, Chen S (2021) Identification of Genes Involved in Fe–S Cluster Biosynthesis of Nitrogenase in Paenibacillus polymyxa WLY78. Int J Mol Sci 22:3771.

Lin Y-F, Cheng C-W, Shih C-S, Hwang J-K, Yu C-S, Lu C-H (2016) MIB: metal ion-binding site prediction and docking server. J Chem Inf Model 56:2287–2291.

Litomska A, Ishida K, Dunbar KL, Boettger M, Coyne S, Hertweck C (2018) Enzymatic thioamide formation in a bacterial antimetabolite pathway. Angewandte Chemie International Edition 57:11574–11578.

Lu Y, Chakraborty S, Miner KD, Wilson TD, Mukherjee A, Yu Y, Liu J, Marshall NM (2013) Metalloprotein design In: Comprehensive Inorganic Chemistry II (Second Edition): From Elements to Applications , pp 565–593. Elsevier Ltd.

Luo Z, Neville SL, Campbell R, Morey JR, Menon S, Thomas M, Eijkelkamp BA, Ween MP, Huston WM, Kobe B (2019) Structure and metal binding properties of Chlamydia trachomatis YtgA. J Bacteriol 202:e00580–19.

Marchler-Bauer A, Lu S, Anderson JB, Chitsaz F, Derbyshire MK, DeWeese-Scott C, Fong JH, Geer LY, Geer RC, Gonzales NR (2010) CDD: a Conserved Domain Database for the functional annotation of proteins. Nucleic Acids Res 39:D225–D229.

McLaughlin MP, Retegan M, Bill E, Payne TM, Shafaat HS, Pena S, Sudhamsu J, Ensign AA, Crane BR, Neese F (2012) Azurin as a protein scaffold for a low-coordinate nonheme iron site with a small-molecule binding pocket. J Am Chem Soc 134:19746–19757.

Naik PK, Ranjan P, Kesari P, Jain S (2011) MetalloPred: A tool for hierarchical prediction of metal ion binding proteins using cluster of neural networks and sequence derived features. Journal of Biophysical Chemistry 02:112–123.

Nakayama M, Akashi T, Hase T (2000) Plant sulfite reductase: molecular structure, catalytic function and interaction with ferredoxin. J Inorg Biochem 82:27–32.

Nemirovskiy O v, Gross ML (1996) Complexes of iron (II) with cysteine-containing peptides in the gas phase. J Am Soc Mass Spectrom 7:977–980.

Pandelia M-E, Lanz ND, Booker SJ, Krebs C (2015) Mössbauer spectroscopy of Fe/S proteins. Biochimica et Biophysica Acta (BBA)-Molecular Cell Research 1853:1395–1405.

Pascualini ME, di Russo N v, Thuijs AE, Ozarowski A, Stoian SA, Abboud KA, Christou G, Veige AS (2015) A high-spin square-planar Fe (II) complex stabilized by a trianionic pincer-type ligand and conclusive evidence for retention of geometry and spin state in solution. Chem Sci 6:608–612.

Passerini A, Lippi M, Frasconi P (2011) MetalDetector v2. 0: predicting the geometry of metal binding sites from protein sequence. Nucleic Acids Res 39:W288–W292.

Pehkonen S (1995) Determination of the oxidation states of iron in natural waters. A review. Analyst 120:2655–2663.

Picciocchi A, Douce R, Alban C (2003) The Plant Biotin Synthase Reaction: IDENTIFICATION AND CHARACTERIZATION OF ESSENTIAL MITOCHONDRIAL ACCESSORY PROTEIN COMPONENTS *. Journal of Biological Chemistry 278:24966–24975.

Pierleoni A, Martelli PL, Fariselli P, Casadio R (2006) BaCelLo: a balanced subcellular localization predictor. Bioinformatics 22:e408–e416.

Pierrel F, Hernandez HL, Johnson MK, Fontecave M, Atta M (2003) MiaB Protein from Thermotoga maritima: CHARACTERIZATION OF AN EXTREMELY THERMOPHILIC tRNA-METHYLTHIOTRANSFERASE *. Journal of Biological Chemistry 278:29515–29524.

Pröfrock D, Prange A (2012) Inductively Coupled Plasma-Mass Spectrometry (ICP-MS) for Quantitative Analysis in Environmental and Life Sciences: A Review of Challenges, Solutions, and Trends. Appl Spectrosc 66:843–868.

Pushie MJ, Pickering IJ, Korbas M, Hackett MJ, George GN (2014) Elemental and Chemically Specific X-ray Fluorescence Imaging of Biological Systems. Chem Rev 114:8499–8541.

Putignano V, Rosato A, Banci L, Andreini C (2018) MetalPDB in 2018: a database of metal sites in biological macromolecular structures. Nucleic Acids Res 46:D459–D464.

Qiao L, Xie D (2019) MIonSite: Ligand-specific prediction of metal ion-binding sites via enhanced AdaBoost algorithm with protein sequence information. Anal Biochem 566:75–88.

Ramadan AM, Alnufaei AA, Khan TK, Ali HM, Eissa HF, Hassan SM (2021) The first report of RNA U to C or G editing in the mitochondrial NADH dehydrogenase subunit 5 (Nad5) transcript of wild barley. Mol Biol Rep 48:6057–6064.

Ravet K, Touraine B, Boucherez J, Briat J-F, Gaymard F, Cellier F (2009) Ferritins control interaction between iron homeostasis and oxidative stress in Arabidopsis. The Plant Journal 57:400–412.

Roldán-Arjona T, García-Ortiz M-V, Ruiz-Rubio M, Ariza RR (2000) cDNA cloning, expression and functional characterization of an Arabidopsis thaliana homologue of the Escherichia coli DNA repair enzyme endonuclease III. Plant Mol Biol 44:43–52.

Sánchez M, Sabio L, Gálvez N, Capdevila M, Dominguez-Vera JM (2017) Iron chemistry at the service of life. IUBMB Life 69:382–388.

Sánchez-Aparicio J-E, Tiessler-Sala L, Velasco-Carneros L, Roldán-Martín L, Sciortino G, Maréchal J-D (2021) BioMetAll: Identifying Metal-Binding Sites in Proteins from Backbone Preorganization. J Chem Inf Model 61:311–323.

Sehnal D, Bittrich S, Deshpande M, Svobodová R, Berka K, Bazgier V, Velankar S, Burley SK, Koča J, Rose AS (2021) Mol* Viewer: modern web app for 3D visualization and analysis of large biomolecular structures. Nucleic Acids Res 49:W431–W437.

Sello MM (2016) Comparative genomics of cytochrome P450 monooxygenases in newly explored pathogenic Oomycetes.

Sharma A, Sharma D, Verma SK (2017) Proteome wide identification of iron binding proteins of Xanthomonas translucens pv. undulosa: focus on secretory virulent proteins. BioMetals 30:127–141.

Shematorova EK, Slovokhotov IY, Shmakov VN, Khaliluev MR, Shpakovski DG, Klykov VN, Babak OG, Spivak SG, Konstantinov YM, Shpakovski G v (2019) Novel Interactions of Adrenodoxin-Related [2Fe-2S] Plant Ferredoxins MFDX1 and MFDX2 Indicate Their Involvement in a Wide Spectrum of Functions in Plant Mitochondria. Proceedings of the Latvian Academy of Sciences Section B Natural, Exact, and Applied Sciences 73:478–486.

Shi W, Chance MR (2008) Metallomics and metalloproteomics. Cellular and Molecular Life Sciences 65:3040–3048.

Sodhi JS, Bryson K, McGuffin LJ, Ward JJ, Wernisch L, Jones DT (2004) Predicting Metal-binding Site Residues in Low-resolution Structural Models. J Mol Biol 342:307–320.

Stairs CW, Kokla A, Ástvaldsson Á, Jerlström-Hultqvist J, Svärd S, Ettema TJG (2019) Oxygen induces the expression of invasion and stress response genes in the anaerobic salmon parasite Spironucleus salmonicida. BMC Biol 17:19.

Storcksdieck S, Bonsmann G, Hurrell RF (2007) Iron-Binding Properties, Amino Acid Composition, and Structure of Muscle Tissue Peptides from in vitro Digestion of Different Meat Sources. J Food Sci 72:S019–S029.

Subramanian B, Gao S, Lercher MJ, Hu S, Chen W-H (2019) Evolview v3: a webserver for visualization, annotation, and management of phylogenetic trees. Nucleic Acids Res 47:W270–W275.

Sun N, Cui P, Jin Z, Wu H, Wang Y, Lin S (2017) Contributions of molecular size, charge distribution, and specific amino acids to the iron-binding capacity of sea cucumber (Stichopus japonicus) ovum hydrolysates. Food Chem 230:627–636.

Todorovic S, Teixeira M (2018) Resonance Raman spectroscopy of Fe–S proteins and their redox properties. JBIC Journal of Biological Inorganic Chemistry 23:647–661.

Valasatava Y, Rosato A, Banci L, Andreini C (2016) MetalPredator: a web server to predict iron–sulfur cluster binding proteomes. Bioinformatics 32:2850–2852.

Valasatava Y, Rosato A, Cavallaro G, Andreini C (2014) MetalS3, a database-mining tool for the identification of structurally similar metal sites. JBIC Journal of Biological Inorganic Chemistry 19:937–945.

Verma SK, Sharma A, Sandhu P, Choudhary N, Sharma S, Acharya V, Akhter Y (2017) Proteome scale identification, classification and structural analysis of iron-binding proteins in bread wheat. J Inorg Biochem 170:63–74.

Vigouroux A, Aumont-Nicaise M, Boussac A, Marty L, lo Bello L, Legrand P, Brillet K, Schalk IJ, Moréra S (2020) A unique ferrous iron binding mode is associated with large conformational changes for the transport protein FpvC of Pseudomonas aeruginosa. FEBS J 287:295–309.

Walters EM, Johnson MK (2004) Ferredoxin:thioredoxin Reductase: Disulfide Reduction Catalyzed via Novel Site-specific [4Fe–4S] Cluster Chemistry. Photosynth Res 79:249–264.

Wang S, Chen W, Yang C, Yao J, Xiao W, Xin Y, Qiu J, Hu W, Yao H, Ying W, Fu Y, Tong J, Chen Z, Ruan S, Ma H (2016) Comparative proteomic analysis reveals alterations in development and photosynthesis-related proteins in diploid and triploid rice. BMC Plant Biol 16:199.

Wiederstein M, Sippl MJ (2007) ProSA-web: interactive web service for the recognition of errors in three-dimensional structures of proteins. Nucleic Acids Res 35:W407–W410.

Yamori W, Kondo E, Sugiura D, Terashima I, Suzuki Y, Makino A (2016) Enhanced leaf photosynthesis as a target to increase grain yield: insights from transgenic rice lines with variable Rieske

FeS protein content in the cytochrome b6/f complex. Plant Cell Environ 39:80–87.

Yan F, Fujimori DG (2011) RNA methylation by Radical SAM enzymes RlmN and Cfr proceeds via methylene transfer and hydride shift. Proceedings of the National Academy of Sciences 108:3930–3934.

Yu C-S, Chen Y-C, Lu C-H, Hwang J-K (2006) Prediction of protein subcellular localization. Proteins: Structure, Function, and Bioinformatics 64:643–651.

Zheng H, Cooper DR, Porebski PJ, Shabalin IG, Handing KB, Minor W (2017) CheckMyMetal: a macromolecular metal-binding validation tool. Acta Crystallogr D Struct Biol 73:223–233.

Zhong Z, Ji Y, Fu Y, Liu B, Zhu Q (2015) Molecular characterization and expression analysis of the duck viperin gene. Gene 570:100–107.

REVIEW ARTICLE
Bull Biotechnol (2023) 4(1):30-35
https://doi.org/10.51539/biotech.1215628 Journal homepage: www.dergipark.org.tr/biotech

Bulletin of Biotechnology

Selected research and dramatic surgery fish cases of incisive complete in fish surgical

Nurdan Filik*, Fethi Filik

[1]*Suleyman Demirel University, Isparta, Turkey*

*Corresponding author : nurdansal@hotmail.com
Orcid No: https://orcid.org/0000-0003-4376-7298

Received : 07/12/2022
Accepted : 15/01/2023

Abstract: Health problems which can be treated exclusively by surgical means are relatively uncommon in fish. Fish surgery feat is vital essential and inevitable for the at fish diseases treatment and fish recovery. Consequently, only a limited number of procedures have been developed and reported in the literature. Despite use of analogous surgical instruments and surgical techniques to those employed in other animals, fish are a very diverse taxon and specific anatomy and physiology should be reviewed before surgical procedures are performed. Surgical planning often requires advanced diagnostics such as ultrasonography and imaging. Essantial surgical procedures include cutaneous and intracoelomic mass excision, ophthalmic procedures, reproductive surgery, brain surgery, visceral organs surgery, gastrointestinal foreign body removal, visceral organs examples, and buoyancy concerns. This article reviews several surgical procedures that have been performed in fish and highlight various aspects of surgical care which relate specifically to fishes. In this review article, administration of sedation and anesthesia, anaesthetic agents, pain in fish, obtrusive fish cases surgery, fish cases surgery operations examples, frequently used anesthetics and preoperative considerations, underwater surgery, out of water surgery, specific surgery procedures, microsurgery techniques, laparoscopy, catheter implantation and laparotomy were discussed for fish researchers. Suggestions for appropriate postoperative management are also discussed.

Keywords: Fish surgery; fish surgical procedures; fish cases; dramatic cases of fish surgery; surgery instruments; anesthesia

1 Introduction

General considerations: although the notion of fish surgery is often greeted with skepticism, fish can make excellent subjects for surgery. Fish surgeries take place in both research and clinical settings. The decision to proceed to surgery in clinical cases can be motivated by the rarity of the species involved, the economic value of the patient, or the owner's emotional attachment to the fish. In the authors' experience with fish-owning clients, fish are certainly not exempt from the human-animal bond. An excellent description of fish surgery for veterinarians has been published previously and an extensive basic review of fish anesthesia and surgical techniques has been written for fish researchers lacking prior surgical experience (Craig and Gregory 2000). Surgery of fish is an exciting and pioneering field for veterinary practitioners (Loh and Chia 2016).

After anesthesia is administered, specific surgical procedures can be performed on fish, including laceration and fin tear repairs, biopsies, celiotomy, liver biopsy, renal biopsy, laparoscopy, mass removals, resection of prolapsed intestines, fracture repair, and abdominal surgery to remove impactions and tumors (Murray 2002).

General surgical knowledge and experience will facilitate successful fish surgery, as will familiarity with normal fish anatomy. Frequently, these are surgeries for external skin or fin tumor excisions and abdominal exploratory surgeries to remove masses or biopsy organs. Other surgical procedures have been performed for repair of lacerations from traumatic injuries, resection of prolapsed cloacal tissues, and orthopedic procedures on fish with spinal fractures (Saint-Erne 2015).

Specific surgical procedures have been performed on fish, including laceration and fin repairs, biopsies, celiotomy, laparoscopy, mass removals, resection of prolapsed intestines, fracture repair, and abdominal surgery to remove impactions and tumors (Murray 2002). Very important incisive surgical operations such as tumor removal (Reid and Backma 1988), gallbladder catheterization in pharmacokinetic studies (Sohlberg et al. 1997), prosthetic eye operation (Mentalfloss 2016), monitoring of heart rate during operations (Saint-Erne 2015) have taken place in the literature.

This review article aims to draw attention to fish surgery for success when surgical intervention is needed, to explain successful fish surgeries, and to encourage the development of a fish operating room in the laboratory to protect the survival rights of fish (natural or cultured fish), which is one of the valuable parts of nature, and to increase their survival.

2 Underwater Surgery and Out of Water Surgery

Main advantage of the underwater surgery type is that it caters to the water needs of patient fish. However wound contamination and osmotic tissue damage, the rippling surface caused by movement in the water and the presence of escaped blood usually obscures the field of view (Wildgoose, 2000). Most surgery on fish is performed out of the water by surgeons. Only brief procedures lasting less than four minutes are manageable without anesthetic delivery system to provide a low maintenance dose of anesthetic and fresh oxygenated water. The lack of reflexes that can be fish may necessitate the use of either an electrocardiograph or a doppler pulse ultrasound probe, particularly during prolonged anaesthesia. Body moist by periodic irrigation of the skin to avoid desiccation of the delicate tissues (Wildgoose 2000).

3 Anesthesia

Anesthesia is an essential tool in the detailed live fish examination. For surgical operation, fish must be tranquilized and anesthetized. Tranquilization is enough for different manipulations such as immobilization, prolonged transport, and facial lesions treatment. Although more complex surgical operations require general anesthesia (Yıldırım et al. 2009).

Commonly utilized chemicals for anesthesia and tranquilization are as follows. MS-222 (3-Aminobenzoic Acid Ethyl Ester), Benzocaine (Ethyl p-Aminobenzoate), Quinaldine Sulfate (2-Methylquinoline Sulfate), Carbon Dioxide (CO_2), Tricaine Methane Sulfonate, Diazepam (Valium), Ethanol (Ethyl Alcohol), Ether (Dimethyl Ether), Eugenol/Isoeugenol (Clove Oil), Isoflurane (1- Chloro- 2, 2, 2- Trifluoroethyldifluoromethyl Ether), Ketamine Hydrochloride, Propofol (2, 6- Diisopropylphenol) (Bowser 2001; Neiffer and Stamper 2009; Saint-Erne 2010; Loh 2012).

According to the principle of modern anesthesiology, anesthetic drugs are not used alone. While reaching the desired level of an anesthesia, the use of anesthetic alone is quite risky. Muscle relaxants such as diazepam, tubocurarine chloride, pancuronium bromide, atropine, xylazine are used to decrease the emergency of anesthesia in fish. This prevents excitation or delirium, rigidity, and respiratory depression (Mattson and Riple 1989).

4 Preoperative Surgical Preparation

The goals of doctor the patient's surgical and anesthetic perioperative mortality and to return him to desirable functioning. It is imperative to realize that "perioperative" risk is multifactorial, the invasiveness of the surgical procedure, and the type of anesthetic administered (Zambouri 2007). Stop fish feeding for a certain period time before the time of surgery. Clean possibly the area to be operated on.

Before the surgical operation, the anamnesis of sick fish should be taken and the case scenario should be investigated in detail. Surgical preparation should not destruction of mucus just because these are majority safety fences to complications, potential risks, contamination and infection.

Infections are prevented by using a protective dose of antibiotics before the operation. It is recommended to continue antibiotic administration for 1 to 4 weeks at the end of the operation (ceftazidime 30 mg/kg) (ScottWeber et al. 2009; Filik 2020).

5 Surgery Instruments

Essential surgery instruments for fish surgery are ophthalmic or microsurgery instruments due to size. In addition many surgeries can be performed with a scalpel, magnifying lens, iris scissors, Metzenbaum scissors, mosquito hemostats, hemostatic forceps and other surgical accessories (Saint-Erne 2015). Commonly used in laboratory, the ocular or microsurgical pack is warranted for fishes (Harms et al. 1995). Head loupe magnification with center mounted illumination helps visualize structures that are small in coelomic cavity. Gelpi or Weitlander retractors for large fish and self-retaining ocular retractors for small fish visceral organs (Craig 2005). Start the incision cranial to vent and continue forward to pectoral fin bones, as needed. Scales along incision may be cut through or removed with forceps before making an incision. Use gentle blunt dissection with the hemostats, Metzenbaum scissors, or gloved fingers to isolate the desired tissues. Ligate blood vessels as needed with 2-0 or smaller absorbable suture material such as Vicryl or Maxon. Stainless steel Hemoclips may also be used for ligation. Bipolar cautery units are useful for small vessel hemostasis (Saint-Erne 2015).

6 Fish Surgery: Postoperative Care and Common Procedures

Surgical operations in fish are also applied in cases of vaccine, organ biopsy, removal of problematic organs and tumors, removal of other pathological and nonpathological tissue, blood collection, drug injection, implant placement, marking, sperm and egg retrieval (Yıldırım et al. 2009). During the surgical operation, and all the environment, surgical instruments while performing the surgical operation must be sterile.

Surgical arae is cleaned with a 1:10 diluted solution of 1% povidone-iodine in 0.9% physiological saline. Small dabs of petroleum jelly will help it adhere to the skin (Saint-Erne 2015).

Scale injuries can also be repaired if the sloughed scale still contains adequate attached epidermis, and is immediate. Clean skin via iodine solution. Remove sutures in a few days, or when the tissue has reattached. Skin and fin wounds can be sutured using fine monofilament nylon sutures. To repair lancinated and injured fin membranes, gently scrape the opposing edges scar tissue, and then tightly oppose the fin edges with a continuous suture pattern. Incorporate fin rays in each side to keep suture from tearing through the fin membrane and topical disinfectant solution apply (Saint-Erne 2015).

Surgeries are practical for clinical and researches in fish. Certain surgery adjustments are necessary to accommodate piscine tissue handling, skin sensitivity, aqueous respiration, anatomic variations, and patient size. Surgerys successfully carried out include celiotomy aciurgy, enucleation, pseudobranchectomy aciurgy, swim bladder surgery, gonadectomy aciurgy, vascular catheterization, visceral organs biopsy techniques, and telemetry device implantation, (Craig and Gregory 2000).

Successful abdominal surgeries have been performed to remove both testicular and ovarian gonadal tumors. These appear as large irregular, fibrous masses in the caudal abdomen. Abdomen to appear quite distended. Following may removal, survey abdominal organs and contralateral gonad to assess any damage. In some cases, fish's gas bladder will become traumatized and distended, creating an appearance similar to an abdominal tumor. An ultrasound, radiograph, and endoscopy (Weber et al. 2009) examination will distinguish between an enlarged gas bladder. The damaged compartment of the gas bladder was isolated. The cranial compartment when removed is ligated at the isthmus. Fish will stabilize its buoyancy with the remaining portion of the gas bladder (Saint-Erne 2015).

A 25 cm Cyclosoma labiatum was presented because of a large growth present on the caudoventral aspect of the dorsal fin. The tumor was approximately eight cm3, hyperemic around its periphery, and well-embedded in the fin. Anesthesia was performed using tricaine methanesulphonate (TMS). Ventral recumbency with the surgical site maintained out of the water. The mass was removed using standard tumor excision techniques. Thermal cautery was used to seal the excision site and prevent electrolyte loss. The fish recovered uneventfully in a separate oxygenated tank and was then transferred to a convalescent tank containing 0.5% NaCl solution for one week (Reid and Backman 1988).

During the surgery procedure, an electrocardiogram (ECG) reading is taken to monitor the heart rate and rhythm. Three ECG lead clips can each be attached to the metal part of 22-gauge hypodermic needles. These needles then are placed through the skin and right pectoral fin (RA lead), left pectoral fin (LA lead), and cranial to the vent opening (LL lead). The P-QRS-T waves produced are of low amplitude (1 mV QRS complex). Heart rates are temperature dependent. Typical heart rates are 40 beats per minute but can range from 15 to 100 beats per minute. Increase freshwater flow across to lessen anesthesia and cause pulse to increase if it slows too much (Saint-Erne 2015).

After surgery, place fish in aerated non-anesthetized water of the same temperature in recovery with dusky lighting, in a quiet area (Saint-Erne 2015). Adhesion (Filik 2019) of biofilm (Bülbül and Filik 2019; Filik 2020) to different material surfaces is a serious problem. For this reason, postoperative follow-up biofilm prevent for the implant material placed during implant surgery.

Post-surgical butorphanol can be administered to control pain at 0.1–0.4 mg/kg IM. Tube feed fish food made into gruel in a blender if fish is not eating by after surgery. Surgical success depends on adequate surgical correction of the serious problem, bacterial prevention, bacterial virulence distruption (Nurcan, 2010), good hemostasis, and proper incision closure (Saint-Erne 2015).

7 Surgical Technique

Primarily and as immutable rule the surgeon should keep all the skin moist throughout the surgical procedure, taking care to avoid irrigating the incision site with anesthesia water. Presoaking the opencell foam V-tray. Due to there is no linea alba, so necessitating a carefully controlled entry into the coelomic cavity to intestinal damage. The body wall is poorly pliable, unless the coelomic cavity is distended. Adequate retraction with self-retaining retractors helps the surgeon maintain coelomic visualization despite the rigid body wall. Organs are not freely mobile, so surgeons must perform manipulations within the coelomic cavity rather than exteriorizing the organs (Craig 2005).

Suture materials are use successful at healing time and tissue reactivity (Gilliland 1994), it seems that monofilament sutures such as polydioxanone or polyglyconate are preferable to multifilament sutures such as silk, chromic gut, polyglactin 910, probably partly because of the ability of multifilament from the surrounding water (Sohlberg et al. 1997).

Needles with a cutting tip facilitate skin penetration. The use of continuous Ford interlocking patterns, simple continuous, simple interrupted, simple incision and horizontal mattress for skin closure has had success and satisfactory results. Continuous patterns have the advantages of reducing drag, minimizing knot surface area available for epibiont colonization, and reducing surgery time, but may be more prone to loosening if adequate tension is not maintained through the entire line and if knots at either end are not secure. Single or two-layer closure is usable depending on the thickness of the body wall; skin and fins is the strength layer of the closure. The subcutaneous layer is minimal, with dermis tightly adhered to the underlying muscle, thus there is barely any dead space and any necrotic focus to eliminate. Ideally, one should remove skin sutures when the incision is recovered, usually in a few weeks in uncomplicated cases. The removal of sutures eliminates a possibility of inflammation and can speed the final stages of incision recovering.

Use of cyanoacrylate tissue adhesive for incision closure, either in combination with sutures or alone, may be problematic in fish. However, they also show some inconvenient characteristics, such as less resistance to toxicity and tension in some sick fish. Also at surgery, cyanoacrylate can causes severe dermatitis in fish (Stoskopf 1993), and when used alone is associated with a higher incidence of incision dehiscence (Petering and Johnson 1991). Irritancied goblet cells rapidly produce mucus and elevate the tissue glue layer away from the skin. When tissue adhesives are used in addition to sutures, the sutures retain the cyanoacrylate with mucus trapped beneath, and the loose glue creates extra drag on the sutures. In spite of tissue adhesive is sometimes advocated to seal the suture line and make it watertight, an appropriately sutured incision suffices to prevent water incursion, and re-epithelialization is rapid in fish. Researchers

and fish surgeons have used surgical staples successfully in fish after operation; these could theoretically reduce skin closure time compared with suturing (Summerfelt and Smith 1990). Many fish surgeons reported surgical staples influentially at skin closure.

In neurological studies involving ablation of specific nervous system targets 2% agar gel in physiological saline (Weltzien et al. 2003; Merriam-Webster 2022) or vaseline-paraffin oil capped with anchored vinyl polysiloxane impression material (Zottoli et al. 2021) have been in use to seal and fill the tissue void in fish (Craig 2005).

Wound closure and anchoring of bio-loggers. Two separate thin nonabsorbable (5–0) suturations were used to anchor loggers (red arrow). The logger was abdominal cavity by tapering end pointing towards the pericardial layer. Both suture needles were loggers and then tied knot logger. Using two anchor sutures give flexibility to place loggers close to the pericardial body cavity and traumatonesis is determined. In Test 1, same thin 5–0 non-absorbable sutures were also used for wound closure (black arrow). In Tests 2 & 3 surgical wound was closed using relatively thick 3–0 non-absorbable sutures whereas same thin 5–0 suture as above used for anchoring the loggers. Fish gills were irrigated with seawater containing MS222 at a dose of 20 mg.l-1 during the surgery (Yousaf et al. 2022).

8 Selected Research and Incisive Cases of Fish Surgery in Fish Surgıcal Procedures

An opercular approach. Researchers have developed a unique surgical model for diabetes mellitus in fish, in which the pancreatic endocrine cells are contained solely in an easily excised single mesentery-bound organ adjacent to the hepatic portal vein, separate from the exocrine pancreatic tissue scattered diffusely throughout the mesenteries (Kelley 1993). Fish reproductive organs are elongated and require a correspondingly long incision for surgical removal. The primary blood supply lies at the cranial pole of the gonad, and caution is also necessary at the caudal pole to avoid damage to the excretory systems (Cloud 2003). Endoscopic techniques have approved useful and success for biopsy of entrail organs (Murray et al. 1998). Catheterization of the dorsal aorta is a well-known procedure for repeated blood sampling without complications (Lo et al. 2003). The apparatus for catheterizing the dorsal aorta all involve placement of a catheter into the dorsal aorta at the confluence of branchial vessels in the roof of the mouth. Connecting tubing then exits dorsally through the nasal bone, with anchors placed strategically intraorally and externally along the dorsum of the fish to prevent the catheter from dislodging if the extension tubing becomes entangled (Sohlberg et al., 1997) and intracoelomic catheterization for delivery of drugs in pharmacokinetics studies (Craig 2005).

The goldfish was threatened by a dangerous case of constipation, and the only way to save its life was by surgery to remove the impaction. Anesthetized the fish and carefully removed a lump from its rectum, and another from its dorsal fin. The constipation surgery on the three-inch fish took 50 minutes and was completely successful. A rockfish was being bullied by other fish because it has only one eye. The researcher thought a prosthetic eye might trick the other fish into thinking the rockfish had both eyes. The researcher stitched a bright yellow fake eye onto the rockfish under aseptic conditions and hence has been realized a prosthetıc eye surgery. A goldfish was born without a lower jaw. This meant he couldn’t keep his mouth constantly open like a normal goldfish, and he struggled to breathe and eat. Fashioned a tiny plastic splint for a prosthetıc jaw surgery and stitched the sterile splint to the bottom of the fish mouth (Mentalfloss 2016).

9 Analgesia

Analgesia is the absence of sensation of pain without loss of consciousness, loss of pain. Depending on the procedure, post-operative analgesia may be necessary. A selection of medicines includes: Meloxicam at 0.1-0.2 mg/kg IM, Flunixin 0.25–0.5 mg/kg IM, Carprofen 2-4 mg/kg IM, Morphine 0.1-0.3 mg/kg IM, Methadone 0.1–0.3 mg/kg IM, Butorphanol 0.1-0.4 mg/kg IM (Loh and Chia 2016).

10 Recovery

To regain consciousness, drug-free water is passed over the gills until spontaneous ventilation returns. Fish may then be returned to clean water to recover unassisted until they are free swimming (Loh and Chia 2016).

11 Fish Autopsy

An autopsy is the most essantial piece at Fish medicine. An autopsy (postmortem examination, obduction, necropsy, or autopsia) is a surgical procedure that consists of a thorough examination of a died fish by dissection to determine the cause, mode, and manner of death or to evaluate any disease or injury. Autopsies are unremarkably conducted by a specialized doctor (Khoroshailo and Gvozdeva 2022; Filik and Filik 2022).

12 Euthanasia

Euthanasia is ending a fish's life by giving a painless or minimally painful lethal injection, administering a high dose of medication, or disconnecting the person from life support because their life is perceived as unbearable (Ferreira et al. 2022).

13 Discussion and Conclusion

The dolphin named "Winter" with a prosthetic tail at the Clearwater Aquarium in Florida, USA, became the world's first bionic sea creature. Winter's tail was severed when she was two months old when she got caught in a Crab trap. Winter, with a 75-centimeter tail made of silicone and plastic, can swim easily. Winter, a bottlenose dolphin that lives in the Atlantic Ocean, was near death when she was rescued from the trap in 2006. "I felt so sorry for Winter. It took me a year and a half to build the tail. We worked hard to get Winter to move her tail in all directions," said Kevin Carroll, the world's leading prosthodontist, who has also implanted artificial organs in dogs and an ostrich (Carroll 2008; Brooks 2018). Fish surgery is advancing day by day. This recent successful operation is an example of this.

In that study, the researcher added an undetermined concentration of the antibiotic kanamycin to the water for an undetermined time period; the author did not address survival and wound healing, but a enough number of fish survived a few weeks after surgery for the aims of the study. Products such as Orabase gel (Garcia et al. 2022) or extracellular matrix protein may be suitable for sealing and promoting healing of surgical defects in fish when such defects are not amenable to suturing (Craig 2005).

Post-surgery can also serious a series of problems. For this reason, it is vital to follow up on the sick fish after the surgery. All sensitivity during the operation should be maintained after the operation. As the number of sick fishes increases, so too will the indications for surgical intervention. In general, the most difficult aspect of fish surgery is the provision of safe and adequate anesthesia. In this sense, several different anesthetic regimens are provided. Once one is familiar with the normal anatomy of the piscine patient, the basic concepts of surgery prevail, including appropriate surgical approach, hemostasis, and gentle tissue manipulation. Common specific surgical procedures in fish include integumentary mass excision, intracoelomic mass removals, reproductive system procedures, gastrointestinal foreign body removal, ocular procedures, celiotomy, liver biopsy, renal biopsy, and laparoscopy and radio-transmitter implantation. With the right medicines and equipment, surgery on fish is within the scope of traditional veterinary practice. Finally, the successful outcome of surgical manipulation often rests in the postoperative management of the surgical patient fish.

Acknowledgements

"This research did not receive any specific grant from funding agencies in the public, commercial, or not-for-profit sectors"

Authors' contributions: All authors contribute equally to our study.

Conflict of interest disclosure: Our work has not been carried out with any organization or employees.

References

Bowser PR (2001) Anesthetic options for fish. In: Gleed R.D., Ludders J.W., eds. Recent Advances in Veterinary Anesthesia and Analgesia: Companion Animals. Ithaca, NY: International Veterinary Information Service 2001. www.ivis.org/advances/Anesthesia_Gleed/bowser/chapter_frm.asp?LA=1. (VIN editor: link access requires IVIS membership).

Brooks A (2018) The New World of Pet Prosthetics.

Bülbül Z, Filik N (2019) Gemi yapımında kullanılan ahşap malzemelerde oluşan biyofilm ve fouling. Mühendislik Bilimleri ve Tasarım Dergisi 7(1): 1-6.

Carroll K (2008) Protez kuyruklu ilk biyonik yunus. https://www.hurriyet.com.tr/dunya/protez-kuyruklu-ilk-biyonik-yunus-8866968 Date:13.10.2022.

Cloud JG (2003) Surgical transplantation of sexually immature ovaries in rainbow trout (Oncorhynchus mykiss). J Exp Zool Part A Comp Exp Biol 298(1): 73-76

Craig A (2005) Surgery in Fish Research: Common Procedures and Postoperative Care. Lab Animal, 34(1): 28-34. https://doi.org/10.1038/laban0105-28.

Craig A, Gregory A (2000) Surgery in Fish. Veterinary Clinics of North America: Exotic Animal Practice. Soft-Tissue Surgery, 3(3): 759-774.

Fajardo AJ (2009) A global view of antibiotic resistance. Bull Biotech 34:44-65

Ferreira JM, Félix L, Jorge S, Monteiro SM, Olsson IAS, Valentim AM (2022) Anesthesia Overdose Versus Rapid Cooling for Euthanasia of Adult Zebrafish. Zebrafish 19(4): 148-159.

Filik F (2019) Bazı Bakteriyel Balık Patojenlerinde Biyofilm Oluşumuna Farklı Maddelerin *İn Vitro* Etkisinin Tespiti. (Doctoral dissertation, ISUBÜ Lisansüstü Eğitim Enstitüsü, Yüksek Lisans Tezi).

Filik N (2020) Kültür Balıklarından İzole Edilen *Aeromonas hydrophila* Suşlarında Fenolik Bileşenlerin Çevreyi Algılama Sistemi Üzerine İnhibisyon Etkisi ve Suşlar Arasındaki Klonal İlişkinin Pulsed Field Jel Elektroforez Yöntemiyle Belirlenmesi. TC. Isparta Uygulamalı Bilimler Üniversitesi Lisansüstü Eğitim Enstitüsü, Doktora Tezi.

Filik N, Filik F (2022) Chapter IX Fish Diseases Doctrine. Engineering Sciences 149.

Garcia CR, Ueda TY, da Silva RA, Cano IP, Saldanha LL, Dokkedal AL, Porto VC, Urban VM, Neppelenbroek KH (2022) Effect of denture liners surface modification with *Equisetum giganteum* and *Punica granatum* on *Candida albicans* biofilm inhibition. Therapeutic delivery 13(3): 157-166.

Gilliland ER (1994) Comparison of absorbable sutures used in largemouth bass liver biopsy surgery. Prog Fish Cult 56(1): 60-61

Harms CA, Bakal RS, Khoo LH, Spaulding KA, Lewbart GA (1995) Microsurgical excision of an abdominal mass in a gourami. J Am Vet Med Assoc, 207(9): 1215-1217.

Kelley KM (1993) Experimental diabetes mellitus in a teleost fish. I. Effect of complete isletectomy and subsequent hormonal treatment on metabolism in the goby, Gilichthys mirabilis. Endocrinology 132(6): 2689-1695.

Khoroshailo TA, Gvozdeva YM (2022) Veterinary and Sanitary Examination of Fish in Veterinary Laboratories.

Lo WL, Chang CF, Song YL (2003) Evaluation of dorsal aorta cannulation for immunological studies of grouper (Epinephelus malabaricus). Fish Shellfish Immunol 14(4): 289-303.

Loh R (2012) Fish Vetting Medicines: Formulary of Fish Treatments. Perth, Australia: Richmond Loh Publishing

Loh R, Chia M (2016) Common Fish Surgical Procedures and Anaesthesia. World Small Animal Veterinary Association Congress Proceedings, Main: Fish Disease: Common Fish Surgery & Anaesthesia, 41st WSAVA Sept 27-30 Cartagena, Colombia

Mattson NS, Riple TH (1989) Metomidate, a better anesthetic for cod (Gadus morhua) in comparison with benzocaine, MS-222, chlorobutanol, and phenoxyethanol, Aquaculture 83: 89-94.

Mentalfloss (2016) https://www.mentalfloss.com/article/78187/7-incisive-cases-fish-surgery.

Merriam-Webster (2022) Cite this Entry "Physiological saline." Merriam-Webster.com Dictionary, Merriam-Webster, https://www.merriam-webster.com/dictionary/physiological%20saline. Accessed 22 Jun. 2022

Murray MJ (2002) Fish Surgery. Seminars in Avian and Exotic Pet Medicine 11(4): 246-257. https://doi.org/10.1053/saep.2002.126571.

Murray MJ, Schildger B, Taylor M (1998) Endoscopy in Birds, Reptiles, Amphibians and Fish. Endo-Press, Tuttlingen, Germany.

Neiffer DL, Stamper MA (2009) Fish sedation, anesthesia, analgesia, and euthanasia: considerations, methods, and types of drugs. ILAR J, 50(4): 343-360. http://vpresearch.louisiana.edu/areas/research/files/NeifferFish Sedation.pdf

Nurcan N (2010) Bazı gram-negatif bakteriyel balık patojenlerinde çevreyi algılama sisteminin incelenmesi (Doctoral dissertation, SDÜ Fen Bilimleri Enstitüsü, Yüksek Lisans Tezi).

Petering RW, Johnson DL (1991) Suitability of a cynoacrylate adhesive to close incisions in black crappies used in telemetry studies. Trans. Am. Fish. Soc 120(4): 535-537

Reid S, Backman S (1988) Surgical Excision of a Tumor in a Fish. The Canadian Veterinary Journal 29(2): 172

Saint-Erne N (2010) Advanced Koi Care. 2nd ed. Glendale, AZ: Erne Enterprises

Saint-Erne N (2015) Surgery in Fish. World Small Animal Veterinary Association World Congress Proceedings, WAVMA-Ornamental Fish, Technical Service Veterinarian, PetSmart, Inc., Phoenix, AZ, USA

ScottWeber EP, Schwarz T, Innis C, Klide AM (2009) Anesthesia, Diagnostic Imaging, and Surgery of Fish Compendium Vet.com, February

Sohlberg S, Martinsen B, Horsberg TE, Soli NE (1997) A method for collecting bile in free swimming fish. J Vet Pharmacol Ther 20(6): 493-495.

Stoskopf MK (1993) In Fish Medicine (ed. Stoskopf, M K) 91-97 (WB Saunders, Philadelphia, 1993)

Summerfelt RC, Smith LS (1990) In Methods for Fish Biology. (eds. Schreck C B & Moyle PB) 213-272 (American Fisheries Society, Bethesda, Maryland)

Weber EP, Weisse C, Schwarz T, Innis C, Klide AM (2009) Anesthesia, diagnostic imaging, and surgery of fish. Europe PMC plus, 31(2): E11

Weltzien F, Höglund E, Hamdani EH, Døving KB (2003) Does the lateral bundle of the medial olfactory tract mediate reproductive behavior in male crucian carp? Chem. Senses 28(4): 293-300.

Wildgoose WH (2000) Fish surgery: an overview. Fish Veterinary Journal 5: 22-36

Yıldırım M, Genç E, Yıldırım YB (2009) Balık Cerrahisi ve Anestezi Uygulamaları. www.akuademi.net. XV. Ulusal Su Ürünleri Sempozyumu 01-04 Temmuz 2009 Rize

Yousaf MN, Røn Ø, Hagen PP, McGurk C (2022) Monitoring fish welfare using heart rate bio-loggers in farmed Atlantic salmon (*Salmo salar* L.): An insight into the surgical recovery. Aquaculture 555: 738211

Zambouri A (2007) Preoperative evaluation and preparation for anesthesia and surgery. Hippokratia 11(1): 13

Zottoli SJ, Faber DS, Hering J, Dannhauer AC, Northen S (2021) Survival and Axonal Outgrowth of the Mauthner Cell Following Spinal Cord Crush Does Not Drive Post-injury Startle Responses. Frontiers in Cell and Developmental Biology 9

REVIEW ARTICLE
Bull Biotechnol (2023) 4(1):36-41
https://doi.org/10.51539/biotech.1239945 Journal homepage: www.dergipark.org.tr/biotech

Bulletin of Biotechnology

miRNAs, cancer, and unconventional miRNA functions

Ibrahim Bozgeyik*

*[1]Department of Medical Biology, Faculty of Medicine, Adiyaman University, Adiyaman, Turkey

*Corresponding author : i.bozgeyik@gmail.com
Orcid No: https://orcid.org/0000-0003-1483-2580

Received : 20/01/2023
Accepted : 14/03/2023

Abstract: MicroRNAs are non-protein-coding RNA molecules that control and fine-tune gene expression at the post-transcriptional level by negatively regulating their target genes. MicroRNAs mature into 22-nucleotide-long RNA transcripts that negatively regulate gene expression by inducing either inhibition of translation or degradation of mRNAs. Increasing evidence suggests that distinct signatures of microRNAs are a feature of human cancers. MicroRNA expression patterns have been linked to tumor development, progression, and response to therapies, implying that they could be used as prognostic and diagnostic biomarkers. Moreover, based on a growing body of research indicating that microRNAs may serve as tumor suppressive or tumor promoter functions, miRNA-based therapy against cancer has lately been utilized, either alone or in conjunction with current targeted strategies. One of the advantages of microRNA-based therapeutics is that they can target numerous components of signaling circuits involved in cell differentiation, proliferation, and survival. In this review, the current available evidence about miRNAs and their diagnostic, prognostic, and therapeutic potential will be discussed. miRNAs may play chief roles in the development and progression of human cancers, offer great advantages in differential diagnosis, and can be therapeutically targeted.

Keywords: Cancer; miRNA; non-coding RNAs; miPEP; unconventional miRNA functions

1 Introduction

Previously, most of the human genome was considered "junk DNA" and transcription at these sites was considered transcriptional noise or waste. On the contrary, scientific developments over the last two decades have shown that "junk DNA" encodes active RNA transcripts that are not converted into proteins but are functional (Esquela-Kerscher and Slack 2006; Mattick 2003; Zaratiegui et al. 2007). The discovery of these non-coding RNAs has allowed scientists to better understand complex molecular mechanisms. In 1993, Lee et al., by a chance, identified the lin-4 transcript, a small non-coding RNA that repress lin-14 protein synthesis (Lee et al. 1993). These short non-coding RNAs were later annotated as microRNAs in the early 2000s (Lee et al. 2004). These findings are the first to demonstrate the existence of functional non-coding transcripts. Later, rapid progress in the analysis of the human transcriptome with the development of advanced technological methods enabled the identification of numerous non-coding RNA transcripts involved in the control of key regulatory pathways.

Although many methods have been proposed for classifying non-coding RNAs, they are most often categorized based on their size (Nagano and Fraser 2011). Depending on their size, non-coding RNAs are classified into two main categories as long non-coding RNAs (lncRNAs) and short or small non-coding RNAs (sncRNAs) (Dozmorov et al. 2013; Nagano and Fraser 2011). Small non-coding RNAs are less than 200 nucleotides long and they include microRNAs (miRNAs), 5S and 5.8S ribosomal RNAs (rRNAs), piwi-interacting RNAs (piRNAs), short interfering RNAs (siRNAs), small nucleolar RNAs (snoRNAs), and small nuclear RNAs (snRNAs) (Dozmorov et al. 2013; Nagano and Fraser 2011). Also, long non-coding RNAs are longer than 200 nucleotides and they comprise natural antisense transcripts (NATs), long intergenic non-coding RNAs (lincRNAs), transcribed ultra-conserved regions (T-UCRs), competing endogenous RNAs (ceRNAs) and ribosomal RNAs (rRNAs) (Dozmorov et al. 2013; Nagano and Fraser 2011; Ponting et al. 2009).

Cumulative evidence strongly suggests that non-coding RNA molecules play fundamental regulatory functions in many vital cellular mechanisms, including proliferation, cell growth, differentiation, and cell death (Calin and Croce 2006; Reddy 2015; Visone and Croce 2009). Coordinated regulation of these molecules is essential for the proper maintenance of cellular hemostasis. However, defects in the

regulation of non-coding RNAs are directly involved in the development of many pathological problems, especially cancer (Calin and Croce 2006; Esquela-Kerscher and Slack 2006; Wapinski and Chang 2011).

2 MicroRNAs

MiRNAs are non-protein-coding RNA molecules that control and fine-tune gene expression at the post-transcriptional level through negative regulation of their target genes (Esteller 2011). MiRNAs mature into 22-nucleotide-long RNA transcripts. A growing mass of evidence indicates miRNAs have central tasks in various dynamic cellular mechanisms such as growth, differentiation, apoptosis and, proliferation (Melo and Esteller 2011; Ruan et al. 2009). More than 60% of human genes are thought to be controlled by miRNAs (Esteller 2011). While some participate in the control of specific target molecules, others can act as principal regulators of a signaling pathway, allowing important miRNAs to control the levels of hundreds of genes at once, and several sorts of miRNAs to work together to regulate their targets (He and Hannon 2004; Mendell 2005). A growing body of evidence suggests that deregulated expression of microRNAs is an important contributor to the development and progression of many diseases, including immune system disorders, diabetes, neurodegenerative diseases, and cancer (Garzon et al. 2009; Melo and Esteller 2011; Ruan et al. 2009).

2.1 Genomic localization, biogenesis, and mechanisms of action of miRNAs

MiRNA genes have been shown to be conserved across species (Rodriguez et al. 2004). They can be found in exons, introns, and intergenic regions of protein-coding genes (Rodriguez et al. 2004). The majority of intronic or exonic miRNAs are oriented in the same direction as the host gene, indicating that they are co-transcribed (Rodriguez et al. 2004). The latter group of miRNAs are synthesized from gene deserts or intergenic regions containing independent transcription elements (Rodriguez et al. 2004). The RNase III enzymes, Drosha and Dicer, are involved in miRNA biogenesis. Biogenesis of miRNAs first begins with the production of the primary miRNA transcript (pri-miRNA) by RNA polymerase II (Bartel 2007). The pri-miRNA is further cleaved by the enzyme Drosha, a double-strand DNA-specific ribonuclease, in the nucleus (Bartel 2007). As a result of this enzymatic cleavage, a 70-100 nt long precursor miRNA (pre-miRNA) transcript is produced (Bartel 2007). The pre-miRNAs are subsequently transported to the cytoplasm from the nucleus by the Exportin-5-RanGTP protein and undergo a second cleavage in the cytoplasm. This second cleavage reaction is catalyzed by the Dicer enzyme. As a result, mature microRNAs with an average length of 22 nucleotides are formed (Bartel 2007). TRBP and Argonaute 2 proteins aid mature miRNAs to interact with their target mRNAs.

2.2 MiRNA-mediated gene silencing

To perform their regulatory functions, miRNAs cooperate with members of the Argonaute proteins to assemble into miRNA-induced silencing complexes (miRISCs) (Ameres and Zamore 2013). Post-transcriptional silencing of mRNAs containing sequences partly or completely complementary to miRNA genes is mediated by these complexes. (Ameres and Zamore 2013; Jonas and Izaurralde 2015). Target mRNAs with excellent complementarity are degraded by enzymatically active AGO proteins (Ameres and Zamore 2013; Jonas and Izaurralde 2015). In mammals, however, mRNA often form partial complementarity with miRNAs, making AGO protein destruction impossible (Ameres and Zamore 2013; Jonas and Izaurralde 2015). Moreover, only AGO2 is catalytically active in humans, while other members including AGO1, AGO3 and AGO4 proteins are not active (Ipsaro and Joshua-Tor 2015). Where degradation is not possible, AGO recruits some additional proteins to mediate silencing (Fabian and Sonenberg 2012; Huntzinger and Izaurralde 2011). In this case, silencing of mRNA is achieved through a collection of translation suppression, deadenylation, decapping, and 5′-to-3′ degradation (Fabian and Sonenberg 2012; Huntzinger and Izaurralde 2011). In this mechanism, the GW182 proteins, which are among the most well-studied AGO-related proteins, play a critical role (Fabian and Sonenberg 2012; Huntzinger and Izaurralde 2011). These proteins act as scaffolds between the AGO proteins and the downstream effector complexes. It has been revealed that the degradation of mRNAs by miRNA-mediated silencing is catalyzed by enzymes of 5′ to 3′ mRNA degradation pathway (Jonas and Izaurralde 2015). In the 5′-to-3′ mRNA decay pathway, mRNAs are deadenylated at first by sequential action of the PAN2-PAN3 and CAF1–CCR4–NOT deadenylase complexes (Wahle and Winkler 2013). Deadenylated mRNAs are further subjected to mRNA decapping by decapping protein 2 (DCP2), which necessitates the assembly of extra cofactors. In metazoans, these factors are DCP1 (decapping protein 1), EDC3 (enhancer of decapping 3), EDC4 (enhancer of decapping 4), PATL1 (PAT1-Like Protein 1), and DDX6 (DEAD box protein 6) proteins. Ultimately, deadenylated and decapped messenger RNAs are degraded by exoribonuclease 1 (XRN1) (Jonas and Izaurralde 2015). Argonaute proteins, GW182 proteins, decapping factors, and XRN1 localize to P-bodies (also known as mRNA-processing bodies). However, the functional relevance of this localization is still a mystery (Jonas and Izaurralde 2015).

3 MiRNAs and cancer

Previously, it was thought that only defects in tumor promoter and tumor suppressive genes play a role in the formation of cancer (Rajasegaran et al. 2021). However, with the discovery of miRNA molecules, diagnostic, prognostic, and therapeutic approaches against cancer gained a new dimension (Rajasegaran et al. 2021). Accumulating evidence indicates that these small RNA molecules are highly deregulated in human cancers. In tumor tissues, certain microRNAs (OncomiRs) are elevated, while other miRNAs (tumor suppressor miRNAs) are downregulated. (Dalmay and Edwards 2006; Ruan et al. 2009). Low levels of tumor suppressive miRNAs and enhanced expression of tumor promoter miRNAs contribute to main hallmarks of cancer such as sustained proliferation and growth, disruption of death mechanisms, modulation of immune surveillance, invasion, and metastasis(Calin and Croce 2006; Rajasegaran

et al. 2021). The first findings between cancer and miRNAs were found in studies of patients with chronic lymphocytic leukemia. Calin, G. A. et al. reported that the genomic region encoding mir-15a and mir-16-1 is frequently deleted or translocated in patients with B-cell chronic lymphocytic leukemia (CLL) (Calin et al. 2002). As a result, the expression level of the anti-apoptotic BCL-2 (B-cell lymphoma 2) protein, which is the target of these miRNAs, increases and apoptosis is suppressed (Calin et al. 2002). Because miRNAs play such an active role in tumorigenesis, mimicking the functions of tumor suppressive miRNAs or inhibiting the functions of tumor promoter miRNAs offers a strong therapeutic potential (Petrocca and Lieberman 2009).

3.1 MiRNAs as tumor suppressive genes

As stated above, many miRNAs are localized in cancer-related genomic areas and thus they play important roles in cancer formation by acting as tumor promoter or tumor suppressive genes (Frixa et al. 2015). Similar to genes that code for proteins, miRNAs can also show tumor suppressive effects (Garzon et al. 2009). Thus, loss of function of miRNAs can initiate malignant transformation of a normal cell or contribute to the oncogenic process (Garzon et al. 2009). Loss of miRNA expression might be due to diverse mechanisms, such as mutation, genomic deletion, alterations in miRNA processing and/or epigenetic silencing (Garzon et al. 2009). For instance, it was determined that the expressions of let-7 family of miRNAs are diminished in multiple kinds of cancer (Garzon et al. 2009). Let-7 family members targets the expression of well-recognized tumor promoter genes such as the Ras family (Johnson et al. 2005). Additionally, latest studies have enabled the identification of many miRNAs with tumor suppressive functions. microRNA-34a is one of the well-known tumor suppressive miRNAs. miR-34a was recognized as a direct transcriptional target of p53 and is known to induce G1 cell cycle arrest, senescence, and apoptosis in response to DNA damage (Saito et al. 2015). Like miR-34a, Ma et al. established that miR-361-5p showed tumor suppressive properties in breast cancer as well as colorectal and gastric cancers (Ma et al. 2017). Moreover, miRNA-329 prevents tumor growth and cell proliferation while facilitating apoptotic death of gastric cancer cells by negatively regulating KDM1A (Cai et al. 2017). MiRNA-211 expression was also shown to be highly reduced in cervical cancer cell lines and tissues compared to controls, and overexpression of miRNA-211 suppressed the expansion and metastasis of cervical cancer cells through modulating ZEB1 (Chen et al. 2017). MiRNA-193a-3p is another miRNA known for its tumor suppressor properties. It has been shown that it is downregulated in colorectal cancer patients and increased expression of miRNA-193a-3p represses expansion and invasion of colorectal cancer cells (Takahashi et al. 2017). Also, miRNA-195 has been shown to be frequently downregulated in melanoma patients. Functional analyzes have shown that miRNA-195 exerts an anti-proliferative effect on human melanoma cancer cells by suppressing Prohibitin 1, which plays an active role in the RAS-RAF-MEK-ERK pathway (Cirilo et al. 2017). In addition to these findings, members of miR-29 family of miRNAs were reported to be downregulated in patients with CLL, AML, cholangiocarcinoma, lung, and breast cancers (Calin et al. 2005; Garzon et al. 2008; Iorio et al. 2005; Mott et al. 2007; Yanaihara et al. 2006). Moreover, overexpression of miR-29b provoked apoptosis in lung cancer and cholangiocarcinoma cell lines and weakened tumorigenic properties in the lung cancer mouse xenograft model (Fabbri et al. 2007; Mott et al. 2007). Anti-apoptotic MCL-1 and TCL-1 oncogenes are two identified targets of miR-29b (Mott et al. 2007; Pekarsky et al. 2006). There is also increasing evidence that miR-139 is frequently suppressed in various human malignancies. Although miR-139 is encoded in the intronic region of the phosphodiesterase 2A (PDE2A) gene, no correlation was found between these two in carcinogenesis (Shen et al. 2014). miR-139 was reported to be directly activated in cells expressing wild type p53 gene during DNA damage (Cao et al. 2016) and silenced by Polycomb repressive complex-2 (PRC2) and RNA Polymerase 2 Subunit M (POLR2M) (Cao et al. 2016; Stavast et al. 2022).

3.2 MiRNAs as oncogenes

Accumulating body of evidence also revealed that many miRNAs show tumor promoter functions. MiR-155 was one of the first oncomiRs discovered and its gene expression level was found to be markedly elevated in various cancers as lung cancer, pancreatic cancer, breast cancer, B-cell lymphoma and Hodgkin's lymphoma. In addition, miR-155 was shown to downregulate TP53INP1 (Tumor protein 53-induced nuclear protein 1) expression (Hemmatzadeh et al. 2016). Another oncogenic miRNA that accelerates tumor formation is miR-21 (Garzon et al. 2009). miR-21 is upregulated in many hematological malignancies such as CLL and AML, as well as breast, lung, prostate, colon, liver, stomach, pancreatic and glioblastoma cancers (Garzon et al. 2009). miR-21 triggers the metastasis and invasion of cancerous cells by suppressing tumor suppressor proteins including PTEN (phosphatase and tensin homolog), PDCD4 (programmed cell death 4) and TPM1 (tropomyosin 1) (Garzon et al. 2009). Moreover, overexpression of miR-21 has been shown to suppress apoptosis of glioblastoma cells (Chan et al. 2005). In addition, suppression of its expression in breast, liver, and glioblastoma cancer cells suppresses cell proliferation, triggers caspase activation, and increases apoptotic cell death (Chan et al. 2005; Frankel et al. 2008; Meng et al. 2007). The miR-17-92 miRNA gene cluster (including miR-19a, miR-19b-1, miR-17, miR-18a, and miR-92-1, miR- 20a) is recurrently amplified in many solid tumors and hematological malignancies, including lung, colon, breast, pancreatic, prostate, gastric cancers and lymphomas (Garzon et al. 2009). These miRNAs trigger proliferative signaling and invasion in cancer cells and suppress apoptosis (Garzon et al. 2009). Interestingly, c-myc, a tumor promoter gene which is commonly stimulated in cancer, transactivates the miR-17-92 miRNA cluster.

3.3 MiRNAs in cancer treatment

Because of the oncogenic and tumor suppressor roles played by miRNAs in cancer expansion and advancement, mimicking the functions of tumor suppressive miRNAs or suppressing the functions of tumor promoter miRNAs emerges as an innovative approach in cancer treatment.

Today, there are pre-clinical and clinical studies that have been made or are being conducted for the use of miRNAs in the therapy of various health manifestations, including cancer (Li and Rana 2014). The use of miRNAs in cancer therapy has several benefits. Mature miRNA sequences are small and conserved among many vertebrate species (van Rooij and Kauppinen 2014). In addition, miRNAs often target many genes in cellular signaling pathways. Thus, therapeutic targeting of disease-associated miRNAs may allow targeting of the entire disease-associated pathway (van Rooij and Kauppinen 2014). Two basic methods have been used to modulate miRNA activity; the first is to restore miRNA activity using synthetic double-stranded miRNAs or viral overexpression vector, and the second is to inhibit miRNA activity using chemically modified antimiR oligonucleotides (Shah et al. 2016; van Rooij and Kauppinen 2014).

4 Unconventional functions of miRNAs

Numerous unconventional regulatory functions of miRNAs have also been reported. Primary transcripts of miRNAs have been found to encode small peptides with regulatory functions, termed miRNA-encoded peptides (miPEPs). Lauressergues et al. were the first to report that miRNAs encode for regulatory peptides. In plants, they have discovered that several pri-miRNAs, comprising pri-miR-165a of *Arabidopsis thaliana* (miPEP165a, 18 amino acids) and pri-miR-171b of *Medicago truncatula* (miPEP171b, 9 amino acids), codes for short regulatory peptides. These pri-miRNA-encoded oligopeptides have been identified to advance transcription of their own pri-miRNA, which increases the production of their respective mature miRNAs (Lauressergues et al. 2015). Although a direct physical interaction has not yet been demonstrated, increased expression of miRNAs has been shown to enhance Toll-like receptor (TLR) activity. Specifically, in lung cancer, miR-29a and miR-21 have been reported to activate the expression of TLR7 in humans. Let-7b has also been reported to directly stimulate the expression of TLR7 and exert a neurodegenerative effect (Lehmann et al. 2012). Another unconventional function of miRNAs is the upregulation of protein expression in response to cell cycle progression. During cell cycle arrest, certain miRNAs promote translation of their target mRNAs while repressing translation in proliferating cells. Specifically, miR-369 was shown to control the association of Argonaute (AGO) and Fragile X Mental Retardation-Related Protein 1 (FXR1) with the AU-rich elements (AREs) in tumor necrosis factor mRNA during cell cycle arrest to enhance translation (Vasudevan et al. 2007). Although the mitochondrial genome lacks miRNAs, Das et al. discovered that miR-181c translocates to mitochondria and represses expression of the mitochondrially encoded cytochrome c oxidase subunit 1 (mt-COX1) protein while increasing expression of mt-COX2 mRNA and protein content (Das et al. 2012). These findings further indicate that miRNAs also participate in the control of genes encoded by the mitochondrial genome to regulate mitochondrial dynamics. AGO-independent actions of miRNAs have also been reported. Eiring et al. identified that miR-328 acts as a molecular decoy for heterogeneous ribonucleoprotein E2 (hnRNP E2) to rescue translation of CEBPA mRNA. When miR-328 binds to hnRNP E2, releasing CEBPA mRNA from hnRNP E2-mediated translational repression (Eiring et al. 2010).

5 Conclusion

Although considerable efforts have been made for many years to identify biomarkers for cancer diagnosis and treatment, no biomarker has attracted as much attention as the potential of miRNAs. A substantial body of research shows that miRNAs have tremendous potential for the development of targeted cancer therapies since they can selectively bind to and repress the target gene. Currently available evidence indicates that suppression of oncogenic miRNAs or replacement of tumor suppressor miRNAs could be an innovative therapeutic strategy in cancer therapy. Furthermore, miRNA profiling of human cancer provides significant advantages for the discovery of effective therapeutic drugs and treatment planning. In further studies, more detailed studies on the clinical use of these molecules are needed.

Acknowledgements

Authors' contributions: I.B. conceptualized the study, reviwed literature and wrote the manuscript.

Conflict of interest disclosure: I am the sole author of the manuscript, and I have no conflicts of interest to declare.

References

Ameres SL, Zamore PD (2013). Diversifying microRNA sequence and function. Nat Rev Mol Cell Bio 14:475-488

Bartel DP (2007). MicroRNAs: Genomics, biogenesis, mechanism, and function (Reprinted from Cell, vol 116, pg 281-297, 2004). Cell 131:11-29

Cai L, Chen Q, Fang S, Lian M, Cai M (2017). MicroRNA-329 inhibits cell proliferation and tumor growth while facilitates apoptosis via negative regulation of KDM1A in gastric cancer. Journal of Cellular Biochemistry

Calin GA, Croce CM (2006). MicroRNA signatures in human cancers. Nature reviews cancer 6:857-866

Calin GA, Dumitru CD, Shimizu M, Bichi R, Zupo S, Noch E, Aldler H, Rattan S, Keating M, Rai K, Rassenti L, Kipps T, Negrini M, Bullrich F, Croce CM (2002). Frequent deletions and down-regulation of micro-RNA genes miR15 and miR16 at 13q14 in chronic lymphocytic leukemia. P Natl Acad Sci USA 99:15524-15529

Calin GA, Ferracin M, Cimmino A, Di Leva G, Shimizu M, Wojcik SE, Iorio MV, Visone R, Sever NI, Fabbri M, Iuliano R, Palumbo T, Pichiorri F, Roldo C, Garzon R, Sevignani C, Rassenti L, Alder H, Volinia S, Liu CG, Kipps TJ, Negrini M, Croce CM (2005). A MicroRNA signature associated with prognosis and progression in chronic lymphocytic leukemia. The New England journal of medicine 353:1793-1801

Cao B, Wang K, Liao J-M, Zhou X, Liao P, Zeng SX, He M, Chen L, He Y, Li W (2016). Inactivation of oncogenic cAMP-specific phosphodiesterase 4D by miR-139-5p in response to p53 activation. Elife 5:e15978

Chan JA, Krichevsky AM, Kosik KS (2005). MicroRNA-21 is an antiapoptotic factor in human glioblastoma cells. Cancer Res 65:6029-6033

Chen G, Huang P, Xie J, Li R (2017). microRNA-211 suppresses the growth and metastasis of cervical cancer by directly targeting ZEB1. Molecular medicine reports

Cirilo PDR, de Sousa Andrade LN, Corrêa BRS, Qiao M, Furuya TK, Chammas R, Penalva LOF (2017). MicroRNA-195 acts as an anti-proliferative miRNA in human melanoma cells by targeting Prohibitin 1. BMC Cancer 17:750

Dalmay T, Edwards DR (2006). MicroRNAs and the hallmarks of cancer. Oncogene 25:6170-6175

Das S, Ferlito M, Kent OA, Fox-Talbot K, Wang R, Liu D, Raghavachari N, Yang Y, Wheelan SJ, Murphy E, Steenbergen C (2012). Nuclear miRNA regulates the mitochondrial genome in the heart. Circ Res 110:1596-1603

Dozmorov MG, Giles CB, Koelsch KA, Wren JD (2013) Systematic classification of non-coding RNAs by epigenomic similarity. In: BMC bioinformatics. BioMed Central, p S2

Eiring AM, Harb JG, Neviani P, Garton C, Oaks JJ, Spizzo R, Liu S, Schwind S, Santhanam R, Hickey CJ, Becker H, Chandler JC, Andino R, Cortes J, Hokland P, Huettner CS, Bhatia R, Roy DC, Liebhaber SA, Caligiuri MA, Marcucci G, Garzon R, Croce CM, Calin GA, Perrotti D (2010). miR-328 functions as an RNA decoy to modulate hnRNP E2 regulation of mRNA translation in leukemic blasts. Cell 140:652-665

Esquela-Kerscher A, Slack FJ (2006). Oncomirs - microRNAs with a role in cancer. Nature Reviews Cancer 6:259-269

Esteller M (2011). Non-coding RNAs in human disease. Nature reviews genetics 12:861-874

Fabbri M, Garzon R, Cimmino A, Liu Z, Zanesi N, Callegari E, Liu S, Alder H, Costinean S, Fernandez-Cymering C (2007). MicroRNA-29 family reverts aberrant methylation in lung cancer by targeting DNA methyltransferases 3A and 3B. Proceedings of the National Academy of Sciences 104:15805-15810

Fabian MR, Sonenberg N (2012). The mechanics of miRNA-mediated gene silencing: a look under the hood of miRISC. Nat Struct Mol Biol 19:586-593

Frankel LB, Christoffersen NR, Jacobsen A, Lindow M, Krogh A, Lund AH (2008). Programmed cell death 4 (PDCD4) is an important functional target of the microRNA miR-21 in breast cancer cells. J Biol Chem 283:1026-1033

Frixa T, Donzelli S, Blandino G (2015). Oncogenic MicroRNAs: Key Players in Malignant Transformation. Cancers 7:2466-2485

Garzon R, Calin GA, Croce CM (2009). MicroRNAs in cancer. Annual review of medicine 60:167-179

Garzon R, Volinia S, Liu C-G, Fernandez-Cymering C, Palumbo T, Pichiorri F, Fabbri M, Coombes K, Alder H, Nakamura T (2008). MicroRNA signatures associated with cytogenetics and prognosis in acute myeloid leukemia. Blood 111:3183-3189

He L, Hannon GJ (2004). MicroRNAs: small RNAs with a big role in gene regulation. Nature reviews genetics 5:522-531

Hemmatzadeh M, Mohammadi H, Jadidi-Niaragh F, Asghari F, Yousefi M (2016). The role of oncomirs in the pathogenesis and treatment of breast cancer. Biomedicine & pharmacotherapy = Biomedecine & pharmacotherapie 78:129-139

Huntzinger E, Izaurralde E (2011). Gene silencing by microRNAs: contributions of translational repression and mRNA decay. Nature Reviews Genetics 12:99-110

Iorio MV, Ferracin M, Liu CG, Veronese A, Spizzo R, Sabbioni S, Magri E, Pedriali M, Fabbri M, Campiglio M, Menard S, Palazzo JP, Rosenberg A, Musiani P, Volinia S, Nenci I, Calin GA, Querzoli P, Negrini M, Croce CM (2005). MicroRNA gene expression deregulation in human breast cancer. Cancer Res 65:7065-7070

Ipsaro JJ, Joshua-Tor L (2015). From guide to target: molecular insights into eukaryotic RNA-interference machinery. Nat Struct Mol Biol 22:20-28

Johnson SM, Grosshans H, Shingara J, Byrom M, Jarvis R, Cheng A, Labourier E, Reinert KL, Brown D, Slack FJ (2005). RAS is regulated by the let-7 microRNA family. Cell 120:635-647

Jonas S, Izaurralde E (2015). Towards a molecular understanding of microRNA-mediated gene silencing. Nature reviews Genetics 16:421-433

Lauressergues D, Couzigou J-M, San Clemente H, Martinez Y, Dunand C, Bécard G, Combier J-P (2015). Primary transcripts of microRNAs encode regulatory peptides. Nature 520:90-93

Lee R, Feinbaum R, Ambros V (2004). A short history of a short RNA. Cell 116:S89-S92

Lee RC, Feinbaum RL, Ambros V (1993). The C-Elegans Heterochronic Gene Lin-4 Encodes Small Rnas with Antisense Complementarity to Lin-14. Cell 75:843-854

Lehmann SM, Krüger C, Park B, Derkow K, Rosenberger K, Baumgart J, Trimbuch T, Eom G, Hinz M, Kaul D, Habbel P, Kälin R, Franzoni E, Rybak A, Nguyen D, Veh R, Ninnemann O, Peters O, Nitsch R, Heppner FL, Golenbock D, Schott E, Ploegh HL, Wulczyn FG, Lehnardt S (2012). An unconventional role for miRNA: let-7 activates Toll-like receptor 7 and causes neurodegeneration. Nature Neuroscience 15:827-835

Li Z, Rana TM (2014). Therapeutic targeting of microRNAs: current status and future challenges. Nature reviews Drug discovery 13:622-638

Ma F, Zhang L, Ma L, Zhang Y, Zhang J, Guo B (2017). MiR-361-5p inhibits glycolytic metabolism, proliferation and invasion of breast cancer by targeting FGFR1 and MMP-1. Journal of experimental & clinical cancer research : CR 36:158

Mattick JS (2003). Challenging the dogma: the hidden layer of non-protein-coding RNAs in complex organisms. Bioessays 25:930-939

Melo SA, Esteller M (2011). Dysregulation of microRNAs in cancer: Playing with fire. Febs Letters 585:2087-2099

Mendell JT (2005). MicroRNAs: critical regulators of development, cellular physiology and malignancy. Cell cycle 4:1179-1184

Meng F, Henson R, Wehbe-Janek H, Ghoshal K, Jacob ST, Patel T (2007). MicroRNA-21 regulates expression of the PTEN tumor suppressor gene in human hepatocellular cancer. Gastroenterology 133:647-658

Mott JL, Kobayashi S, Bronk SF, Gores GJ (2007). mir-29 regulates Mcl-1 protein expression and apoptosis. Oncogene 26:6133-6140

Nagano T, Fraser P (2011). No-nonsense functions for long noncoding RNAs. Cell 145:178-181

Pekarsky Y, Santanam U, Cimmino A, Palamarchuk A, Efanov A, Maximov V, Volinia S, Alder H, Liu C-G, Rassenti L (2006). Tcl1 expression in chronic lymphocytic leukemia is regulated by miR-29 and miR-181. Cancer Res 66:11590-11593

Petrocca F, Lieberman J (2009). Micromanipulating cancer microRNA-based therapeutics? Rna Biology 6:335-340

Ponting CP, Oliver PL, Reik W (2009). Evolution and functions of long noncoding RNAs. Cell 136:629-641

Rajasegaran Y, Azlan A, Rosli AA, Yik MY, Kang Zi K, Yusoff NM, Moses EJ (2021). Footprints of microRNAs in Cancer Biology. Biomedicines 9:1494

Reddy KB (2015). MicroRNA (miRNA) in cancer. Cancer cell international 15:1-6

Rodriguez A, Griffiths-Jones S, Ashurst JL, Bradley A (2004). Identification of mammalian microRNA host genes and transcription units. Genome research 14:1902-1910

Ruan K, Fang XG, Ouyang GL (2009). MicroRNAs: Novel regulators in the hallmarks of human cancer. Cancer Letters 285:116-126

Saito Y, Nakaoka T, Saito H (2015). microRNA-34a as a Therapeutic Agent against Human Cancer. J Clin Med 4:1951-1959

Shah MY, Ferrajoli A, Sood AK, Lopez-Berestein G, Calin GA (2016). microRNA therapeutics in cancer—an emerging concept. EBioMedicine 12:34-42

Shen K, Mao R, Ma L, Li Y, Qiu Y, Cui D, Le V, Yin P, Ni L, Liu J (2014). Post-transcriptional regulation of the tumor suppressor miR-139-5p and a network of miR-139-5p-mediated m RNA interactions in colorectal cancer. The FEBS journal 281:3609-3624

Stavast CJ, van Zuijen I, Karkoulia E, Özçelik A, van Hoven-Beijen A, Leon LG, Voerman JSA, Janssen GMC, van Veelen PA, Burocziova M, Brouwer RWW, van Ijcken WFJ, Maas A, Bindels EM, van der Velden VHJ, Schliehe C, Katsikis PD, Alberich-Jorda M, Erkeland SJ (2022). The tumor suppressor MIR139 is silenced by POLR2M to promote AML oncogenesis. Leukemia 36:687-700

Takahashi H, Takahashi M, Ohnuma S, Unno M, Yoshino Y, Ouchi K, Takahashi S, Yamada Y, Shimodaira H, Ishioka C (2017). microRNA-193a-3p is specifically down-regulated and acts as a tumor suppressor in BRAF-mutated colorectal cancer. BMC cancer 17:723

van Rooij E, Kauppinen S (2014). Development of microRNA therapeutics is coming of age. Embo Molecular Medicine 6:851-864

Vasudevan S, Tong Y, Steitz JA (2007). Switching from Repression to Activation: MicroRNAs Can Up-Regulate Translation. Science 318:1931-1934

Visone R, Croce CM (2009). MiRNAs and cancer. The American journal of pathology 174:1131-1138

Wahle E, Winkler GS (2013). RNA decay machines: deadenylation by the Ccr4-not and Pan2-Pan3 complexes. Biochimica et biophysica acta 1829:561-570

Wapinski O, Chang HY (2011). Long noncoding RNAs and human disease. Trends in cell biology 21:354-361

Yanaihara N, Caplen N, Bowman E, Seike M, Kumamoto K, Yi M, Stephens RM, Okamoto A, Yokota J, Tanaka T (2006). Unique microRNA molecular profiles in lung cancer diagnosis and prognosis. Cancer cell 9:189-198

Zaratiegui M, Irvine DV, Martienssen RA (2007). Noncoding RNAs and gene silencing. Cell 128:763-776